University of Stavanger

Faculty of Science and Technology

MASTER'S THESIS

Study program/ Specialization: Offshore Technology-Marine Technology and Subsea Engineering	Spring semester, 2012 Open / Restricted access
Writer: **Nima Ghanemnia**	………………………………………… (Writer's signature)
Faculty supervisor: **Professor Dr. Ljlijana Djapic Oosterkamp** External supervisor(s): Youhannes Ayele (Det Norske Veritas)	
Titel of thesis: **Non-Linear Finite Element Analysis of tubular X joint with selected geometry**	
Credits (ECTS):30	
Key words: Tubular Joints, Theory of Elasticity and Plasticity, Finite Element Analysis, Element Types, Abaqus	Pages: 105 + enclosure: CD contains ABAQUS files Stavanger, 27.06.2012 Date/year

Abstract

"Tubular Joints" play a very important and quite vital role in most of the marine structures; we can see maybe hundreds of them in every even simple jacket or steel platforms. It is obvious that having full control about capacity and strength of tubular joints would be very worthy to have good knowledge about total performance of the structure. During recent years the application of the finite element (FE) method has become very popular in the analyses of different types of welded circular tubular joints. The rapid development of commercial FE programs and computation facilities has extended the analyses from elastic to elasto-plastic, from linear to non-linear, from uniplanar joints to multiplanar joints, from un cracked joints to cracked joints, from traditional study of stress distribution, SCF calculation and load displacement behavior of a joint to the assessment of the ultimate capacity of a joint (21). Due to complexity of these kinds of elements, Lots of world level codes and standards have covered some chapters about tubular joints and their capacity, and in some of them the mentioned relations and formula are extremely conservative and are not showing the real ability of the joints. As mentioned FE analysis has opened new horizons to tubular joints capacity. In these technical notes first off all I am trying make a good introduction about what we have already about tubular joints in different standards, comparing different mentioned relations and formula and general classifications of the joints, after that we will a choose real case for our study, a X joints from a real jacket located in north sea. We discuss the concept of theory of elasticity and theory of plasticity in detail later on and finally we are aiming to perform elastic and also a plastic analysis on that specific joint.

We will perform linear and non-linear finite element analysis by very powerful FE software which is called ABAQUS, ways of meshing and choosing element types are always important concern in each FE analysis. In addition of performing FE analysis we will perform some studies about different kinds of element type and meshing sizes. Comparing of these results would be a interesting guide for choosing optimum way of meshing, Since as we know different types of elements and meshing have direct relation with needed time and a skilled FE analyst can choose the optimum way.

Acknowledgment

In 27th of June, at 15:20 pm my thesis finished after about 5 mounts every day work. This period was one of the strangest periods in my life; I have experienced lots of up and downs, lots of hopeful and disappointing moments But I as I am not kind of quitter person finally I could finish it. My thesis is always associated with some names that I will never ever forget them and if these people were not in my life this could never be happened.

First of all I would like to thank my great and knowledgeable university supervisor Professor **Dr. Ljlijana Djapic Oosterkamp**, she spent lots of energy and attention in beginning and along my thesis way and I am always thankful of her because of everything. In addition of significant technical and scientific skills she has a great sense of sympathy which I have been really influenced by it.

Also I would like to say special thank you to my ever beloved teacher, **Professor Ove Tobias Gudmestad** who supported me in every aspect and I will never forget what he has done for me till end of my life, **He is a great real man that if he was not I would not be here now**. And of course I cannot forget the dear name of Tanja Bergby who always has done her best for me and the all students to reach their educational goals, thank you very much dear Tanja.

And about **Det Norske Veritas**…

I have had this honor and chance to my thesis at DNV office in Stavanger, words cannot describe what a memorable moments I have experienced there and how much did I learn from every one there. The name of DNV will always stay in my heart for ever.

Very specifically and sincerely I would like to say my best of thanks to **Mr. Ole Gabrielsen** head of the structural section in DNV. He is a really great man that have spent lots of his worthy time on my thesis, I have learnt bunch of valuable lessons from him which is a lifelong treasure for me.

He is valuable human for everyone around himself and I am so happy that I had this chance to meet him every day for around six mounts. Dear Ole I will never forget your great sense of responsibility and I wish you all the best in your life.

The last but not the least I would like to name a person who spent his time and energy on my thesis even more than me, a busy man who was always so kind to me to answer all my even stupid questions, a person who I have learnt a lot from him and I am always thankful of him.

Mr. Yohannes Ayele, a perfect and knowledgeable senior engineer in dnv and my mentor. Dear Yohannes I will never forget all your kindness and I wish you all the perfects in your life.

Nima Ghanemnia
27 June 2012, Stavanger

Table of Contents

List of tables and Figures

Acknowledgment

In 27th of June, at 15:20 pm my thesis finished after about 5 mounts every day work. This period was one of the strangest periods in my life; I have experienced lots of up and downs, lots of hopeful and disappointing moments But I as I am not kind of quitter person finally I could finish it. My thesis is always associated with some names that I will never ever forget them and if these people were not in my life this could never be happened.

First of all I would like to thank my great and knowledgeable university supervisor Professor **Dr. Ljlijana Djapic Oosterkamp**, she spent lots of energy and attention in beginning and along my thesis way and I am always thankful of her because of everything. In addition of significant technical and scientific skills she has a great sense of sympathy which I have been really influenced by it.

Also I would like to say special thank you to my ever beloved teacher, **Professor Ove Tobias Gudmestad** who supported me in every aspect and I will never forget what he has done for me till end of my life, **He is a great real man that if he was not I would not be here now**. And of course I cannot forget the dear name of Tanja Bergby who always has done her best for me and the all students to reach their educational goals, thank you very much dear Tanja.

And about **Det Norske Veritas**…

I have had this honor and chance to my thesis at DNV office in Stavanger, words cannot describe what a memorable moments I have experienced there and how much did I learn from every one there. The name of DNV will always stay in my heart for ever.

Very specifically and sincerely I would like to say my best of thanks to **Mr. Ole Gabrielsen** head of the structural section in DNV. He is a really great man that have spent lots of his worthy time on my thesis, I have learnt bunch of valuable lessons from him which is a lifelong treasure for me.

He is valuable human for everyone around himself and I am so happy that I had this chance to meet him every day for around six mounts. Dear Ole I will never forget your great sense of responsibility and I wish you all the best in your life.

The last but not the least I would like to name a person who spent his time and energy on my thesis even more than me, a busy man who was always so kind to me to answer all my even stupid questions, a person who I have learnt a lot from him and I am always thankful of him.

Mr. Yohannes Ayele, a perfect and knowledgeable senior engineer in dnv and my mentor. Dear Yohannes I will never forget all your kindness and I wish you all the perfects in your life.

Nima Ghanemnia
27 June 2012, Stavanger

1 Comparison of tubular joint strength requirements in codes and standards (1)

*(Attention: this chapter has been mainly taken from Tubular joint strength provisions in codes and standards, HSE) (1)

1.1 Introduction

“The purpose of chapter is to present an analogy of the technical provisions concerning the static strength of tubular joints given in the following documents:

1. API RP2A WSD and LRFD
2. HSE 4th Edition Guidance Notes (GNs)
3. Draft ISO standard for fixed steel offshore structures
4. NORSOK standard for the design of steel offshore structures (1).

Generically, code provisions for the static strength of tubular joints in offshore steel structures cover the following areas:

1. Joint capacity
    a. axial and moment strength
    b. geometric effects
    c. Chord stress effects
    d. Brace load interaction
    e. validity ranges
2. Relative joint / member strength
3. Joint categorization
4. Joint detailing
5. Safety format (10).

1.2 General background (1)

1.2.1 Tubular joint strength in the design ground

Code provisions for the static strength of tubular joints in offshore structures

Basically cover the following:

1. Joint strength
    a. figure (T/Y, X/DT, K; complexe grouted, multiplanar etc.)

b. loading modes (P, Mipb, Mopb)
c. geometric factors (Qu)
d. chord stress factor(Qf)
e. brace load interactions (P-M)
f. credibility range
2. Relative joint / member strength
3. Joint grouping
4. Joint detailing
5. Safety format.

Joint capacity requirements are largely experimental given the complex interaction between shell bending and coat action which forms the basis of tubular joint capacity (2).

For complex joints and joint detailing practices for which test data are sparse, practice and engineering point of view influence the theories. Finite element analysis is being used largely in complex cases, but the data catch is limited by the difficulties related with modeling fracture failure modes. Joint configurations and provisions for relative joint and member capacities are based on rules of engineering mechanics (1).

1.2.2 Basis of equations (1)

In applying a design code or standard it is vital to respect the basis of the given equations, particularly the way uncertainty and inherent variability are derived, the case of tubular joints:

- Many tests are undertaken for the simplest joints and loading modes in different exams to determine capacity.
- The results are assembled (usually by a third party) and screened to ensure as far as possible that results are comparable and useful to offshore tubular joints.
- Best-fit relations are derived upon on measured material and geometric specifications, relating strength to non-dimensional elements. However, the information exhibit serious scatters about the mean due, for example, to differences in component testing ways, as well as to substantial mutability that may be showed within jacket structures (3).
- Design relations are developed to provide efficient assurance that the actual capacity will be larger than the nominal value assumed in design. In some cases, this may be based on a lower bound fit to the data or on a specification evaluation (i.e. mean minus N standard deviations - where N depends on the number of results available and the degree of assurance needed, say, 95% survivability with 50% assurance).
- The formulae to account for simple joint capacity are combined with allowances for chord stress effects, the combined action of different loading modes, etc., to give all-

snuggled equations for joint capacity. Few information Exist for a realistic combination of loads and geometries against which to compare the resulting calculated capacities (9).

The experimental expressions for axial capacity, P, and moment capacities, M, of tubular joints is generally fixed across all standards taking the form:

$$P = K \frac{FyT^2}{\sin\theta} Q_u Q_f$$

$$M = K \frac{FyT^2}{\sin\theta} d Q_u Q_f$$

Where:

Fy = chord yield stress

T = chord wall thickness

θ = included angle between brace and chord

d = brace diameter

Qu = geometric modifier, f (b, g, z, etc.)

Qf = chord stress modifier

β = brace diameter (d) / chord diameter (D) ratio

γ = chord slenderness (D/2T)

ζ = K joint gap (g) to chord diameter ratio (g/D)

K = constant / multiplier.

The specific formulations for Qu and Qf differ as do the forms for axial and moment interaction (2).

1.2.3 Design stages (1)

The strength relations are put into a standard checking equation to define if the load demand is less than the available strength with a good margin of safety. Working stress design (WSD) or limit state (alternatively formulated as load and resistance factors design (LRFD) approaches may be used. In traditional WSD practice the check is that:

$$\frac{nominal\_strength}{safety\_factor} \geq \sum nominal\_loads$$

Whereas for LRFD partial factors reflect the different degree of uncertainty in the different elements of loading and resistance giving:

$$resistance\_factor \times nominal\_strength \geq \sum load\_factor \times nominal\_load$$

Resistance factors are basically less than one and account for the potential variability in capacity due to substantial uncertainty in the material (thickness) and fabrication endurance in the structure (5).

Limit state approaches provide the process to design to safe target with partly factors selected accordingly. However the evaluation of standards is made to move from WSD to LRFD practices, calibrating partial factors to deliver safety levels on average equivalent to earlier WSD designs.

In the design check process, component forces or stresses are defined by linear elastic analysis methods and entered into programmed post-processors effecting the standard relations. In specific respects, the analytical assumptions differ from those underlying the relations. For example, an axially loaded T joint in the laboratory produces bending stresses in the chord but their effect is generally ignored in formulating capacity equations. Extreme fiber stresses calculated in the chord of a T joint in a jacket, however, combine the equilibrium stress with additional load effects (4).

The total is then used to assess chord stress effects. It is comfortable to extract total stresses in this way but it is not practical to re-evaluate the test data; the degree of end fixity in the test (pinned vs fixed) is generally unknown and to extract their influence would require a priori quantification of the effect on capacity.

The complexities of real jacket nodes are generally simplified to render them amenable to assessment against the empirical equations. Individual planes are extracted and assessed independently from out-of-plane influences.

The assessment is subject also to a classification of the joint action within the plane. A combined evaluation based on geometry and a conservative hierarchy of load effects is generally applied. The degree of tolerance on the classification (e.g. K joint load balanced to within ±5%, 10% etc.) varies with software package and user.

The above is by no means an exhaustive list of the steps but it serves to highlight the implicit assumptions and approximations in assessing the design requirements for tubular joints. It also presents the framework against which many of the subsequent observations in this technical note can be interpreted.

1.3 HSE 4th edition guidance notes (1)

Although the 15th Edition of RP2A represented a step change in API practice, subsequent work identified a significant body of additional test data. This was included in expanded databases which formed the basis of static strength equations in the HSE 4th Edition Guidance Notes. The additional data enabled different load and geometry effects to be distinguished giving a more 'refined' set of equations. In addition the derivation of design equations was based on a lower characteristic formulation rather than the lower bound approach in RP2A. However the overall approach for code checking was based on working stress, with characteristic capacities being reduced by a safety factor to give allowable loads.

Although the Guidance Notes were withdrawn in 1998 (for regulatory reasons rather than any specific concern over technical rigor of the tubular joint provisions), the background to the static strength guidance is openly available (8).

In BOMEL's Tubular Joints Group project, the HSE database was further expanded and re-screened and the goodness of fit of existing design equations assessed.

Focusing on the basic Qu geometric influence for different loading modes and joint types, the HSE equations represented the underlying data most consistently compared with RP2A and other Canadian, Norwegian and European practices.

Although individual equations provided a better fit to the data in certain cases a 'mix and match' selection is inappropriate. The HSE equations continue to represent the best available set of equations for assessing tubular joint capacity, until the proposed ISO equations are accepted and adopted.

A further advantage is that the background document provides the mean equations, as well as design characteristic values. The former are particularly required for the assessment of existing structures, where joints may fail to satisfy design criteria and the 'actual' capacity needs to be considered.

1.4 API RP2A (1)

The reference editions for RP2A in this study are WSD 20th Edition and LRFD 1st Edition both published in 1993. The tubular joint provisions are identical in respect of basic nominal capacities between WSD and LRFD and date from the 15th edition of WSD published in 1984.

Their introduction represented a step change in API practice. Earlier editions from the 1970s were generally based on an underestimate of capacity and had been presented in a punching shear format, which does not represent the failure mode for many tubular joints. Although improvements had been introduced as knowledge of different joint characteristics emerged, the 15th Edition brought a major overhaul of the provisions. The capacity equations are presented as a lower bound representation of the available data. In the transition from WSD to LRFD the opportunity was taken to revise the interaction formula to avoid numerical solution problems for highly utilized joints. The commentary to LRFD presents detailed discussion of the calibration process. In summary, reasonably uniform and consistent reliabilities between the WSD and LRFD versions were obtained with resistance factors of 0.95 generally and 0.9 in the specific case of tension loaded T/Y and X joints. The distinction reflects the additional uncertainty associated with crack initiation on which the tension equations are based rather than ultimate strength (4).

The API-LRFD calibration exercise also included a direct comparison of resulting interaction ratios (IRs) for specific combinations of load and resistance factors as opposed to blanket WSD safety factors. The LRFD: WSD ratio of IRs generally fell in the ±20% range but the comparison with IRs from earlier editions showed much greater variation (±60% in the extreme).

1.5 ISO 13819-2 (1)

The first edition of ISO 13819 adopts the provisions of RP2A-LRFD. The starting point for the technical core group preparing the second edition was to carry the existing recommendations forward without change unless they were shown to be inadequate. A number of factors influenced the approach. The lower bound formulation in RP2A is not consistent with the more rigorous statistical approach generally adopted for limit state codes. Work by the TJ Group as well as others had shown that the RP2A formulae did not present the best representation of newly available data. As a result more recent better formulae had been produced. The ISO technical core group therefore took these equations as the basis for the second edition of ISO 13819-2 and worked these in conjunction with other design considerations for achieving adequate static strength of tubular joints.

Development of the proposed text has been an iterative process with a number of internal drafts within the core group, some of which have formed part of consolidated drafts of the whole standard circulated for industry comment. The draft text presents design formulae and within the commentary mean bias and coefficient of variation (COV) statistics are presented enabling the formulae to be used for assessment purposes. It is understood that the chord stress parameter, Qf, is among a number of areas still under scrutiny by the ISO Technical Core Group.

1.6 NORSOK (1)

The NORSOK standard has, to a very large extent, adopted the provisions of contemporaneous drafts of the ISO standard. This would therefore lead to some differences between NORSOK and the current draft ISO, which are pointed out in the detailed comparisons below (10).

1.7 Comparison of technical provisions (1)

1.7.1 Preamble

This section compares the principal provisions of the API, withdrawn HSE, and draft ISO and NORSOK codes. Shorthand reference to 'API', 'HSE', 'ISO' and ‘NORSOK’ will be made for convenience. In addition to quantified recommendations, the reference documents provide other general guidance, but it is not practicable for every aspect to be covered here. To apply the codes, the reader must refer to the original documents. The comparison covers the aspects of tubular joint strength.

1.7.2 Axial and moment capacities (1)

All four codes adopt the basic axial and moment capacity formulations however; the expressions for Qu and Qf differ as shown below. The constant K in the moment equation is unity in HSE, ISO and NORSOK, but 0.8 in API. For the purpose of comparison the 0.8 factor is therefore combined with the API Qu values. Similarly for axial loading HSE includes a multiplier Ka (a function of brace inclination) and again this is presented with Qu.

1.7.3 Geometric effects (1)

Geometric effects are embodied in the Qu factor. Table below compares the Qu formulae presented in the four codes for each joint geometry (T/Y, DT/X, K) and loading mode (axial tension, axial compression, in-plane bending, out-of-plane bending). For the most part the expressions used by NORSOK follow those in the latest ISO, the only exception is for DT/X joints in compression, for which NORSOK follows the provisions set out in ISO Draft C. In all cases the expressions are reached as an empirical fit to the available data (a lower bound in API and statistically determined characteristics in HSE, ISO and NORSOK). Each set was derived on the basis of independent datasets and the constants differ as a result. In terms of the fundamental relationships expressed in the equations the following observations with respect to Table can be made:

- **T/Y joints in compression**. ISO and NORSOK, as HSE, identify a strength enhancement for high β joints. At low β ISO/NORSOK indicate less capacity than either API or HSE. At high β the ISO/NORSOK capacity is between API and HSE values.
- **Ÿ T/Y joints in tension.** ISO, NORSOK and API equations are based on a 'first crack' limit whereas the HSE formula relates to ultimate strength; HSE therefore indicates significantly higher capacities. ISO/NORSOK capacities are generally greater than API (for b > 0.3). At b = 1.0 the ISO/NORSOK first crack design capacity is equivalent to the ultimate strength value given in HSE.
- **Ÿ DT/X joints in compression.** The ISO formula is modified from Draft C to introduce a g influence neglected in NORSOK, API and HSE. For g » 20 the

DT joint design capacities from API, HSE, ISO and NORSOK are almost identical across a range of b. The latest ISO equations give a reduced enhancement with increasing b for low g but for high g joints the effect is stronger.DT/X joints in tension. As for T/Y joints in tension, ISO and NORSOK, as API, relate to first crack whereas HSE is based on ultimate strength therefore giving the greatest capacities. Where HSE indicated a gradual enhancement in capacity for high b by including a Qb factor, in ISO/NORSOK the influence is limited to b in the range 0.9 to 1.0 where the membrane influence becomes strongest. As for DT/X joints in compression ISO and NORSOK introduce a g influence; with high g / high b joints having greater capacity. As for T/Y joints in tension, ISO first crack capacities at b = 1.0 are comparable (depending on g) to the ultimate values given by HSE. For b < 0.9 the ISO/NORSOK capacity is somewhat lower than API.

- Ÿ **K joints axial.** ISO and NORSOK, as HSE, give a relative increase in strength for high b joints (viaQb0.5) not seen in API. At low β the ISO/NORSOK capacity is in some instances less than API depending on the gap between K joint weld toes. The gap influence is complex and is expressed differently in all four codes. ISO, NORSOK and HSE equations can be expressed in terms of the g/D ratio although the applicability for ISO/NORSOK is based on g/T. The power of the ISO/NORSOK approach is that it provides continuity between gap and overlap configurations. In API and HSE a separate formulation addressing shear at the common weld of overlapping joints is invoked.
- **Ÿ All joints IPB.** ISO and NORSOK, as HSE, includes a g influence on IPB capacity (γ 0.5) which is not included in API. Evidence for the sing influence in HSE was not found for the ISO/NORSOK equations. In general the ISO/NORSOK IPB capacities are greater than in API.
- **All joints OPB.** Where API and HSE include a β or Qβ influence on OPB capacity of a similar form, the relationship in ISO/NORSOK is quite different. Capacity relates to the γ ratio but the strength of influence varies with β (expressed as a $\beta \wedge 2$ power). Where HSE distinguished between X and Y / T /K joints, ISO/NORSOK and API, present a single equation for all joint types.

Despite the change in the formulation the capacities are reasonably similar between the four codes for moderate γ (3).

1.1 Comparison of Qu in standards

Code	T/Y Compression	T/Y Tension	DT/X Compression	DT/X Tension	K/YT Balanced axial	IPB	OPB
API-WSD & LRFD	$3.4 + 19\beta$		$(3.4 + 13\beta)Q_\beta$	$3.4 + 19\beta$	$(3.4 + 19\beta)Q_g$	$0.8(3.4 + 19\beta)$ Note a	$0.8(3.4 + 7\beta)Q_\beta$ Note a
HSE	$(2\ 20\beta +)Q_\beta^{0.5}K_a$ Note b	$(8 + 22\beta)K_a$ Note b	$(2.5 + 14\beta)Q_\beta K_a$ Note b	$(7 + 17\beta)Q_\beta K_a$ Note b	$(2 + 20\beta)Q_\beta^{0.5}Q_g K_a$ Note b	$5\beta\gamma^{0.5}\sin\theta$	$(1.6 + 7\beta)Q_\beta$ (Y/K) $(1.6 + 7\beta)Q_\beta^{0.5}$ (X)
ISO & NORSOK	$(1.9 + 19\beta)Q_\beta^{0.5}$	30β	$(2.8+X\beta)Q_\beta$ Note c	23β for $\beta \le 0.9$ else $21+(\beta-0.9)(17\gamma-220)$	$(1.9+19\beta)Q_\beta^{0.5}Q_g$ Note d	$4.5\beta\gamma^{0.5}$	$3.2\gamma^{(0.5\beta^2)}$

where $\beta = d/D$, $\gamma = D/2T$, $\zeta = g/D$, $Q_\beta = \frac{0.3}{\beta(1-0.833\beta)}$ $K_a = 0.5\,(1+\frac{1}{\sin\theta})$

and Q_g for the respective codes is given by:

API $1.8 - 0.1\frac{g}{T}$ for $\gamma \le 20$ or $1.8 - 4\frac{g}{D}$ for $\gamma > 20$ $Q_g \ge 1.0$

HSE $1.7 - 0.9\left(\frac{g}{D}\right)^{0.5}$ $Q_g \ge 1.0$

ISO & NORSOK $1.9 - 0.7\gamma^{0.5}\left(\frac{g}{T}\right)^{0.5}$ for $\frac{g}{T} \ge 2.0$ or $0.13 + 0.65\phi\gamma^{0.5}$ for $\frac{g}{T} \le -2.0$

with interpolation between for $-2.0 \le \frac{g}{T} \le 2.0$

$\phi = \frac{t F_{yb}}{T F_y}$ in which t and F_{yb} are the brace thickness and yield stress and T and F_y relate to the chord

a In API 0.8 is presented as a multiplier on moment capacity rather than an element of Q

b In HSE K_a is presented as a multiplier on axial capacity rather than an element of Q

c In ISO draft C & NORSOK expression for DT/X joints is X = 14 (ie. independent of γ); latest ISO X = (12+0.1γ) (ie. dependent on γ)

d In ISO draft C & NORSOK an additional angle capacity factor Q_ψ was included for joints where $Q_{\psi} = 1.0$, when $\theta_t \le 4\theta_c - 90°$ or $(110° + 4\theta_c - \theta_t) / 200°$ otherwise

1.7.4 Chord stress effects (1)

The chord effects are embodied in the Qf factor. The HSE and API formulations are identical on account of the limited data available to both background studies. The HSE formula is however presented in terms of forces and moments as opposed to stresses. The ISO provisions are different in a number of respects:

- The chord stress effects are independent from γ.
- The interaction is based on the comparison between factored loads and section capacities rather than stresses and yield.
- Ÿ the significance of chord forces and moments varies with joint type and loading mode in an attempt to separate the influence of equilibrium effects due to brace loading already accounted for in Qu.

- Ÿ In addition to a detrimental effect of chord compression, the Qf factor also applies for DT/X joints with $\beta > 0.9$ if chord axial tension stress is less than the combined stress due to moments.

The changes result in a significant increase in calculated capacity for high g joint with net compressive stresses in the chord.

NORSOK uses expressions from Draft C of ISO. Key aspects of the NORSOK formulation used are that:

- Ÿ the interaction is based on factored applied stresses on the action side, and yield strength and characteristic chord bending strength on the resistance side. Thus, no partial safety factors are applied to the resistance components.
- Ÿ In addition to a detrimental effect of chord compression, the Qf factor also applies for DT/X joints with b > 0.9 if chord axial tension stress is less than the combined stress due to moments.

  AS example Qf formulation in NORSOK is presented below:

  Qf is a design factor to account for the presence of factored actions in the chord.

$$Q_f = 1.0 - \lambda A^2$$

Where

λ = 0.030 for brace axial force in Equation

= 0.045 for brace in-plane bending moment in Equation

= 0.021 for brace out-of-plane bending moment in Equation

The parameter A is defined as follows:

$$A^2 = C_1\left(\frac{\sigma_{a,Sd}}{f_y}\right)^2 + C_2\left(\frac{\sigma_{my,Sd}^2 + \sigma_{mz,Sd}^2}{1.62\, f_y^2}\right)$$

Where

$\sigma_{a,Sd}$ = design axial stress in chord

$\sigma_{my,Sd}$ = design in-plane bending stress in chord

$\sigma_{mz,Sd}$ = design out-of-plane bending stress in chord

f_y = yield strength

C1, C2 = coefficients depending on joint and load type as given in Table

Joint type	C_1	C_2
T/Y under brace axial loading	25	11
X joints under brace axial loading	20	22
K joints under balanced axial loading	20	22
All joints under brace moment loading	25	30

1.2 Coefficients depending on Joint length

1.7.5 Brace Load Interaction (1)

Table below compares the interaction formulae in all four codes. It can be seen that the hyperbolic expressions have not been retained in ISO from API, and the ISO formulation is identical to HSE. The NORSOK formula, whilst different in appearance from that of ISO, is identical in format. This format is more amenable to assessment of joints in existing structures where utilization may be beyond current design capacities for which the API expressions may be insoluble. The expressions are similar, as they are intended to be, at and around full utilization of the joint. However for lower levels of load, very significant differences result on account of the different representation of non-linear interactions at failure. Utilization comparisons away from unity should therefore by viewed with caution (6).

1.7.6 Validity ranges (1)

Table 1.3 compares the validity ranges stated within the codes. Although limitations are not presented by API, the ISO, NORSOK and HSE conditions are very similar.

The significant expansion in the ISO and NORSOK codes is on yield stress extending the validity from 400 to 500 N/mm2, together with a relaxation in the restriction on yield to ultimate strength ratio (Fy:Fu). Where the yield strength of the chord was to be taken as the minimum of the nominal yield or 0.7 times the ultimate stress, Fu (0.66 in API), the ISO/NORSOK limit is 0.8 Fu, which is above the level of practical significance for most structural steels in current offshore use for fixed structures.

Code	γ	β	θ	F_y (N/mm²)
API*	10 - 50	0.2 - 1.0	30 - 90	333 - 500
HSE	9 - 50	0.15 - 1.0	30 - 90	≤ 400
ISO	10 - 50	0.2 - 1.0	30 - 90	≤ 500
NORSOK	10 - 50	0.2 - 1.0	30 - 90	≤ 500
* not specified in code but deduced from background in [9] i.e. ranges in databases stated above.				

1.3 Validity ranges in codes

$$\beta = \frac{d}{D}, \ \gamma = \frac{D}{2T}, \ \tau = \frac{t}{T}$$

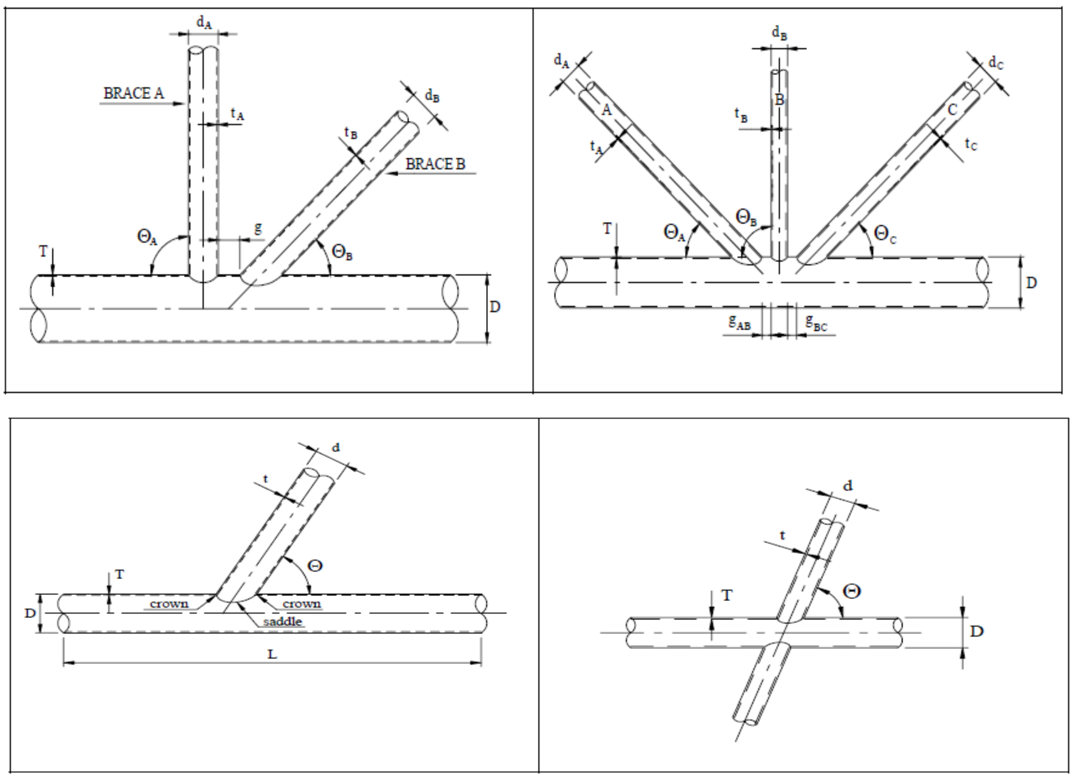

1.4 Geometrical factors in tubular joints

1.7.7 Relative joint / member strength (1)

The principal requirement is for joints to be sized to withstand the design loads.

The additional provisions regarding the relative strength of joints compared to the incoming members is different in ISO compared with API. No specific requirements were set down in the HSE Guidance Notes which did not give explicit treatment of member design. In ISO the requirement for primary or significant' joints are:

IR joint $\leq$ 85% IR brace

Whereas in API the provision is expressed as:

joint capacity $\geq$ 50% brace capacity

Or alternatively

$$\frac{F_{yb}}{F_{yc}} \frac{(\gamma \tau \sin\theta)}{\left(11+\frac{1.5}{\beta}\right)} \leq 1$$

In which Fyb, Fyc are the brace and chord yield stresses and t is the brace to chord wall thickness ratio.

ISO provisions are an attempt to ensure that joints are stronger than the adjoining braces to give adequate ductility in extreme conditions. It could be argued that this is not an appropriate strategy for assuring ductility, but accepting the premise the basis of utilization is more rational than inherent capacity. It is assumed that the 15% margin accounts for the greater variability in tubular joint strength and hence different mean bias and partial resistance factors for joint and member equations. In light of the use of modern analysis and automated code checking computer software there are difficulties associated with fulfilling this 15% criterion, however. A comparison of IRs for brace and joint would only be possible after the code checking has been completed; an impractical iteration process would be necessary in the event that the 15% margin was not achieved.

The ISO focus on primary joints means that for many secondary joints, previously governed by minimum capacity requirements, the change represents a relaxation.

However for some primary joints the effects may be significantly more onerous. The ISO commentary suggests the net impact should be negligible. The effect may be greatest in regions where fatigue considerations do not play a part in the sizing of joints.

1.7.8 Joint classification (1)

The principles in all four codes are similar in that classification should be based on a combination of geometry and axial load paths within each plane on a conservative basis. ISO and NORSOK suggest the tolerance on 'balanced' loads can be ±10%. The diagrams used to aid classification of joints are identical in NORSOK and ISO. In comparing these with the equivalent diagram in API, it is found that API covers the same examples, with one exception. ISO/NORSOK includes a DT/Y joint in which 50% of the diagonal force is balanced with a force in the vertical on the same side of the chord in a K-joint, and 50% is balanced with a force in the vertical on the opposite side of the chord in a X-joint. The diagram given in HSE differs from the rest entirely, concentrating on simple Y and X-joints, and the treatment of various K-joints depending on the degree to which the brace loads balance. Other configurations where brace members occur on opposite sides of the chord are dealt with by textual provisions (1) (4).

1.7.9 Joint detailing (1)

HSE gives general considerations for joint detailing whereas API and ISO give identical quantified recommendations on the minimum extent of chord can beyond the outermost intersection (D/4 or 300mm) and brace stub lengths (d or 600mm).

API, ISO and NORSOK also provide equations to quantify the partial effectiveness of a short chord can. For K joints, loads are generally transferred in the gap region whereas the influence of the can in resisting overall bending is more significant for Y and X joints.

In API the requirements (which apply only to X joints) take the form:

$$P_{uj} = P_1 + \frac{L}{2.5D}[P_2 - P_1] \quad \text{for } L < 2.5D$$

where P1 is the joint capacity based on the chord member thickness, T

P2 is the joint capacity based on the chord can thickness, Tc and L is the can length based on the shortest distance between the brace and can transition.

In ISO the expression applies both to X and Y joints and has been developed further to be:

$$P_{uj} = [r - (1 - r)(\frac{T}{T_c})^2] P_2$$

where $r = \frac{L}{2.5D}$ for $\beta \leq 0.9$

and $r = (4\beta - 3)\frac{L}{1.5D}$ for $\beta > 0.9$

where $r \leq 1$.

As joint capacity is proportional to T2 the ISO equation reduces to the API expression for Y joints and tension X joints for β < 0.9. However for compression X joints and all High β X and Y configurations advantage is taken of the can thickness in the γ contribution to Qu (see Table 3.1). It is not clear whether this is intentional. For high β joints the alternative formulation for r means that, because of the predominance of local membrane action, even short cans contribute to enhanced capacity.

In NORSOK the formula for Puj is the same as that for ISO. The computation of r is different, however, as follows:

$$r = \frac{L}{D} \text{ for } \beta \leq 0.9$$
$$r = \beta + (1 - \beta)(10\frac{L}{D} - 9) \text{ for } \beta > 0.9.$$

where $r \leq 1$.

1.7.10 Safety format (1)

As described in Section 2 the safety format of the WSD (HSE and API WSD) and LRFD (NORSOK, ISO and API LRFD) codes is different.

For both working stress approaches (HSE and API WSD) the allowable joint capacities compared with unfactored loads have all-encompassing safety factors of 1.7 for operating conditions and 1.28 for extreme environmental events comprising live (L), dead (D), environmental (W) load components.

$$\frac{\text{nominal\_strength}}{1.7(\text{or } 1.28)} \geq \sum L, D, W, \text{etc.}$$

In API LRFD and ISO, the format is:

$$\phi_j \times \text{nominal\_strength} \geq \sum \gamma_L L + \gamma_D D + \gamma_W W$$

Where, for API LRFD:

ϕj = 0.95 for all joints and loading modes except T/Y and DT/X joints in tension for which j = 0.9 and γL and γD equal 1.1, or 0.9 and 0.8 if lower loads are more onerous

γW = 1.35 but may vary with region, etc.

In ISO it is proposed that a uniform fj of 0.95 be adopted across all joints. Although the load factors remain to be confirmed, the CD of May 1999 indicates that:

γL and γD equal 0.9, 1.1 and 1.5, depending on which actions predominate

γW = 1.35 but may vary with region, etc. In NORSOK, the design values are obtained by dividing the characteristic values from the generalized formulae for axial and moment resistance by a material partial safety factor γM. This takes a fixed value of 1.15 in all cases (which represents a f value of 0.87).

In general terms the safety format appears as:

$$\frac{\text{characteristic\_strength}}{\gamma M} \geq \sum \gamma_f S_k$$

Where Sk are the characteristic values of action effects, and gf are the partial safety factors on actions. The latter are to follow the ISO recommendations. Thus NORSOK design strengths can potentially be 1/ (1.15 x 0.95) = 0.92 times those of ISO. The tubular joint checks are in fact expressed not in the linear form as indicated here but in the more complex P-M interaction given in Table 3.3, although the above is illustrative.

It should also be noted that the safety format also affects elements within the nominal strength calculation.

1.7.11 Conclusions (1)

1. In this technical note comparisons have been made between the following documents:

. API RP2A WSD and LRFD and

. HSE 4th edition Guidance Notes

. Draft ISO standard for fixed steel offshore structures [6]

. NORSOK standard for the design of steel offshore structures [8]

2. All four use the same basic formulae for computing the characteristic strengths in respect of axial and moment resistances. Differences do occur in the Qu (geometric) and Qf (chord effects) factors, leading to differences in the characteristic strengths calculated.

3. The NORSOK standard tends to follow the ISO document, but the older draft C version, so that differences between the two relate to the revisions made to ISO, hence in NORSOK:

. Qu - the expression for DT/X joints is taken to be independent of g

. Qf - the expression uses design axial and bending stresses in the actions components, along with characteristic yield strength and chord bending strength in the resistance components, i.e. without the partial safety factors on resistance.

4. The interaction criterion (P - M) for NORSOK takes the same format as that for ISO and HSE, which in turn is different from those used for both API codes. Where the formula used is similar, differences occur because of the differences between the safeties formats of the codes (i.e. working stress versus limit state/LRFD formats):

	In Axial Load - Bending Interaction Equation:	
Code	Applied loads factored?	Resistances factored?
API WSD	No	Yes
HSE	No	Yes
API LRFD	Yes	Yes
ISO	Yes	Yes
NORSOK	Yes	Yes

1.5 Axial Load-Bending interactions in Codes

5. In terms of safety formats, API WSD and HSE are working stress ("partial" safety factor on resistances only), whereas API LRFD, ISO and NORSOK are limit state/LRFD (partial safety factors on load and resistance)."

<table>
<tr><td></td><td colspan="2">“Partial Safety” Factors on:</td></tr>
<tr><td>Code</td><td>Actions/Loads</td><td>Resistances/Strengths</td></tr>
<tr><td>API WSD</td><td>N/A</td><td rowspan="2">Divisors: 1.7 or 1.28 depending on design condition</td></tr>
<tr><td>HSE</td><td>N/A</td></tr>
<tr><td>API LRFD</td><td>Multipliers: 0.8, 0.9, 1.1 & 1.35, depending on load type and design condition</td><td>Multiplier: 0.95</td></tr>
<tr><td>ISO</td><td rowspan="2">Multipliers: 0.9, 1.1, 1.35 & 1.5 depending on action type and design condition</td><td>Multiplier: 0.95</td></tr>
<tr><td>NORSOK</td><td>Divisor: 1.15</td></tr>
</table>

1.6 Partial Safty Factors in Standards

2 Introduction to Elastic & Plastic Analysis (11), (12)

2.1 Theory of Elasticity (11), (12)

In physics, elasticity is a physical property of materials which return to their original shape after the stress that caused their deformation is no longer applied.

Linear elasticity is the mathematical study of how solid objects deform and become internally stressed due to prescribed loading conditions. Linear elasticity models materials as continua. Linear elasticity is a simplification of the more general nonlinear theory of elasticity and is a branch of continuum mechanics. The fundamental "linearizing" assumptions of linear elasticity are:

Infinitesimal strains or "small" deformations (or strains) and linear relationships between the components of stress and strain. In addition linear elasticity is valid only for stress states that do not produce yielding. These assumptions are reasonable for many engineering materials and engineering design scenarios. Linear elasticity is therefore used extensively in structural analysis and engineering design, often with the aid of finite element analysis.

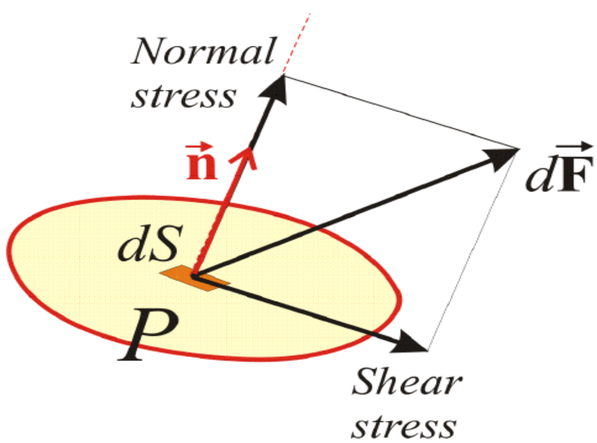

2.1 Stress definition

At point P, force dF acts on any infinitesimal area dS Stress, with respect to direction n, is a vector: lim(dF/dS) (as dS→0)

Stress is measured in [Newton/m2], or Pascal which is a unit of pressure, dF can be decomposed in two components relative to n: Parallel (normal stress) and Tangential (shear stress) Stress, in general, is a tensor: It is described in terms of 3 force components acting across each of 3 mutually orthogonal surfaces 6 independent parameters Force dF/dS depends on the orientation n, but stress does not Stress is best described by a matrix:

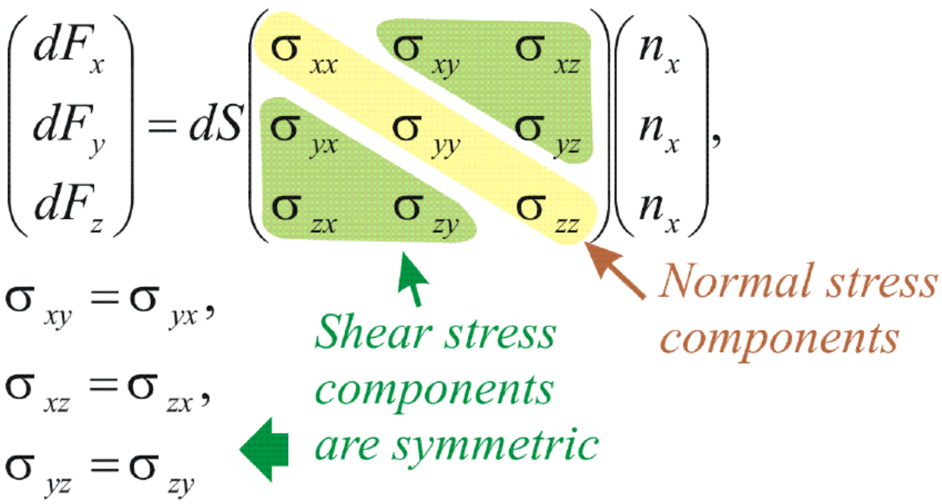

Finally, in a continuous medium, stress depends on (x,y,z,t) and thus it is a field.

Consider a small cube within the elastic body. Assume dimensions of the cube equal '1' both the forces and torque acting on the cube from the outside are balanced (12).

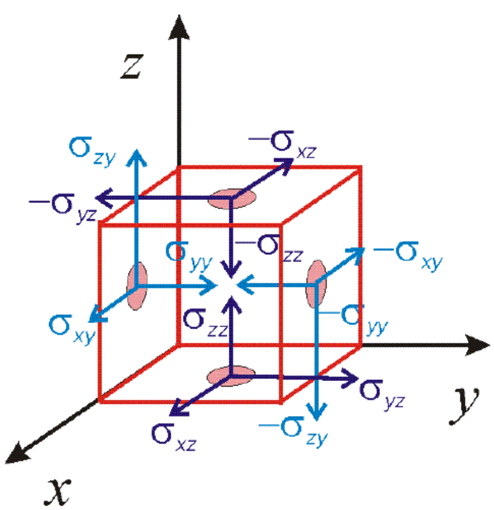

$$\begin{pmatrix} \sigma_{xx} & \sigma_{xy} & \sigma_{xz} \\ \sigma_{yx} & \sigma_{yy} & \sigma_{yz} \\ \sigma_{zx} & \sigma_{zy} & \sigma_{zz} \end{pmatrix}$$

2.2 Stress tensor

In consequence, the stress tensor is symmetric: $\sigma ij = \sigma ji$ Just 6 independent parameters out of 9 strain is a measure of deformation, i.e., variation of relative displacement as associated with a particular direction within the body It is, therefore, also a tensor represented by a matrix like stress, it is decomposed into normal and shear components Seismic waves yield strains of (10∧-10) - (10∧-6) So we rely on infinitesimal strain theory.

Elementary Strain: (12)

When a body is deformed, displacements (U) of its points are dependent on (x,y,z), and consist of:

- Translation (blue arrows below)
- Deformation (red arrows)

Elementary strain is simply:

$$e_{ij} = \frac{\partial U_i}{\partial x_j}$$

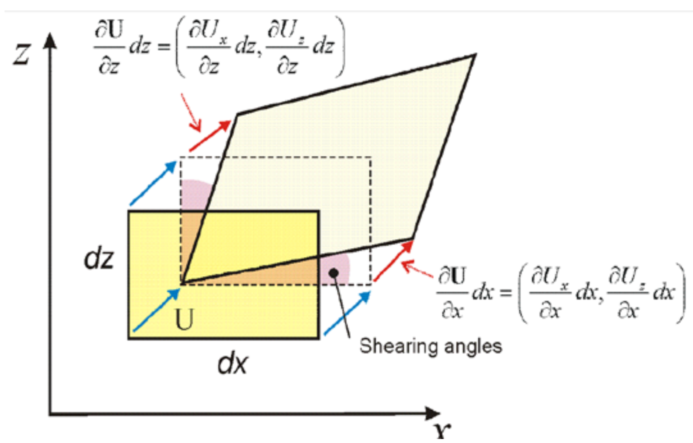

2.3 Elementry strain

Strain Components (12)

However, anti-symmetric combinations of eij above yield simple rotations of the body without changing its shape:

To characterize deformation, only the symmetric component of the elementary strain is used:

$$\varepsilon_{ij} = \frac{1}{2}\left(\frac{\partial U_i}{\partial x_j} + \frac{\partial U_j}{\partial x_i}\right),$$
$$\varepsilon_{ij} = \varepsilon_{ji}, \text{ where } i, j = x, y, \text{ or } z$$

$$\varepsilon = \begin{pmatrix} \frac{\partial U_x}{\partial x} & \frac{1}{2}\left(\frac{\partial U_x}{\partial y} + \frac{\partial U_y}{\partial x}\right) & \frac{1}{2}\left(\frac{\partial U_x}{\partial z} + \frac{\partial U_z}{\partial x}\right) \\ \frac{1}{2}\left(\frac{\partial U_y}{\partial x} + \frac{\partial U_x}{\partial y}\right) & \frac{\partial U_y}{\partial y} & \frac{1}{2}\left(\frac{\partial U_y}{\partial z} + \frac{\partial U_z}{\partial y}\right) \\ \frac{1}{2}\left(\frac{\partial U_z}{\partial x} + \frac{\partial U_x}{\partial z}\right) & \frac{1}{2}\left(\frac{\partial U_z}{\partial y} + \frac{\partial U_y}{\partial z}\right) & \frac{\partial U_z}{\partial z} \end{pmatrix}$$

Dilatational Strain (relative volume change during deformation)

Original volume: $V=\delta x\delta y\delta z$

Deformed volume:

$V+\delta V= (1+\varepsilon xx)\ (1+\varepsilon yy)\ (1+\varepsilon zz)\ \delta x\delta y\delta z$

Dilatational strain:

$$\Delta = \frac{\delta V}{V} = (1+\varepsilon_{xx})(1+\varepsilon_{yy})(1+\varepsilon_{zz}) \approx \varepsilon_{xx} + \varepsilon_{yy} + \varepsilon_{zz}$$
$$= \frac{\partial U_x}{\partial x} + \frac{\partial U_y}{\partial y} + \frac{\partial U_z}{\partial z}$$
$$= div\mathbf{U} = \nabla\mathbf{U}$$

Notice that (as expected) shearing strain does not change the volume

Hooke's Law (general) (12)

Describes the stress developed in a deformed body:

F = -kx for an ordinary spring (1-D)

$\sigma \sim \varepsilon$ (in some sense) for a '*linear*', '*elastic*' 3-D solid. This is what it means:

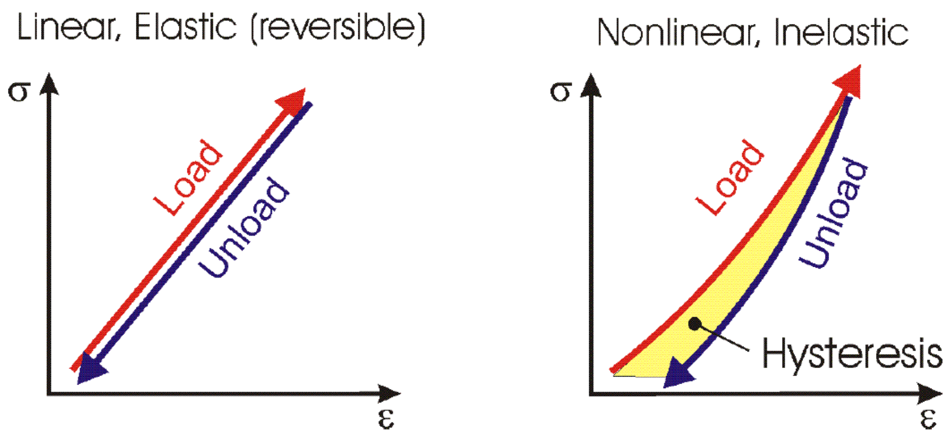

2.4 Linear & non linear Strain

For a general (anisotropic) medium, there are 36 coefficients of proportionality between six independent σ_{ij} and six ε_{ij}.

2.2 Theory of Plasticity (13)

Plastic deformation is a non-reversible process where Hooke's law is no longer valid.

One aspect of plasticity in the viewpoint of structural design is that it is concerned with predicting the maximum load, which can be applied to a body without causing excessive yielding.

Another aspect of plasticity is about the plastic forming of metals where large plastic deformation is required to change metals into desired shapes. (13), (14)

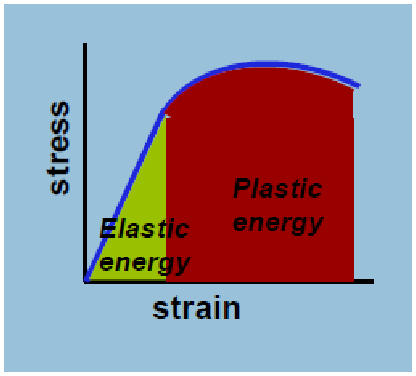

2.5 Elastic &plastic Strain Energy

True stress-strain curve for typical ductile materials, i.e., aluminum show that the stress - strain relationship follows up the Hooke's law up to the yield point, σo.

Beyond σo, the metal deforms plastically with strain-hardening. This cannot be related by any simple constant of proportionality.

If the load is released from straining up to point A, the total strain will immediately decrease from

$\varepsilon 1$ to $\varepsilon 2$. by an amount of σ/E.

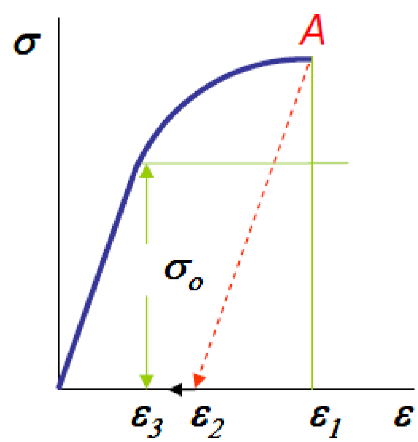

2.6 Stress-strains in plasticity

The strain $\varepsilon 1$-$\varepsilon 2$ is the recoverable elastic strain. Also there will be a small amount of the plastic strain $\varepsilon 2$-$\varepsilon 3$ known as an elastic behavior which will disappear by time. (Neglected in plasticity theories)(13) (15)

The strain $\varepsilon 1$-$\varepsilon 2$ is the recoverable elastic strain. Also there will be a small amount of the plastic strain $\varepsilon 2$-$\varepsilon 3$ known as an elastic behavior which will disappear by time. (Neglected in plasticity theories)

Usually the stress-strain curve on unloading from a plastic strain will not be exactly linear and parallel to the elastic portion of the curve.

On reloading the curve will generally bend over as the stress pass through the original value from which it was unloaded. With this little effect of unloading and loading from a plastic strain, the stress strain curve becomes a continuation of the hysteresis behavior. (But generally neglected in plasticity theories)

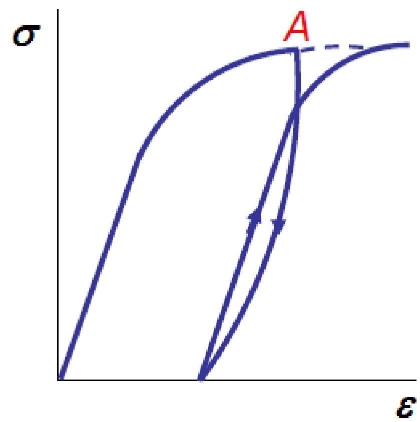

2.7 Stress-strain curve on unloading from a plastic strain

If specimen is deformed plastically beyond the yield stress in tension (+), and then in compression (-), it is found that the yield stress on reloading in compression is less than the original yield stress. (13)(14)

The dependence of the yield stress on loading path and direction is called the Bauschinger effect. (However it is neglected in plasticity theories and it is assumed that the yield stress in tension and compression are the same).

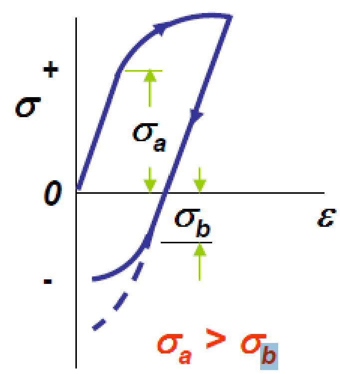

2.8 Bauschinger effect

A true stress – strain curve provides the stress required to cause the metal to flow plastically at any strain it is often called a 'flow curve'.

A mathematical equation that fit to this curve from the beginning of the plastic flow to the maximum load before necking is a power expression of the type

$$\sigma = K\varepsilon^n$$

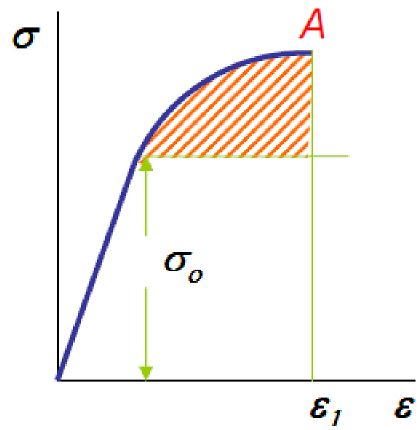

2.9 Typical true stress-strain curves for a ductile metal

Where K is the stress at ε = 1.0

n is the strain – hardening exponent

Note: higher σo will cause greater elastic region, but less ductility (less plastic region).

Idealized fllow curves (13)

Due to considerable mathematical complexity concerning the theory of plasticity, the idealized flow curves are therefore utilized to simplify the mathematics.

1) Rigid ideal plastic material: no elastic strain, no strain hardening.

2) Perfectly plastic material with an elastic region, i.e., plain carbon steel.

3) Piecewise linear (strain-hardening material): with elastic region and strain hardening region more realistic approach but complicated mathematics.

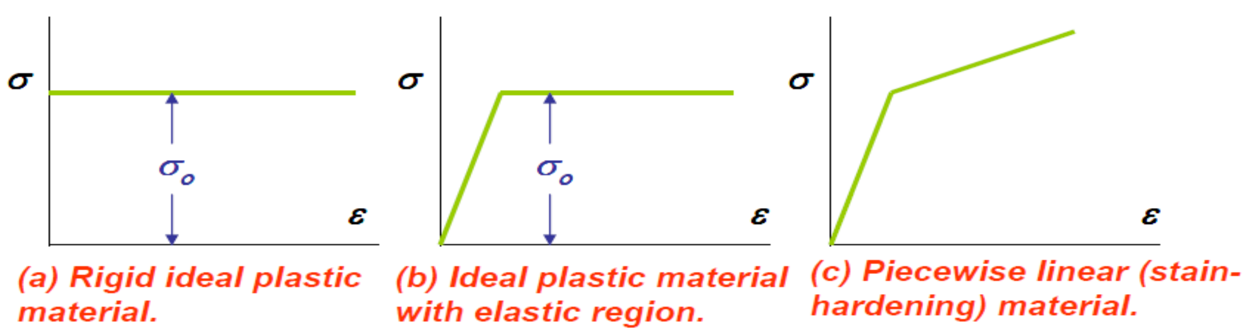

2.10 Rigid, ideal and piecewise plastic materials

True stress and true strain (13) (15)

The engineering stress – strain curve is based entirely on the original dimensions of the specimen therefore this cannot represent true deformation characteristic of the material.

The true stress – strain curve is based on the instantaneous specimen dimensions.

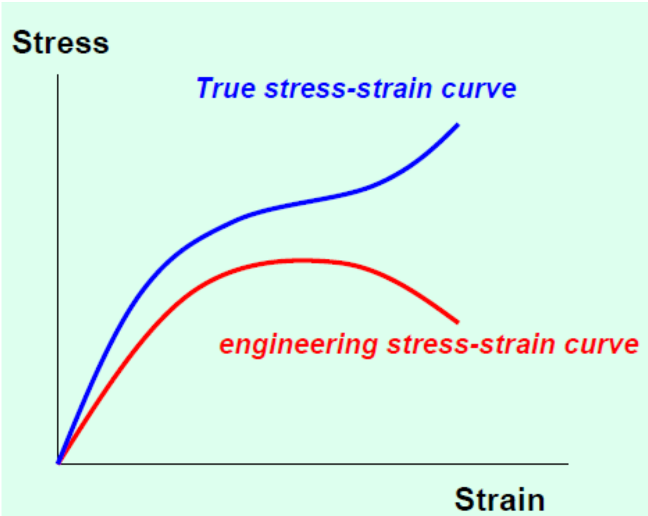

2.11 Engineering stress-strain and true stress-strain curves

The true strain (13)

According to the concept of unit linear strain,

$$e = \frac{\Delta L}{L_o} = \frac{1}{L_o}\int_{L_o}^{L} dL$$

This satisfies for elastic strain where Delta L is very small, but not for plastic strain.

Definition: true strain or natural strain (first proposed by Ludwik) is the change in length referred to the instantaneous gauge length.

Hence the relationship between the true strain and the conventional linear strain becomes

$$\varepsilon = \sum \frac{L_1 - L_o}{L_o} + \frac{L_2 - L_1}{L_1} + \frac{L_3 - L_2}{L_2} + \ldots$$

$$\varepsilon = \int_{L_o}^{L} \frac{dL}{L} = \ln \frac{L}{L_o}$$

$$e = \frac{\Delta L}{L_o} = \frac{L - L_o}{L_o} = \frac{L}{L_o} - 1$$

$$e + 1 = \frac{L}{L_o}$$

$$\varepsilon = \ln \frac{L}{L_o} = \ln(e+1)$$

The volume strain (13)

According to the volume strain

$$\Delta = \frac{\Delta V}{V} = \frac{(1+e_x)(1+e_y)(1+e_z)d_x d_y d_z - d_x d_y d_z}{d_x d_y d_z}$$

$$\Delta = (1+e_x)(1+e_y)(1+e_z) - 1$$

During plastic deformation, it is considered that the volume of a solid remain constant

$$\Delta + 1 = (1+e_x)(1+e_y)(1+e_z)$$

$$\ln 1 = 0 = \ln(1+e_x) + \ln(1+e_y) + \ln(1+e_z)$$

But εx = ln (1+ex), hence

$$\varepsilon_x + \varepsilon_y + \varepsilon_z = \varepsilon_1 + \varepsilon_2 + \varepsilon_3 = 0$$

Due to the constant volume AoLo = AL, therefore…

$$\varepsilon = \ln \frac{L}{L_o} = \ln \frac{A_o}{A}$$

<u>The true stress (13)</u>

Definition: the true stress is the load divided by the instantaneous area.

True stress: $\sigma = \frac{P}{A}$ Engineering stress: $s = \frac{P}{A_o}$

Relationship between the true stress and the engineering stress

Since: $\sigma = \frac{P}{A} = \frac{P}{A_o}\frac{A_o}{A}$

But

$$\frac{A_o}{A} = \frac{L}{L_o} = e + 1$$

$$\sigma = \frac{P}{A_o}(e+1) = s(e+1)$$

Example: A tensile specimen with a 12 mm initial diameter and 50 mm gauge length reaches maximum load at 90 kN and fractures at 70 kN. The maximum diameter at fracture is 10 mm.

Determine engineering stress at maximum load (the ultimate tensile strength), true fracture stress, and true strain at fracture and engineering strain at fracture

Engineering stress at maximum load:

$$\frac{P_{\max}}{A_{\max}} = \frac{90 \times 10^3}{\pi(12 \times 10^{-3})^2 / 4} = 796 \quad MPa$$

True fracture stress:

$$\frac{P_f}{A_f} = \frac{70 \times 10^3}{\pi(10 \times 10^{-3}) / 4} = 891 \quad MPa$$

True strain at fracture:

$$\varepsilon_f = \ln\frac{A_o}{A_f} = \ln\left(\frac{12}{10}\right)^2 = 2\ln 1.2 = 0.365$$

Engineering strain at fracture:

$$e_f = \exp(\varepsilon) - 1 = \exp(0.365) - 1 = 0.44$$

Yielding criteria for ductile metals (13) (15)

Plastic yielding of the material subjected to any external forces is of considerable importance in the field of plasticity. For predicting the onset of yielding in ductile material, there are at present two generally accepted criteria,

1) Von Misses' or Distortion-energy criterion

2) Tresca or Maximum shear stress criterion

Von Misses criterion (13)

Von Misses proposed that yielding occur when the second invariant of the stress deviator J2 > critical value k2.

$$\left[(\sigma_1 - \sigma_2)^2 + (\sigma_2 - \sigma_3)^2 + (\sigma_3 - \sigma_1)^2\right] = 6k^2$$

For yielding in uniaxial tension, σ1 = σo , σ2 = σ3 = 0

$$2\sigma_o^2 = 6k^2, then\ k = \frac{\sigma_o}{\sqrt{3}}$$

Substituting k from Eq.14 in Eq.13, we then have the von Misses' yield criterion

$$\left[(\sigma_1 - \sigma_2)^2 + (\sigma_2 - \sigma_3)^2 + (\sigma_3 - \sigma_1)^2\right]^{\frac{1}{2}} = \sqrt{2}\sigma_o$$

In pure shear, to evaluate the constant k, note σ1 = σ3 = τy, σ2 = 0,

Where σo is the yield stress; when yields: τy 2+τy 2+4τy 2 = 6k2 then k = τy

$$\tau_y = 0.577\sigma_o$$

Example: Stress analysis of a spacecraft structural member gives the state of stress shown below. If the part is made from 7075-T6 aluminum alloy with σo = 500 MPa, will it exhibit yielding? If not, what is the safety factor?

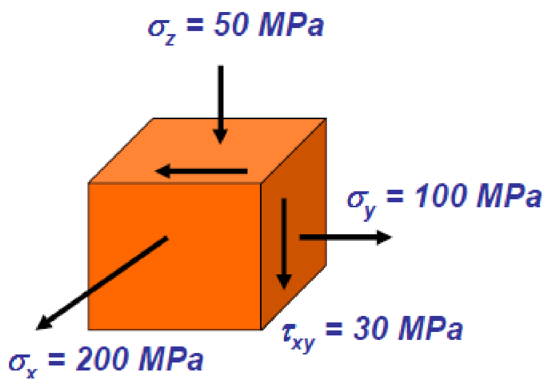

$$\sigma_o = \frac{1}{\sqrt{2}}\left[(\sigma_x - \sigma_y)^2 + (\sigma_y - \sigma_z)^2 + (\sigma_z - \sigma_x)^2 + 6(\tau_{xy}^2 + \tau_{yz}^2 + \tau_{xz}^2)\right]^{1/2}$$

$$\sigma_o = \frac{1}{\sqrt{2}}\left[(200 - 100)^2 + (100 - (-50))^2 + (-50 - 200)^2 + 6(30)^2\right]^{1/2}$$

$$\sigma_o = 224 \quad MPa$$

The calculated σo = 224 MPa < the yield stress (500 MPa), therefore yielding will not occur.

Safety factor = 500/224 = 2.2.

Tresca yield criterion (13)

Yielding occurs when the maximum shear stress τmax reaches the value of the shear stress in the uniaxial-tension test, τo.

$$\tau_{\max} = \frac{\sigma_1 - \sigma_3}{2}$$

Where σ1 is the algebraically largest and σ3 is the algebraically smallest principal stress.

For uniaxial tension, σ1 = σo, σ2 = σ3 = 0, and the shearing yield stress τo = σo/2.

$$\tau_{max} = \frac{\sigma_1 - \sigma_3}{2} = \tau_o = \frac{\sigma_o}{2}$$

Therefore the maximum – shear stress criterion is given by:

$$\sigma_1 - \sigma_3 = \sigma_o$$

In pure shear, σ1 = -σ3 = k, σ2 = 0, τmax = τy

$$\tau_y = 0.5\sigma_o$$

Example: Use the maximum-shear-stress criterion to establish whether yielding will occur for the stress state shown in the previous example.

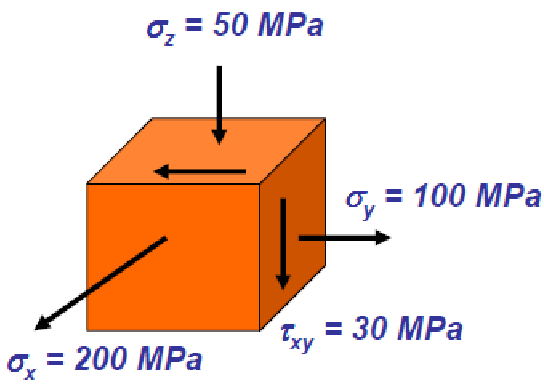

$$\tau_{max} = \frac{\sigma_x - \sigma_z}{2} = \frac{\sigma_o}{2}$$

$$200 - (-50) = \sigma_o$$

$$\sigma_o = 250 \quad MPa$$

The calculated value of σo is less than the yield stress (500 MPa), therefore yielding will not occur.

Summation (13)

1) Von Misses' yield criterion

Yielding is based on differences of normal stress, but independent of hydrostatic stress. Complicated mathematical equations used in most theoretical work.

$$\tau_y = 0.577\sigma_o$$

2) Tresca yield criterion

Less complicated mathematical equation used in engineering design.

$$\tau_y = 0.5\sigma_o$$

Combined stress tests (13)

In a thin-wall tube, states of stress are various combinations of uniaxial and torsion with maybe a hydrostatic pressure being introduced to produce a circumferential hoop stress in the tube.

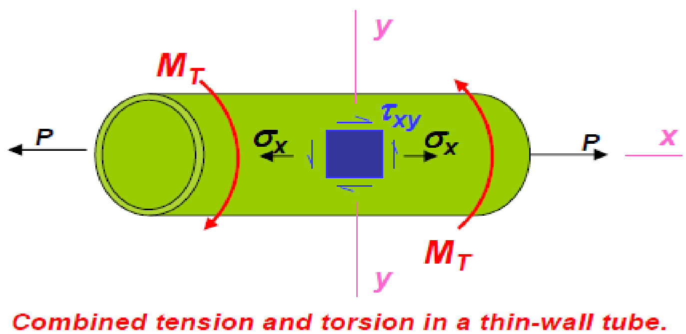

2.12 Combined tension and torsion in a thin-wall tube

In a thin wall, σ1 = -σ3, σ2 = 0 the maximum shear-stress criterion of yielding in the thin wall tube is given by:

$$\left(\frac{\sigma_x}{\sigma_o}\right)^2 + 4\left(\frac{\tau_{xy}}{\sigma_o}\right)^2 = 1$$

The distortion-energy theory of yielding is expressed by:

$$\left(\frac{\sigma_x}{\sigma_o}\right)^2 + 3\left(\frac{\tau_{xy}}{\sigma_o}\right)^2 = 1$$

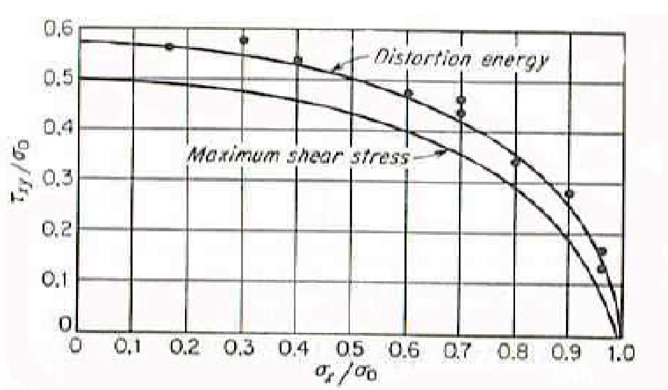

2.13 Comparison between maximum-shear-stress theory and distortion-energy (von Mises') theory

The yield locus (13) (15)

For a biaxial plane-stress condition (σ2 = 0) the von-Misses' yield criterion can be expressed as

$$\sigma_1^2 + \sigma_3^2 - \sigma_1\sigma_3 = \sigma_o^2$$

The equation is an ellipse type with -major semi axis $\sqrt{2}\sigma_o$

- Minor semi axis $\sqrt{\frac{2}{3}}\sigma_o$

The yield locus for the maximum shear stress criterion falls inside the von Misses' yield ellipse.

The yield stress predicted by the von Misses' criterion is 15.5% > than the yield stress predicted by the maximum-shear-stress criterion.

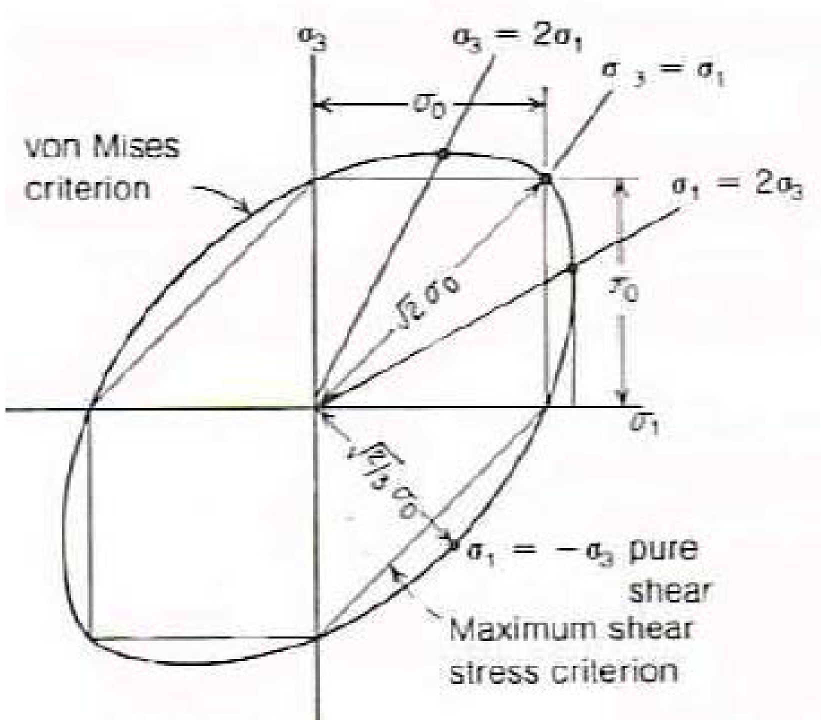

2.14 The yield stress predicted by the von Misses' criterion

2.3 Romberg Osgood Relationship (16)

The Romberg–Osgood equation was created to describe the nonlinear relationship between stress and strain—that is, the stress–strain curve—in materials near their yield points. It is especially useful for metals that harden with plastic deformation (see strain hardening), showing a smooth elastic-plastic transition. In its original form, the equation for strain (deformation) is:

$$\epsilon = \frac{\sigma}{E} + K\left(\frac{\sigma}{E}\right)^n$$

Where

ϵ is strain,

σ is stress,

E is Young's modulus, and

K and n are constants that depend on the material being considered

The first term on the right side, σ/E, is equal to the elastic part of the strain, while the second term, $K(\sigma/E)^n$, accounts for the plastic part, the parameters K and n describing the hardening behavior of the material. Introducing the yield strength of the material, σ_0, and defining a new parameter, α, related to K as

$\alpha = K(\sigma_0/E)^{n-1}$, it is convenient to rewrite the term on the extreme right side as follows:

$$K\left(\frac{\sigma}{E}\right)^n = \alpha\frac{\sigma_0}{E}\left(\frac{\sigma}{\sigma_0}\right)^n$$

Replacing in the first expression, the Romberg–Osgood equation can be written as

$$\epsilon = \frac{\sigma}{E} + \alpha\frac{\sigma_0}{E}\left(\frac{\sigma}{\sigma_0}\right)^n$$

Hardening behavior and yield offset (16)

In the last form of the Romberg–Osgood model, the hardening behavior of the material depends on the material constants α and n. Due to the power-law relationship between stress and plastic strain, the Romberg–Osgood model implies that plastic strain is present even for very low levels of stress. Nevertheless, for low applied stresses and for the commonly used values of the material constants α and n, the plastic strain remains negligible compared to the elastic strain. On the other hand, for stress levels higher than σ_0, plastic strain becomes progressively larger than elastic strain.

The value $\alpha\frac{\sigma_0}{E}$ can be seen as a yield offset, as shown in figure 1. This comes from the fact that $\epsilon = (1+\alpha)\sigma_0/E$, when $\sigma = \sigma_0$.

Accordingly (see Figure):

Elastic strain at yield = σ_0/E
Plastic strain at yield = $\alpha(\sigma_0/E)$= yield offset

Commonly used values for n are ~5 or greater, although more precise values are usually obtained by fitting of tensile (or compressive) experimental data. Values for α can also be found by means of fitting to experimental data, although for some materials, it can be fixed in order to have the yield offset equal to the accepted value of strain of 0.2%, which means:

$$\alpha\frac{\sigma_0}{E} = 0{,}002$$

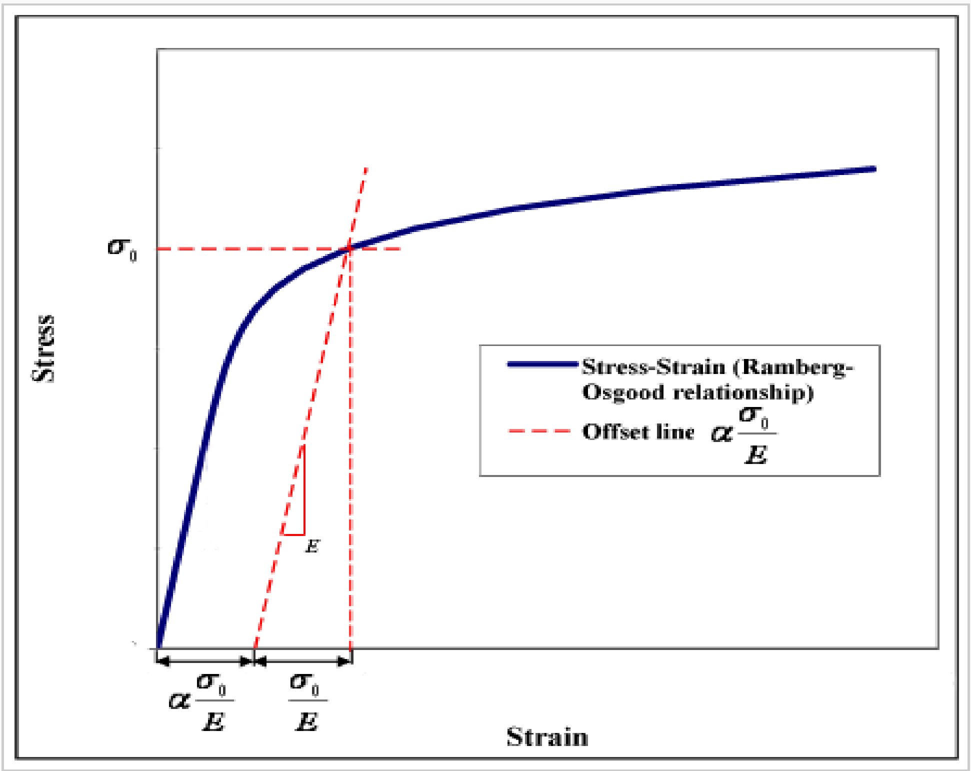

Generic representation of the Stress-Strain curve by means of the Ramberg–Osgood equation. Strain corresponding to the yield point is the sum of the elastic and plastic components.

<u>**2.15 Stress-strains, Romberg-Osgood**</u>

3 Model Description & Elastic Analysis by ABAQUS

3.1 Introduction and methodology

Here in this chapter we are trying to perform two main kind of analysis in one special case; we will select X joint with specific geometrical data from a jacket,

First of all according to capacity formulations (For X joint) which is mentioned in NORSOK N-004 we derive loads related to first crack due to the geometry of the joint and we are going to apply them to the joint.

We want to perform two kinds of analysis on it, linear finite element analysis & non linear finite element analysis. In this way we will use powerful FE software called ABAQUS. In the meantime we will do some studies about different meshing techniques and element types and their effect on FE analysis results. Trying to find out an optimum way of meshing is a main target of these studies.

3.2 General

The jacket is standing in the North Sea. The jacket is relatively tall and slender, and the lift weight was close to the capacity of the available heavy lift crane vessels. Structural design and weight optimization were therefore important.

3.1 Jacket

An X joint has been selected from a jacket to be analyzed.

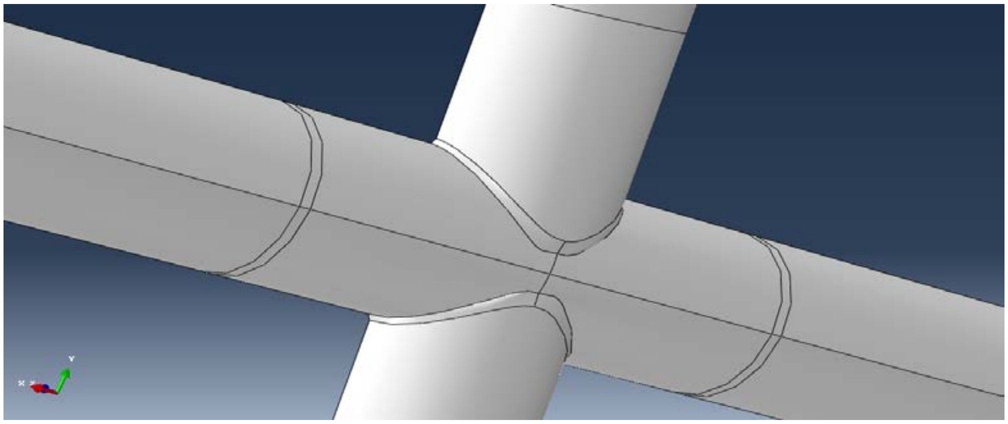

3.2 Typical X joint

3.3 Geometry of analysis model

X joint at level of -23 with following dimensions is presented:

Geometrical Data		
Brace Diameter	d [mm]	900
Chord/can Diameter	D [mm]	900
Brace wall thickness	t [mm]	35
Chord wall thickness	Tn [mm]	32
Angle bn chord and brace	q [deg]	84.6
Can wall thickness	Tc [mm]	45
Effective Can Length	Lc [mm]	2400
Diameter ratio	b	1
Diameter-thickness ratio	g	10.00
Thickness ratio	t	0.777778
Geometric factor	Q_b	1.796
Strength facto	Q_u	16

3.3 Geometrical characteristics of the selected joint

3.4 Material properties

The steel is modeled as a linear isotropic material with the following properties:

• Density: 7850 kg/m3

• Elastic modulus: 2.1x1011 N/m2

• Poisson ratio: 0.3

• Material factor: ALS: 1.0

Minimum yield and ultimate tensile strength for steel grade I and VI and castings are given in below.

3.4 Mechanical steel properties

Mechanical steel properties (MPa)

	Thickness (mm)	Cast	Grade I	Grade VI
Yield	< 16	-	340	235
	17 – 40	310	340	235
	41-63	310	325	215
	64-100	310	310	-
Tensile	Min	450	460	360
	Max		610	460

3.5 Modeling and Analysis with ABAQUS

In this chapter we are aiming to model and analyses selected tubular joint from mentioned jackets, geometrical characteristics and jacket information have been provided in pervious chapter. Finite element software which we have used is ABAQUS.

3.5.1 General introduction about ABAQUS cae

Abacus FEA (formerly ABAQUS) is a suite of software applications for finite element analysis and computer-aided engineering, originally released in 1978. The name and logo of this software is derived from abacus and the Greek word, “abax” (ἄβαξ), meaning “board covered with sand” [citation needed]. The Abaqus product suite consists of four core software products

1) Abaqus/CAE, or "Complete Abaqus Environment” (an acronym with an obvious root in Computer-Aided Engineering [7]) It is a software application used for both the modeling and analysis of mechanical components and assemblies (pre-processing) and visualizing

the finite element analysis result. A subset of Abaqus/CAE including only the post-processing module can be launched independently in the Abaqus/Viewer product.

2) Abaqus/CFD, a Computational Fluid Dynamics software application which is new to Abaqus 6.10
3) nAbaqus/Standard, a general-purpose Finite-Element analyzer that employs implicit integration scheme (traditional).
4) Abaqus/Explicit, a special-purpose Finite-Element analyzer that employs explicit integration scheme to solve highly nonlinear systems with many complex contacts under transient loads.

The Abaqus products use the open-source scripting language Python for scripting and customization. Abaqus/CAE uses the fox-toolkit for GUI development.

3.5.1.1 Abaqus Applications

Abaqus is used in the automotive, aerospace, and industrial products industries. The product is popular with academic and research institutions due to the wide material modeling capability, and the program's ability to be customized. Abaqus also provides a good collection of multiphasic capabilities, such as coupled acoustic-structural, piezoelectric, and structural-pore capabilities, making it attractive for production-level simulations where multiple fields need to be coupled.

Abaqus was initially designed to address non-linear physical behavior; as a result, the package has an extensive range of material models such as elastomeric (rubberlike) material capabilities.

3.5.1.2 Solution Sequence

Every complete finite-element analysis consists of 3 separate stages:

Pre-processing or modeling: This stage involves creating an input file which contains an engineer's design for a finite-element analyzer (also called "solver").

Processing or finite element analysis: This stage produces an output visual file.

Post-processing or generating report, image, animation, etc. from the output file: This stage is a visual rendering stage.

Abaqus/CAE is capable of pre-processing, post-processing, and monitoring the processing stage of the solver; however, the first stage can also be done by other compatible CAD software, or even a text editor. Abaqus/Standard, Abaqus/Explicit or Abaqus/CFD is capable of accomplishing the processing stage. Dassault Systems also produces Abaqus for CATIA for adding advanced processing and post processing stages to a pre-processor like CATIA.

As it is shown in the picture, Abacus cae has 11 modules which will be used one after the other in order to modeling, loading, defining boundary conditions and finally analysis and after that showing the results, diagrams and etc…

These 11 modules are: Part-Property-Assembely-Step-Intreaction-Load-Mesh-Optimization-Job-Vizualation-Sketch

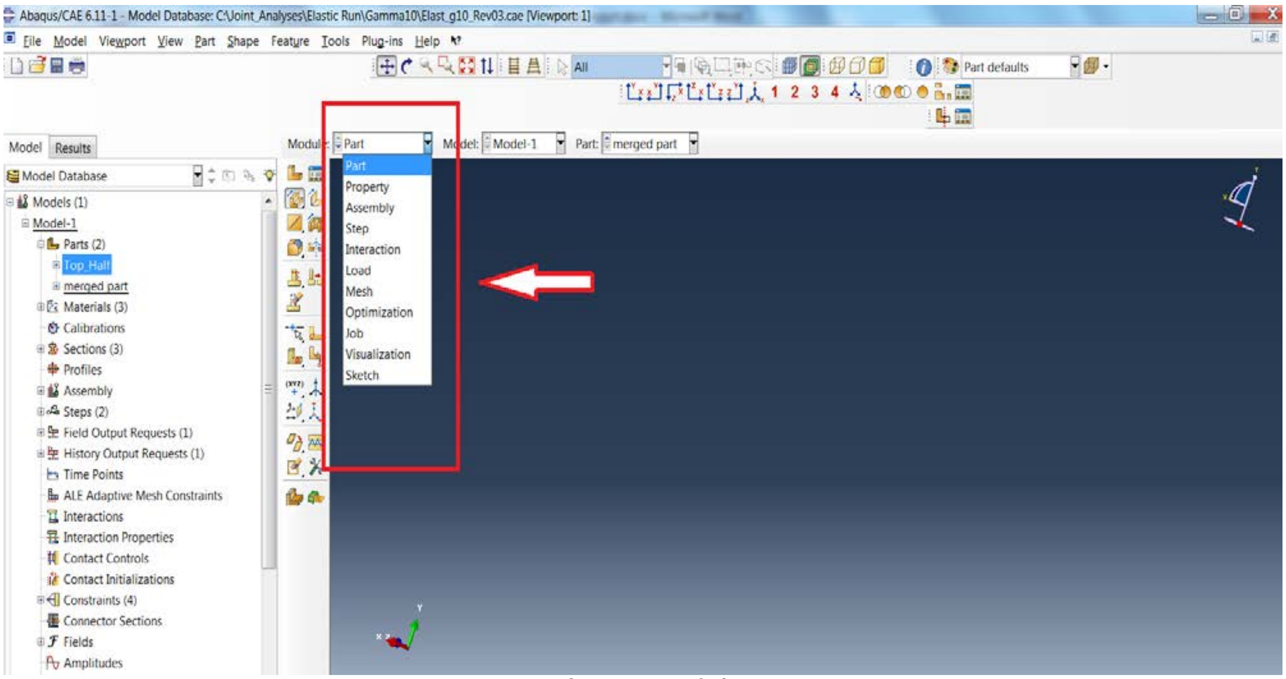

3.5 Abaqus Modules

3.6 Elastic Model

Due to symmetry in geometry and loading, only half of the joint will be modeled.

3.6.1 Geometry

The geometrical characteristics of the selected joint are provided below.

Part Module in Abaqus is dedicated part for drawing and creating the model geometry. Lots of drawing tool and techniques are available to create simplest and also most complex geometrical models.Mainly there are 3 general techniques for drawing a model.

1) Extrusion
2) Revolution
3) Sweep

Geometrical Data		
Brace Diameter	d [mm]	900
Chord/can Diameter	D [mm]	900
Brace wall thickness	t [mm]	35
Chord wall thickness	Tn [mm]	32
Angle bn chord and brace	q [deg]	84.6
Can wall thickness	Tc [mm]	45
Effective Can Length	Lc [mm]	2400
Diameter ratio	b	1
Diameter-thickness ratio	g	10.00
Thickness ratio	t	0.777778
Geometric factor	Q_b	1.796
Strength facto	Q_u	16

3.6 Geometrical characteristics of selected joint

As it is shown in the pictures at first step geometrical model of the joint with mentioned dimensions are created. All welled parts are also included in appropriate place.

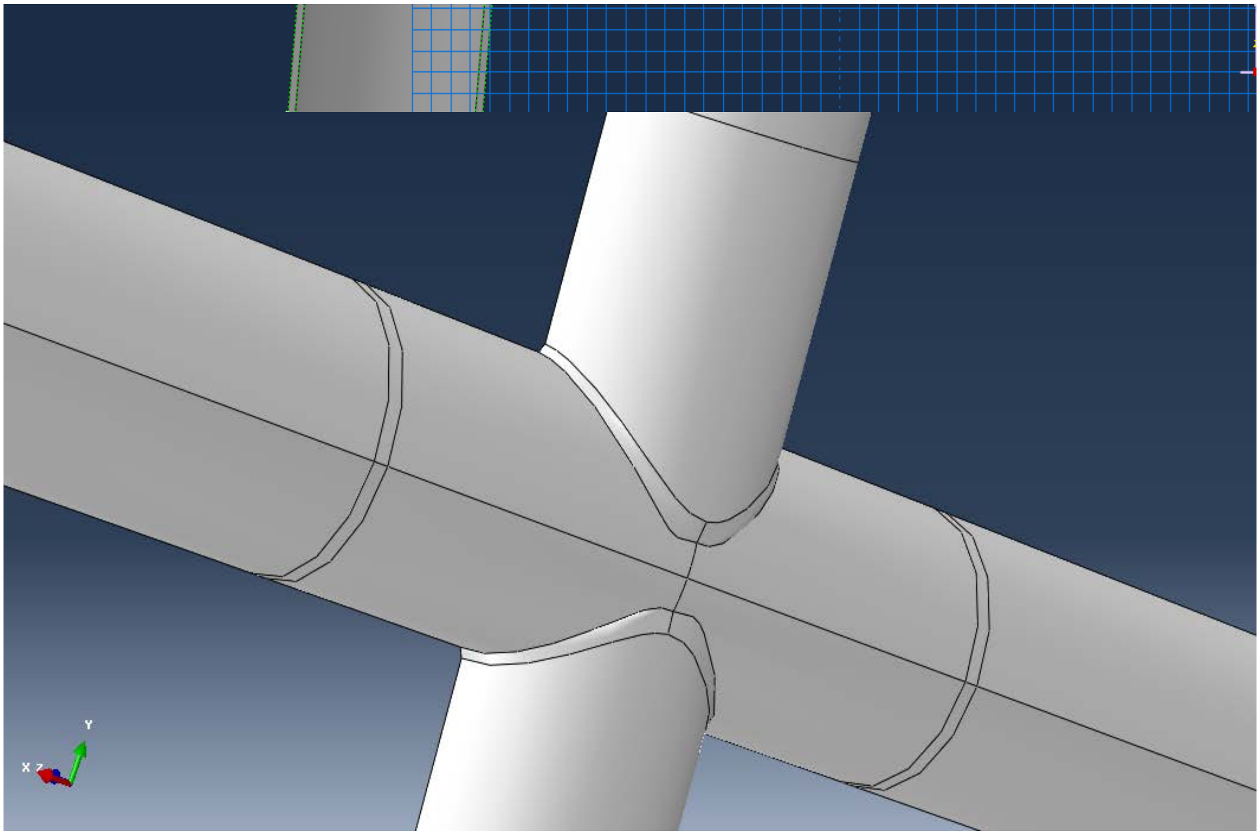

3.7 Snap shot from part module in abaqus

3.8 Snap shot from modul in abaqus

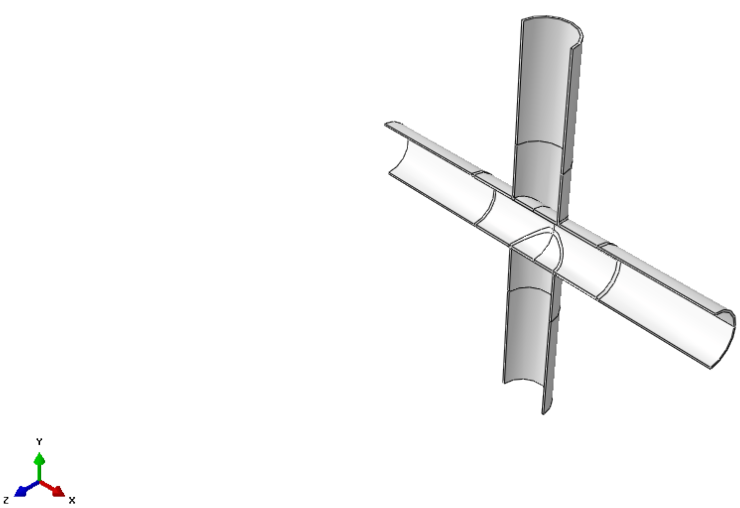

3.9 Final created model

3.6.2 Material Data

Property module is a part which we should define the material properties, since in this step we just want to perform an elastic analyses therefore the defined material are elastic material.

The FEM-material has following properties:

- Density, $\rho = 7850\ kg/m^3$
- Young's Modulus, $E = 210000\ MPa$
- Poisson's ratio, $\upsilon = 0.3$

After defining the material property and creating a section with that specific material we assign that section to whole the joint because as mentioned before it is going to be just elastic analysis in this step.

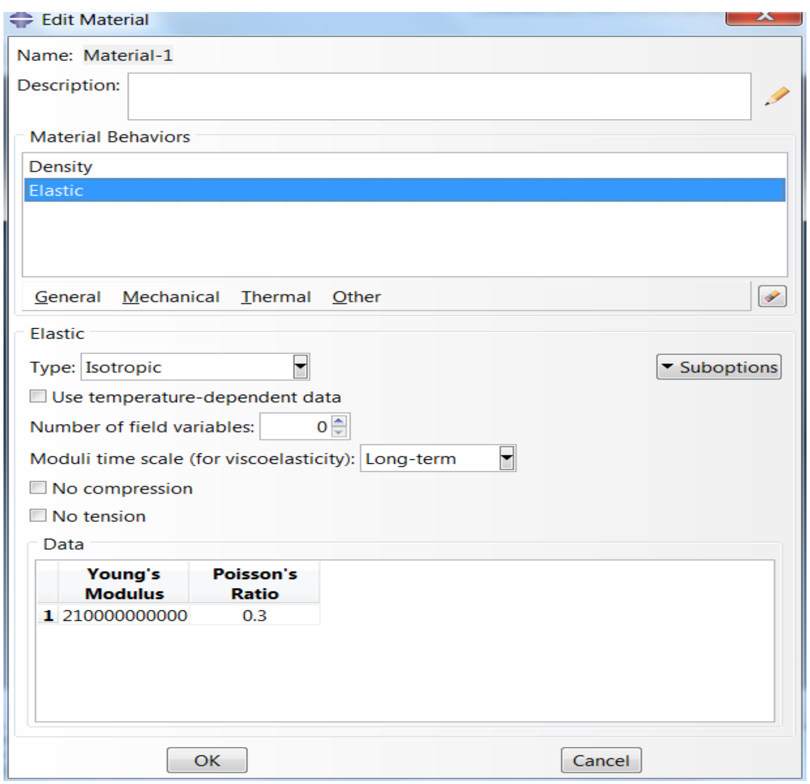

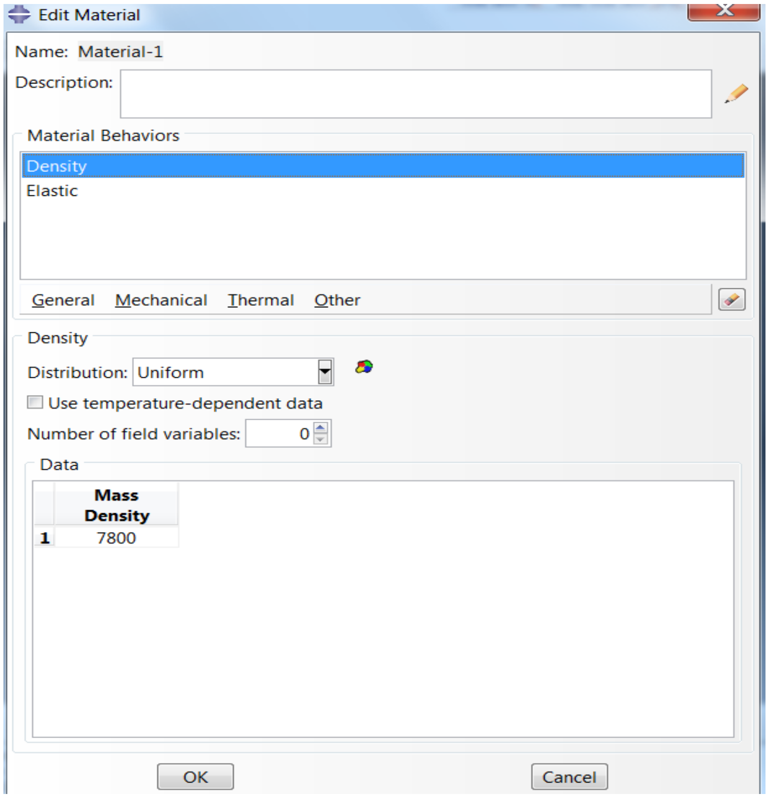

3.10 Material defining in abaqus

3.6.3 Element Mesh (17)

In this step we assign appropriate element nodes for finite element analysis.
There some different techniques and element types for meshing.
Some common techniques in ABAQUS are listed below:

1) Structured
2) Sweep
3) Bottom up

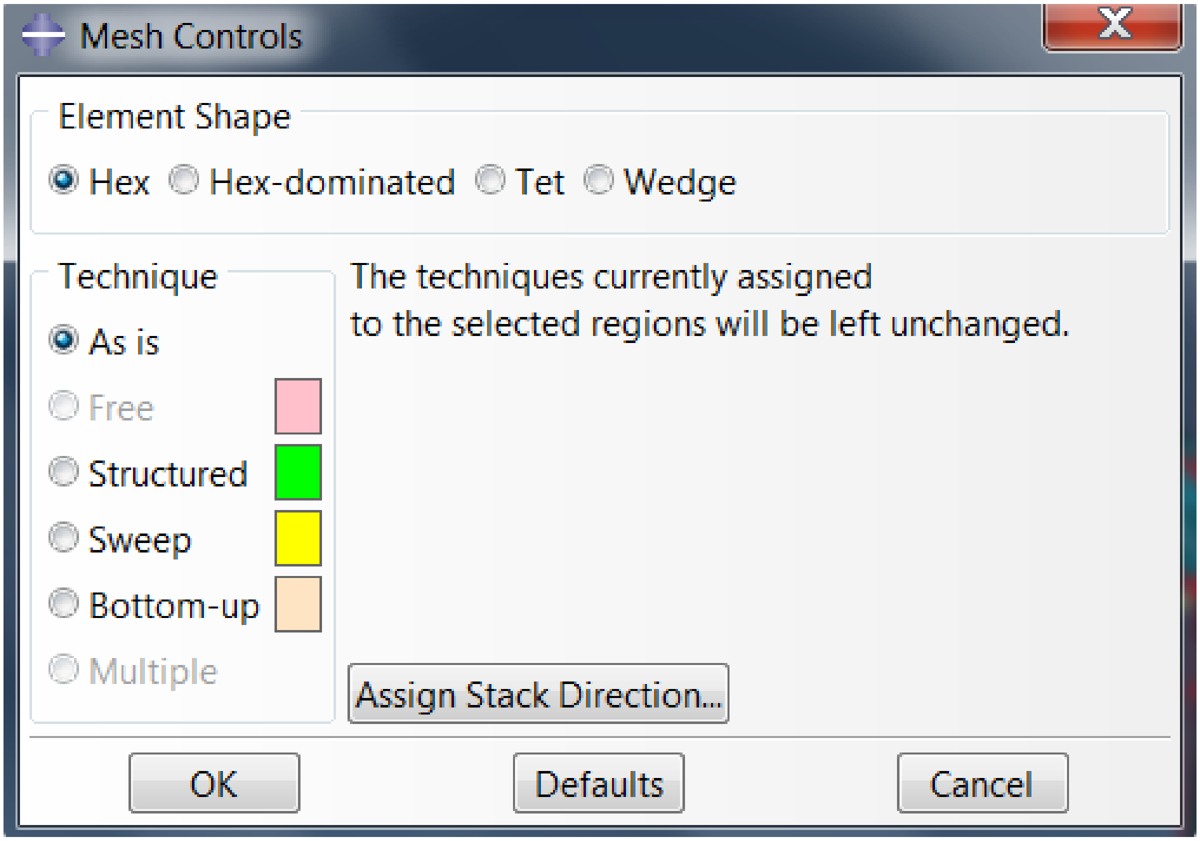

3.11 Mesh control in abaqus

Structured method: (17)

The structured meshing technique generates structured meshes using simple predefined mesh topologies. Abaqus/CAE transforms

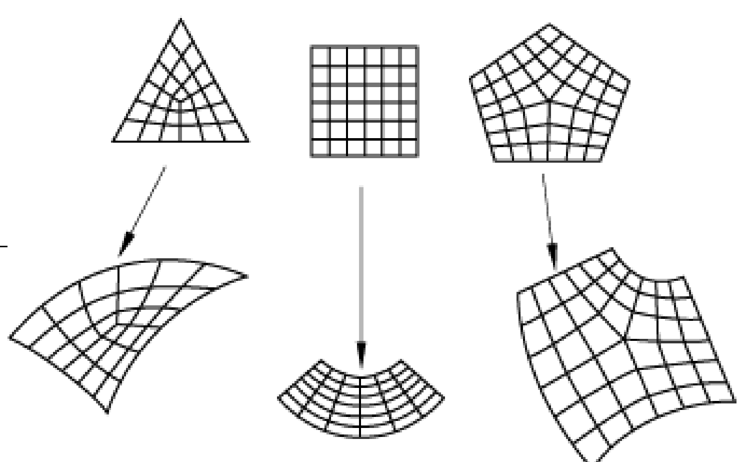

the mesh of a regularly shaped region, such as a square or a cube, onto the geometry of the region you want to mesh. For example, these illustrated figures show simple mesh patterns for triangles, squares, and pentagons are applied to more complex shapes.

3.12 Structured meshing method

Sweep method (17)

Abaqus/CAE uses swept meshing to mesh complex solid and surface regions. The swept meshing technique involves two phases:

Abaqus/CAE creates a mesh on one side of the region, known as the source side. Abaqus/CAE copies the nodes of that mesh, one element layer at a time, until the final side, known as the target side, is reached. Abaqus/CAE copies the nodes along an edge, and this edge is called the sweep path. The sweep path can be any type of edge—a straight edge, a circular edge, or a spline. If the sweep path is a straight edge or a spline, the resulting mesh is called an extruded swept mesh. If the sweep path is a circular edge, the resulting mesh is called a revolved swept mesh.

For example, this figure shows an extruded swept mesh. To mesh this model, Abaqus/CAE first creates a two-dimensional mesh on the source side of the model. Next, each of the nodes in the two-dimensional mesh is copied along a straight edge to every layer until the target side is reached.

Figure bellow shows the swept meshing technique for an extruded solid:

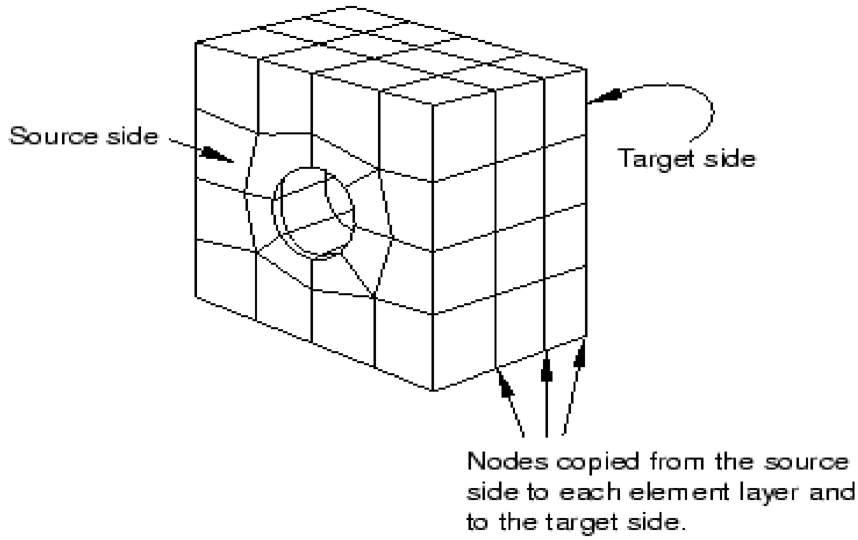

3.13 Sweep method

To determine if a region is swept meshable, Abaqus/CAE tests if the region can be replicated by sweeping a source side along a sweep path to a target side. In general, Abaqus/CAE selects the most complex side (for example, the side that has an isolated edge or vertex) to be the source side. In some cases you can use the mesh controls to select the sweep path. If some regions of a model are too complex to be swept meshed, Abaqus/CAE asks if you want to remove these regions from your selection before it generates a swept mesh on the remaining regions. You can use the free meshing technique to mesh the complex regions, or you can partition the regions into simplified geometry that can be structured or swept meshed.

When you assign mesh controls to a region, Abaqus/CAE indicates the direction of the sweep path and allows you to control the direction. If the region can be swept in more than one direction, Abaqus/CAE may generate a very different two-dimensional mesh on the faces that it can select as the source side. As a result, the direction of the sweep path can influence the uniformity of the resulting three-dimensional swept mesh, as shown in this Figure

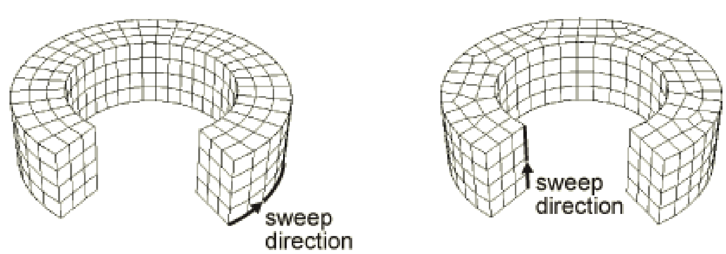

3.14 Sweep method

Bottom up Method (17)

Bottom-up meshing is a manual, incremental meshing process that allows you to build a hexahedral mesh in any solid region. Structured, swept, and free meshing techniques all work in a top-down manner—they are tied directly to the geometry such that the resulting mesh fills the geometry. Bottom-up meshing relaxes the constraint that ties the mesh to the geometry so that you can build a mesh that ignores some geometric features. You can also use bottom-up meshing techniques to modify an orphan mesh part, in which case there are no geometric features to consider. If you work with native geometry, the elements that you create in a bottom-up mesh are always associated with the solid region that you meshed, but the mesh boundaries may not be associated with the geometric boundaries of the region. This allows you to create a mesh using only hexahedral elements where top-down meshing techniques might require extensive partitioning or the use of tetrahedral elements to complete the mesh. However, the relaxed geometry constraints also mean that you must carefully choose the parameters used to create the mesh, since it can vary significantly from the geometry. Once Abaqus has generated a bottom-up mesh, you need to evaluate whether it is suitable for the analysis and, if geometry is present, verify that the mesh is correctly associated with it.

You can apply bottom-up meshing to any solid region, including regions that can be meshed using the top-down techniques, and to orphan meshes. Since bottom-up meshing is a manual process that can be very time consuming, it is recommended that you use this method only when the top-down methods fail to produce a satisfactory mesh.

Generating the desired mesh may require multiple applications of the bottom-up meshing technique. If multiple applications are required, each bottom-up mesh becomes an incremental building block for the next mesh until you complete the mesh for the region. Each application of the bottom-up meshing technique involves three phases:

1) You select the method that Abaqus/CAE will use to create the mesh. You can choose from the following methods:
    - Sweep
    - Extrude
    - Revolve
    - Offset (available only for orphan mesh selections)

2) You select the side, called the source side that Abaqus/CAE will use to create a two-dimensional mesh to be swept, extruded, or revolved to fill a three-dimensional region.

3) You select the remaining parameters to complete the definition of the bottom-up mesh. For example, if you chose the sweep method, you can choose connecting sides and a target side.

Most of the times structured method is using for simple shapes. As an example in our case for braces and chords this techniques has been used. Sweep technique is used in more complex shapes. Like in this case in Can part and welding parts has been meshed by the sweeping.

3.6.3.1 Element shapes in ABAQUS (17)

There are various kinds of element types in ABAQUS:

- **Quad**

Use exclusively quadrilateral elements. The following figure shows an example of a mesh that was constructed using this setting:

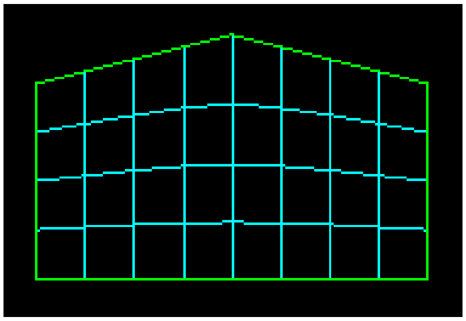

3.15 Quad meshing

- **Quad-dominated**

Use primarily quadrilateral elements, but allow triangles in transition regions. This setting is the default. The following figure shows an example of a mesh that was constructed using this setting:

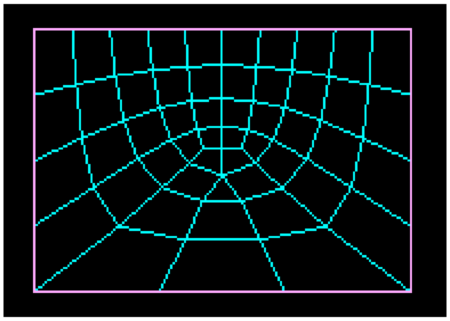

3.16 Quad dominate meshing

- **Tri**

Use exclusively triangular elements. The following figure shows an example of a mesh that was constructed using this setting:

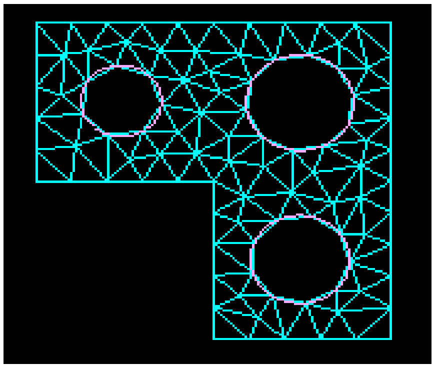

3.17 Tri dominate element

- **Hex**

Use exclusively hexahedral elements. This setting is the default. The following figure shows an example of a mesh that was constructed using this setting:

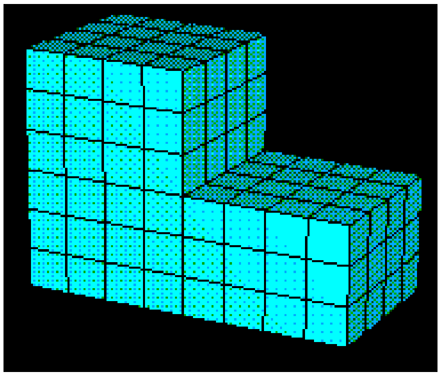

3.18 Hex dominate element

- **Hex-dominated**

Use primarily hexahedral elements, but allow some triangular prisms (wedges) in transition regions. The following figure shows an example of a mesh that was constructed using this setting:

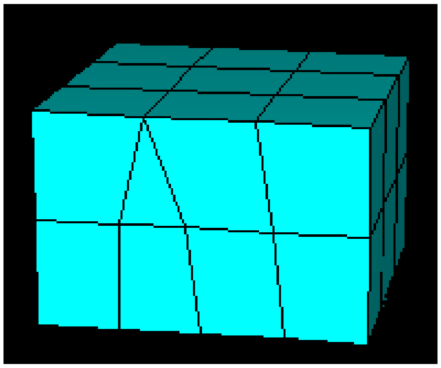

3.19 Hex element

➢ Tet

Use exclusively tetrahedral elements. The following figure shows an example of a mesh that was constructed using this setting:

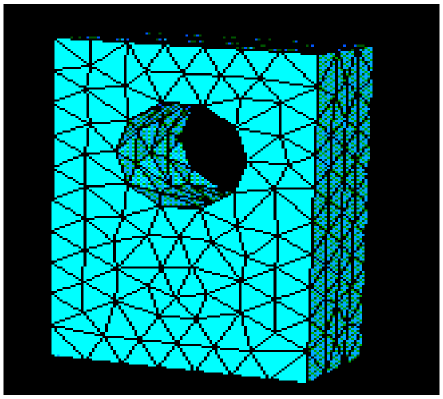

3.20 Tet dominate element

➢ Wedge

Use exclusively wedges elements. The following figure shows an example of a single-element mesh that was constructed using this setting:

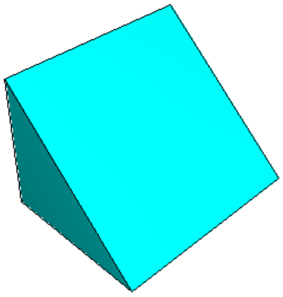

3.21 Wedge element

Element Type (17) (18)

In this part we are supposed to choose the element type, there variety of element types in ABAQUS.

The wide range of elements in the ABAQUS/Explicit element library provides flexibility in modeling different geometries and structures.

– Each element can be characterized by considering the following:

• Family

– Continuum, shell, membrane, rigid, beam, truss elements, etc.

• Number of nodes

– Element shape

– Geometric order

• Linear or quadratic interpolation

• Degrees of freedom

– Displacements, rotations, temperature

• Formulation

– Small- and finite-strain shells, etc.

• Integration

– Reduced and full integration

Each element in ABAQUS has a unique name, such as S4R, B31, M3D4R, C3D8R and C3D4. The element name identifies primary element characteristics. (18)

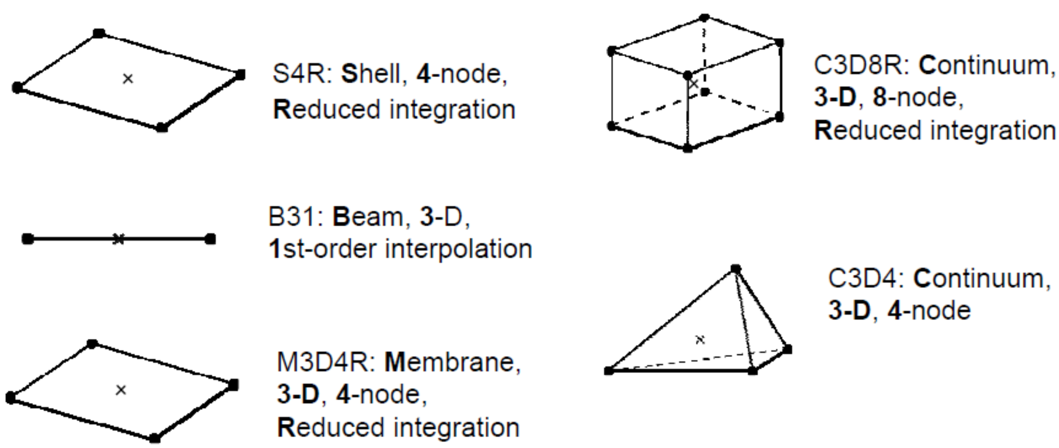

3.22 Elopement naming in abaqus

3.6.3.2 Linear and Quadratic element types (19)

The choice of the elements depends on the type of problem and the material. In General, the Quadratic meshes give more accurate results than the Linear meshes. But the quadratic elements should NOT be used for the faces coming in contact. This will produce unrealistic jump in Contact Pressure values. In that case, better to refine the mesh and use linear elements.

Many non-linear problems use nearly incompressible materials. Usage of Fully Integrated Elements in this case will lead to volumetric locking and therefore excessive stiffness. Usage of Reduced Integration elements (e.g. C3D8R) will relax it and provide more realistic results. But, one should be careful with the effect of hour glassing (Hour glassing is a phenomenon that creates an artificial stress field on the top of the real field. Therefore you see geometric stress patterns that do not have any physical basis.

Hour glassing causes problem in accuracy. The way to check for hour glassing is to look at the artificial energy and compare it to strain energy. The ratio should not exceed 1%) when using Linear Reduced Integration Elements.

Hour glassing is the phenomena of elements distorting in such a way that there is no change in Strain Energy. It behaves like a rigid body mode. One should be concerned with hour glassing effect only in Linear Reduced Integration elements. In Quadratic Reduced Integration Elements, Hour glassing doesn't propagate and therefore has no big effect. Most of the times, hour glassing can be controlled by using enhanced hour glass stiffness option. When using hour glass stiffness one must keep an eye on the artificial energy created in the system and make sure it is low.

As it is shown in figure below, this model has been mashed by C3D8R :An 8- node linear brick , reduced integration elements.

21377 elements have been produced in this stage.

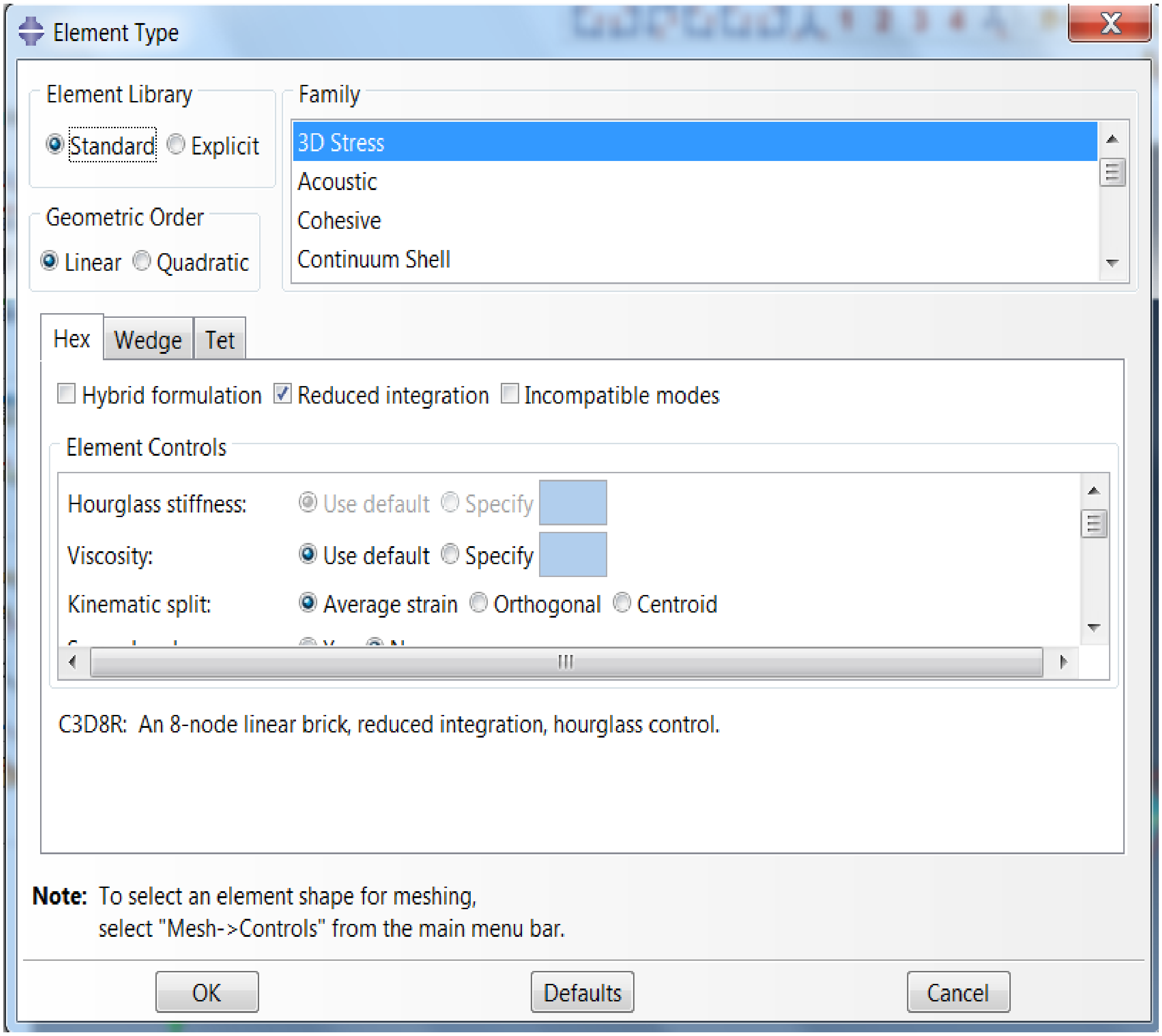

3.23 Element type in abaqus

```
***WARNING: DEGREE OF FREEDOM 3 HAS BEEN ELIMINATED AT NODE 1495 INSTANCE
            MERGED PART-1 BOUNDARY CONDITION TYPE ZSYMM MAY NOT BE APPLIED AT
            THIS NODE

***WARNING: DEGREE OF FREEDOM 3 HAS BEEN ELIMINATED AT NODE 1536 INSTANCE
            MERGED PART-1 BOUNDARY CONDITION TYPE ZSYMM MAY NOT BE APPLIED AT
            THIS NODE

***WARNING: 12 nodes have dof on which incorrect boundary conditions may have
            been specified. The nodes have been identified in node set
            WarnNodeBCIncorrectDof.



                          P R O B L E M   S I Z E


         NUMBER OF ELEMENTS IS                                       21377
         NUMBER OF NODES IS                                          31724
         NUMBER OF NODES DEFINED BY THE USER                         31724
         TOTAL NUMBER OF VARIABLES IN THE MODEL                      96444
         (DEGREES OF FREEDOM PLUS MAX NO. OF ANY LAGRANGE MULTIPLIER
          VARIABLES. INCLUDE *PRINT,SOLVE=YES TO GET THE ACTUAL NUMBER.)



                            END OF USER INPUT PROCESSING
```

2 elements along the braces and 3 elements along the chords and cans, also we have assigned elements in welded area are more complicated.

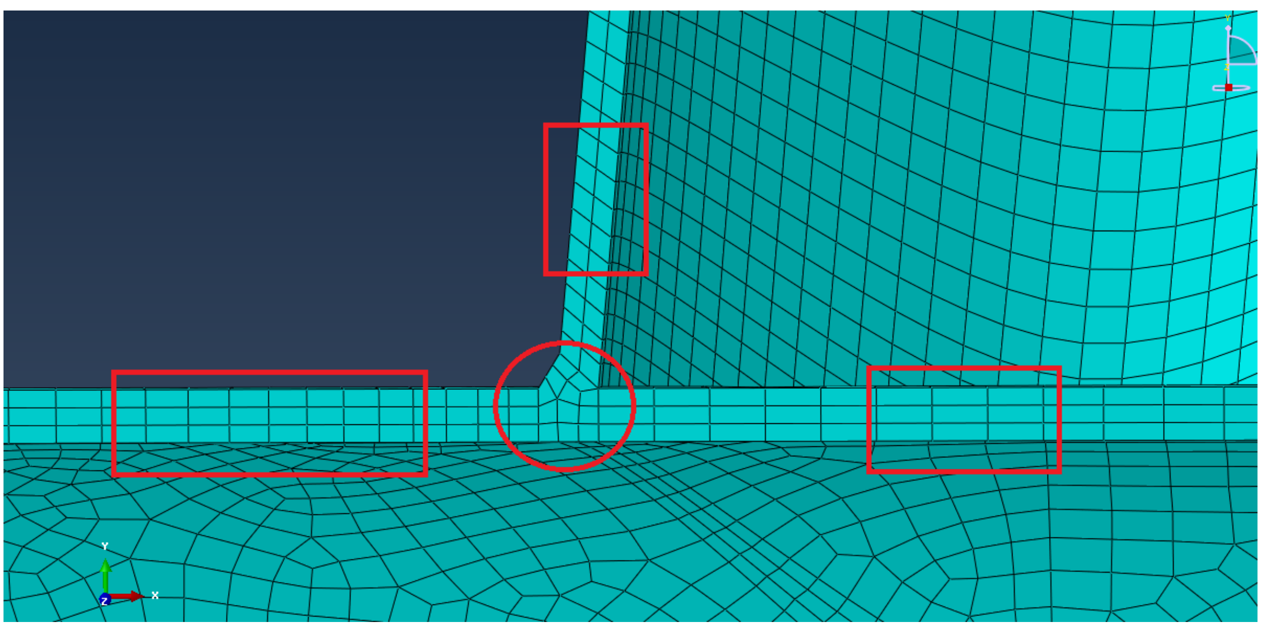

3.24 Snap shot from abaqus

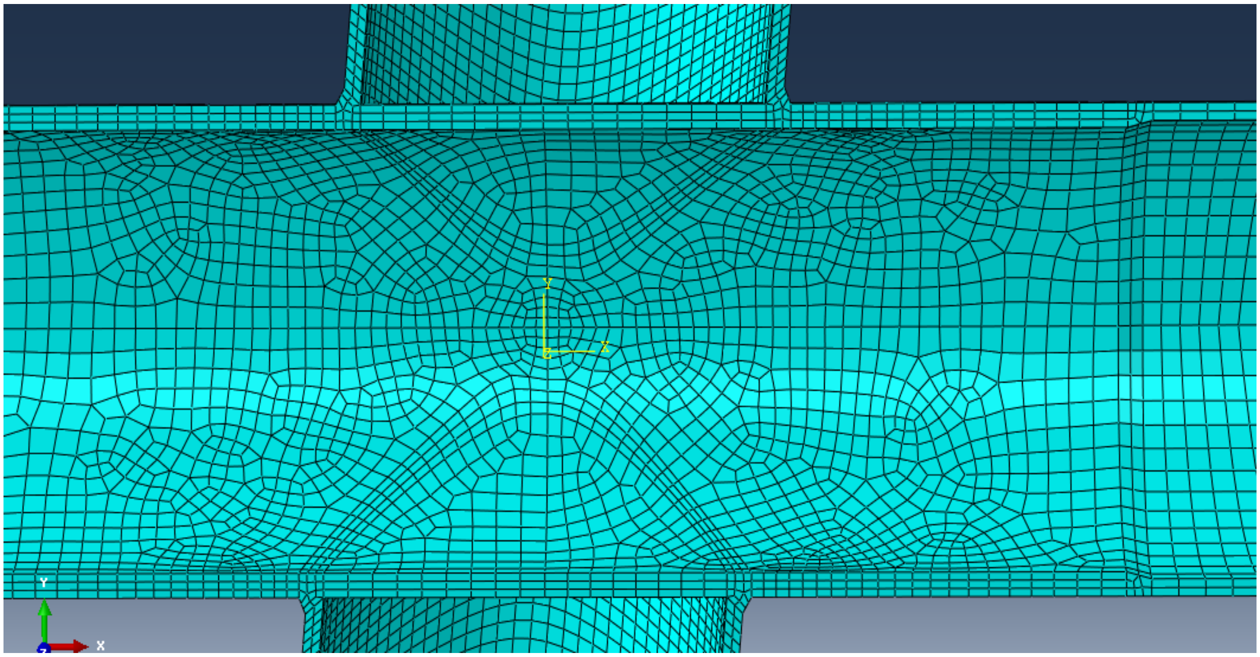

3.25 Snap shot from abaqus

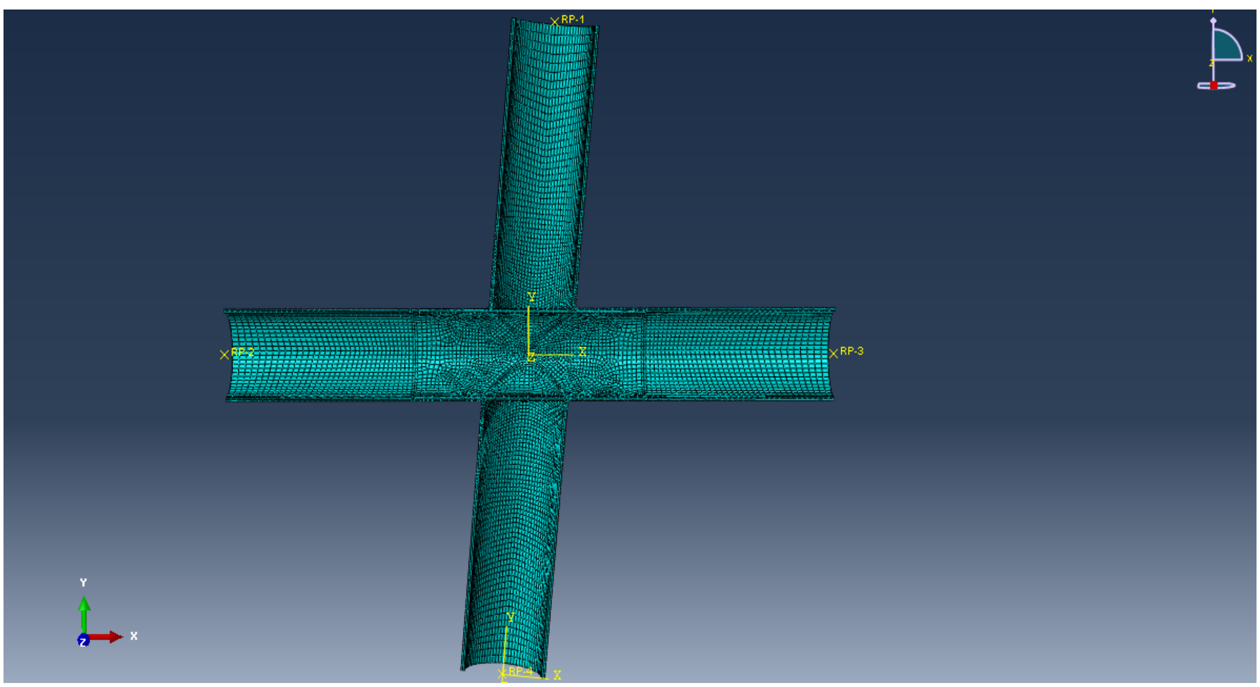

3.26 Snap shot from abaqus (21377 elements)

3.6.4 Boundary Conditions

In this step we are aiming to define the boundary conditions for the joint, this is necessary before applying the loads. As mentioned before, due to symmetry of the joint against the Z axis, we fix it against Z axis, (U3=UR1=UR3=0)

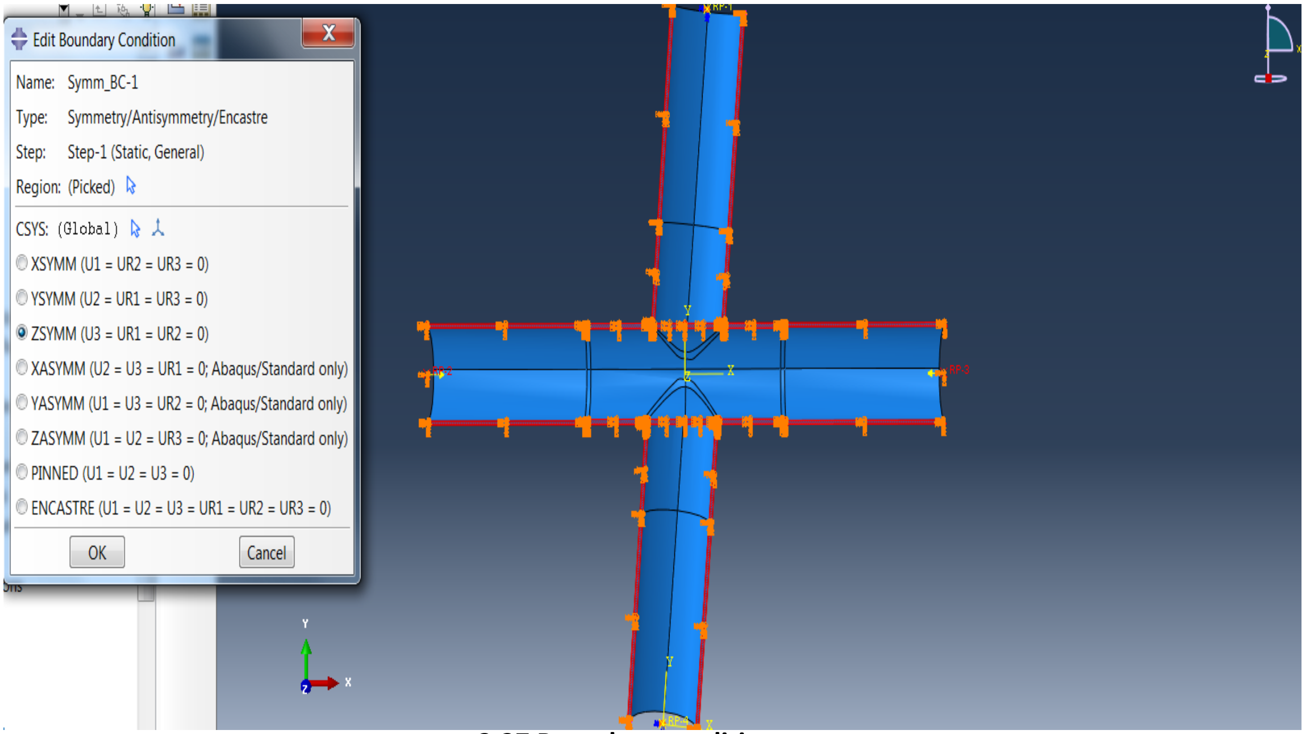

3.27 Boundary conditions

This has been done due to Global axis.

Two cords ends also are fixed due to Y direction and again this has been done according to global axis.

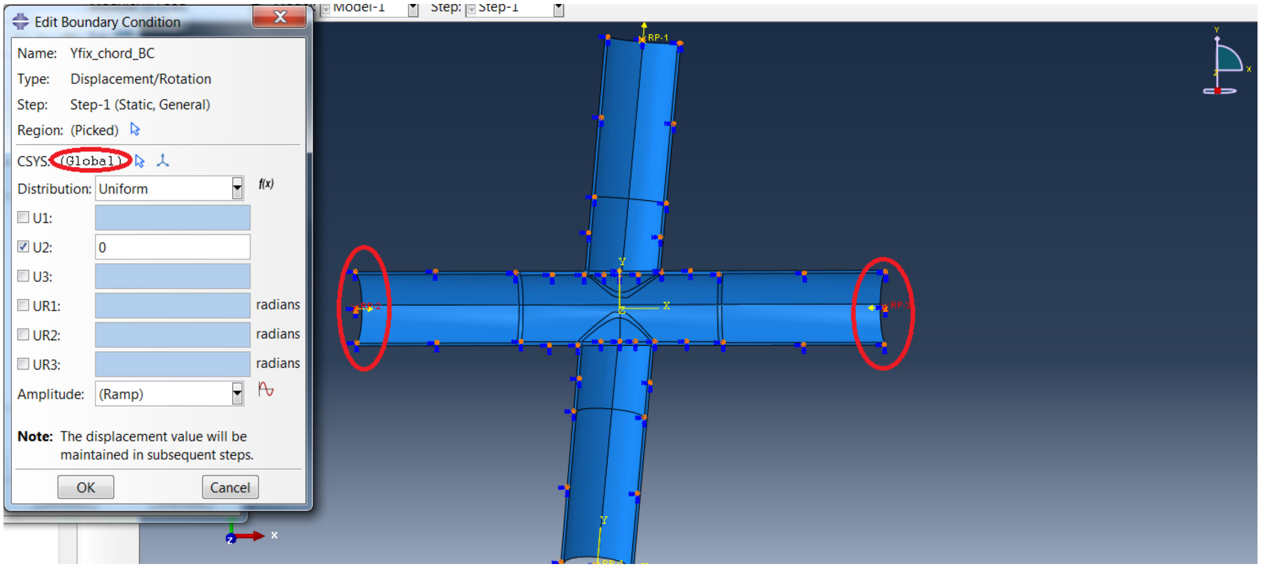

3.28 Boundary conditions

Two brace ends also should be fixed against X direction, the important point here is that we should pay attention to their inclination regarding global Y direction. Otherwise we will face some difficulties in loading since in this situation we need to separate loads which are being applied into the two brace topes.

Because of the we define two local axes in these two areas to make loading easier.

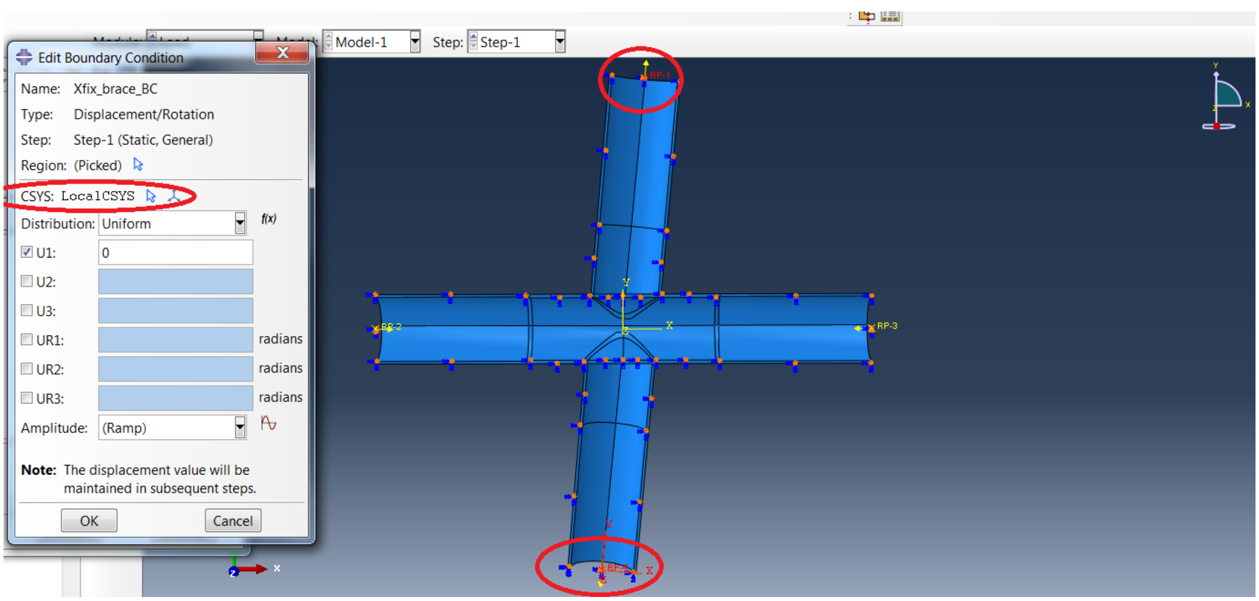

3.29 Boundary conditions

As it is shown in the picture these tow ends in the braces are fixed against the X direction but due to LOCAL axis.

3.7 Applying the Loads

For calculating and applying the loads for the first crash limit we have taken advantage of Norsok standards N004, an Excel spread sheet has been created.

fx =(D30+(1-D30)*(D7/D10)^2)*D28

Copy of N-004 - Joint Capacity_02+++.xlsx

	A	B	C	D	E	F
1						
2				Tension	Compression	
3		**Geometrical Data**				
4		Brace Diameter	d [mm]	900	900	
5		Chord/can Diameter	D [mm]	900	900	
6		Brace wall thickness	t [mm]	35	35	
7		Chord wall thickness	Tn [mm]	32	32	
8		Angle bn chord and brace	θ [deg]	84.6	84.6	
9						
10		Can wall thickness	Tc [mm]	45	45	
11		Effective Can Length	Lc [mm]	2400	2400	
12						
13		**Material Data**				
14		Yield Strength - Brace	σ_{yb} [MPa]	355	355	
15		Yield Strength - Chord/can	σ_{yc} [MPa]	345	345	
16						
17						
18		Diameter ratio	β	1	1	
19		Diameter-thickness ratio	γ	10.00	10.00	
20		Thickness ratio	τ	0.7777778	0.77777778	
21		Geometric factor	$Q_β$	0.448	0.448	
22		Strength facto	Q_u	16	7.522	
23		Chord Cross-section Area	Ac [mm^2]	87261	87261	
24		Cooeficient for Qf	λ	0.03	0.03	
25		Cooeficient for Qf	C1	25	25	
26		parameter 1	m	1.16E+07	5.43E+06	
27		parameter 2	n	8.28E-16	8.28E-16	
28		Joint Axial capacity	$N_{Rd.can}$ [N]	1.05E+07	5.31E+06	
29		**Can Effect**				
30			r	1.00	1.00	
31		Joint Axial capacity with can effect	N_{Rd} [N]	1.05E+07	5.31E+06	
32						

3.30 Capacity spread sheet

In this case we just evaluating joint in Tension, According to spread sheet which has been created due to norsok formulation for joint capacities, for first crash limitation our selected joint with that especial geometry has capacity of

1.05E+06 N, since we are modeling half of it due to symmetry we will apply 50% of the derived capacity as applied load in all braces and chord ends which it means 5.25E+6 N.

3.7.1 Defining Constraints Points Connected to whole surface of the end

It is better to define constraints point in each end of braces and chords and connect and fasten the whole surface of the end to that point. It helps to prevent some unwanted moments in ends also we have used them before also in creating boundary condition. After creating these points we can apply the load of each end surface to these points instead of whole surface.

3.31 Constraints points

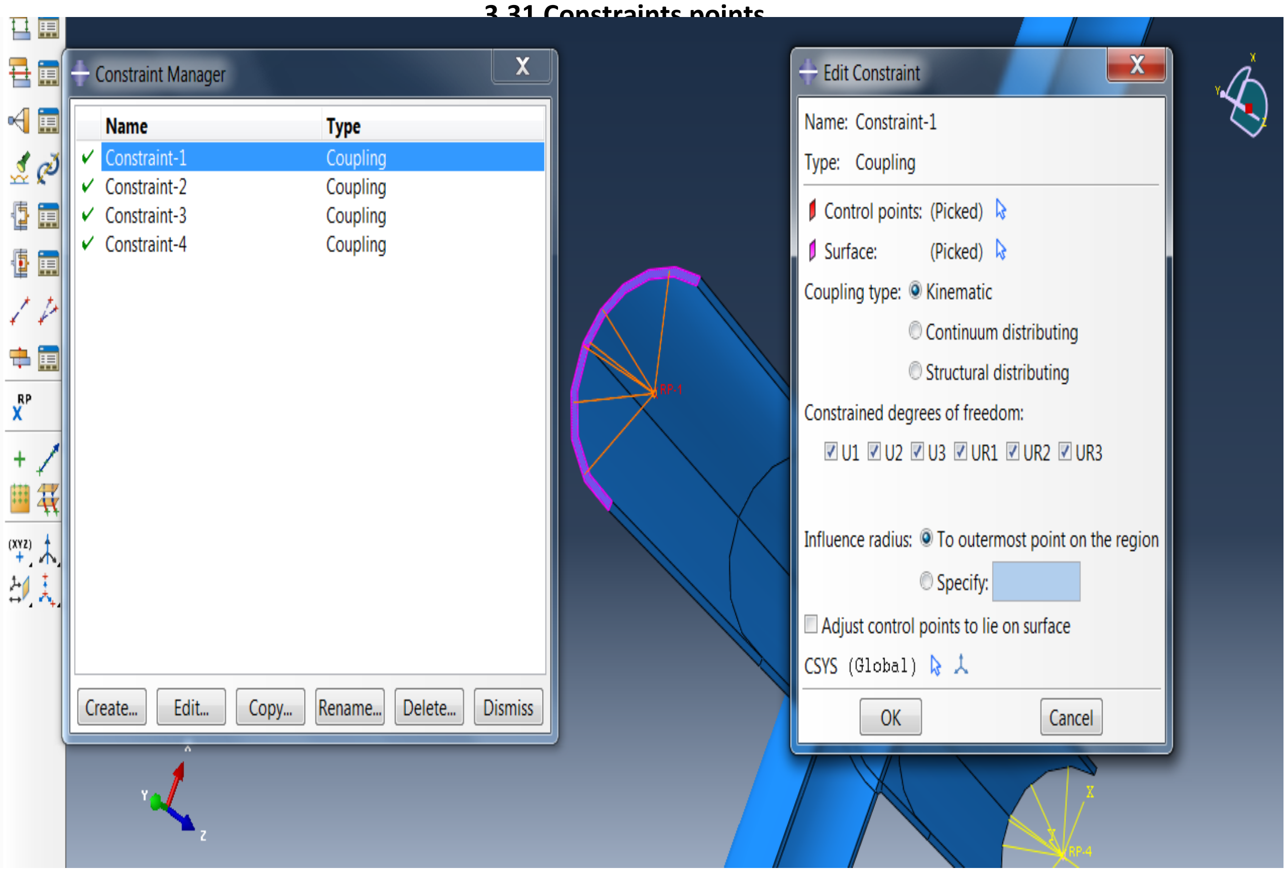

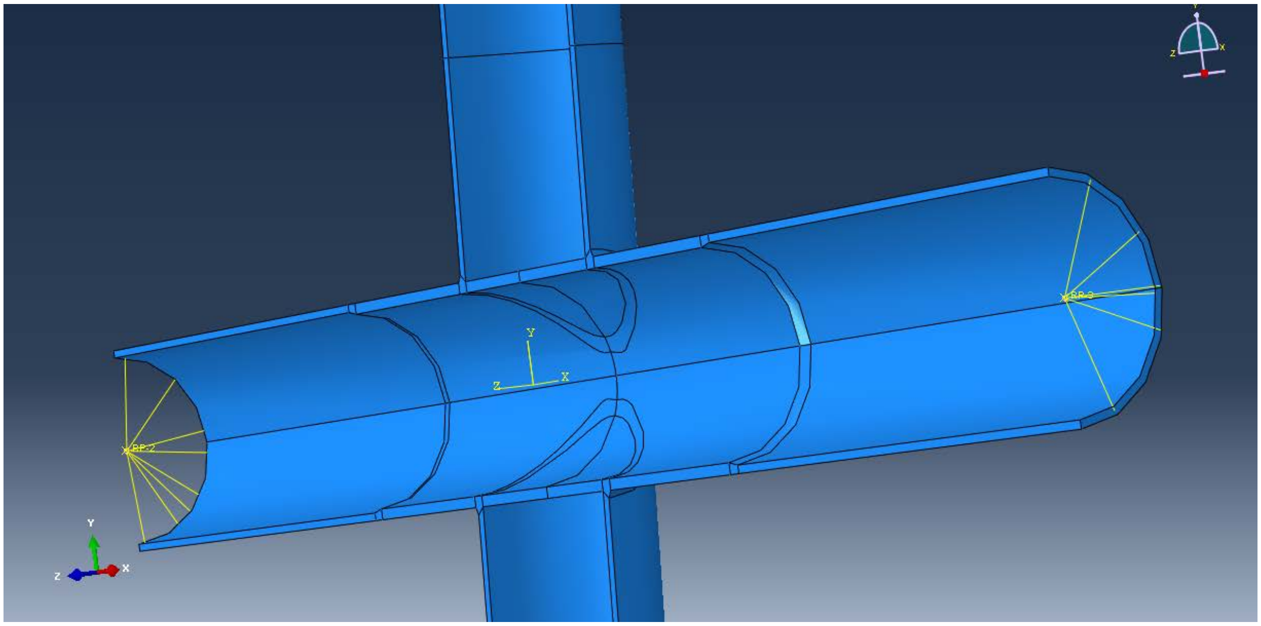

Now we can apply the calculated load to each end.

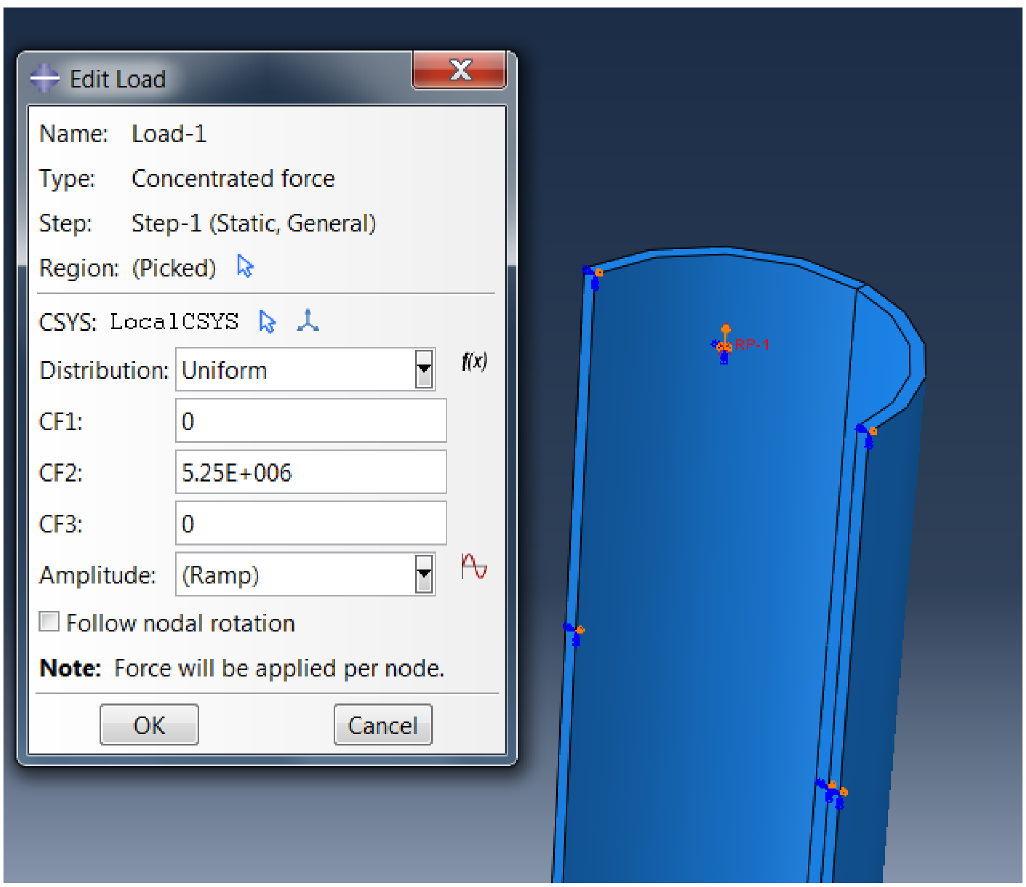

As it is clear loads in the braces are in puling and loads in chords are pushing the joint.

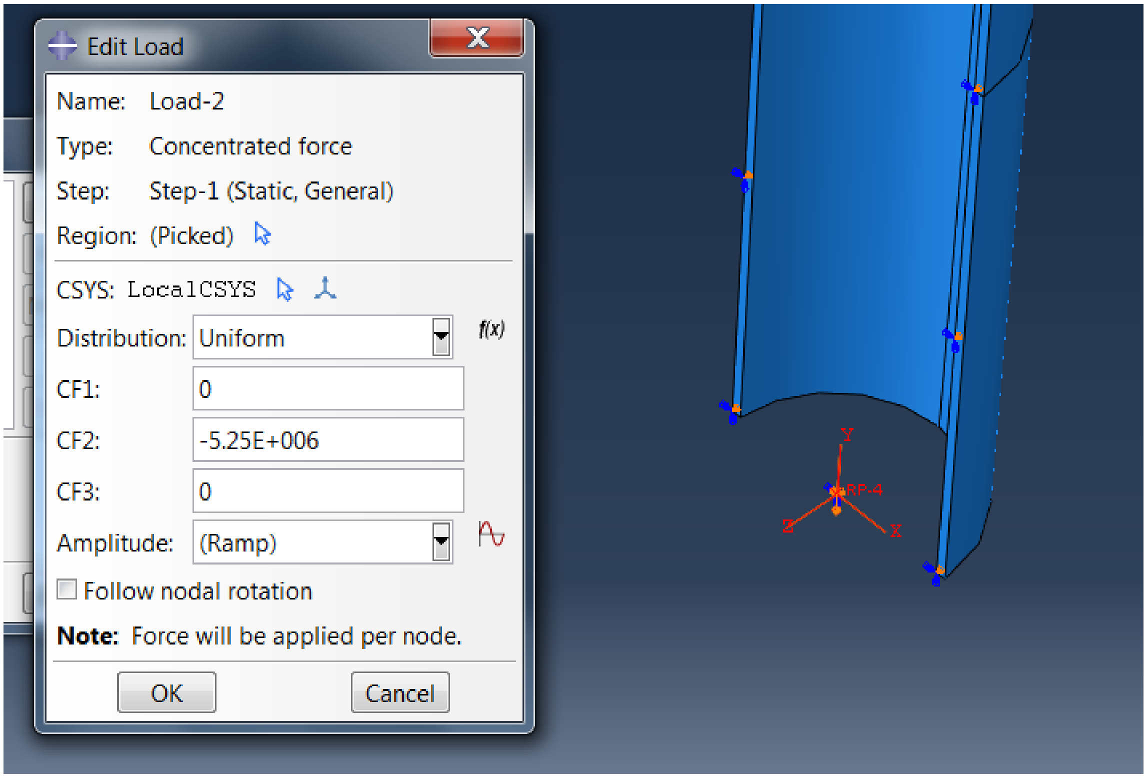

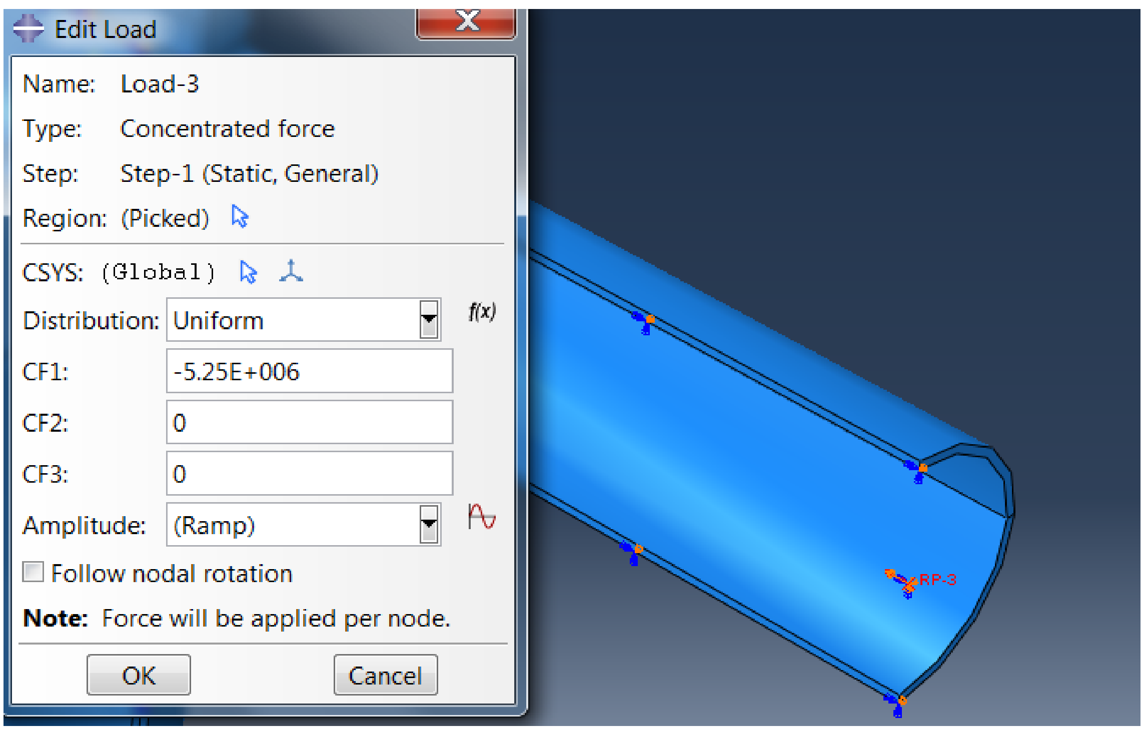

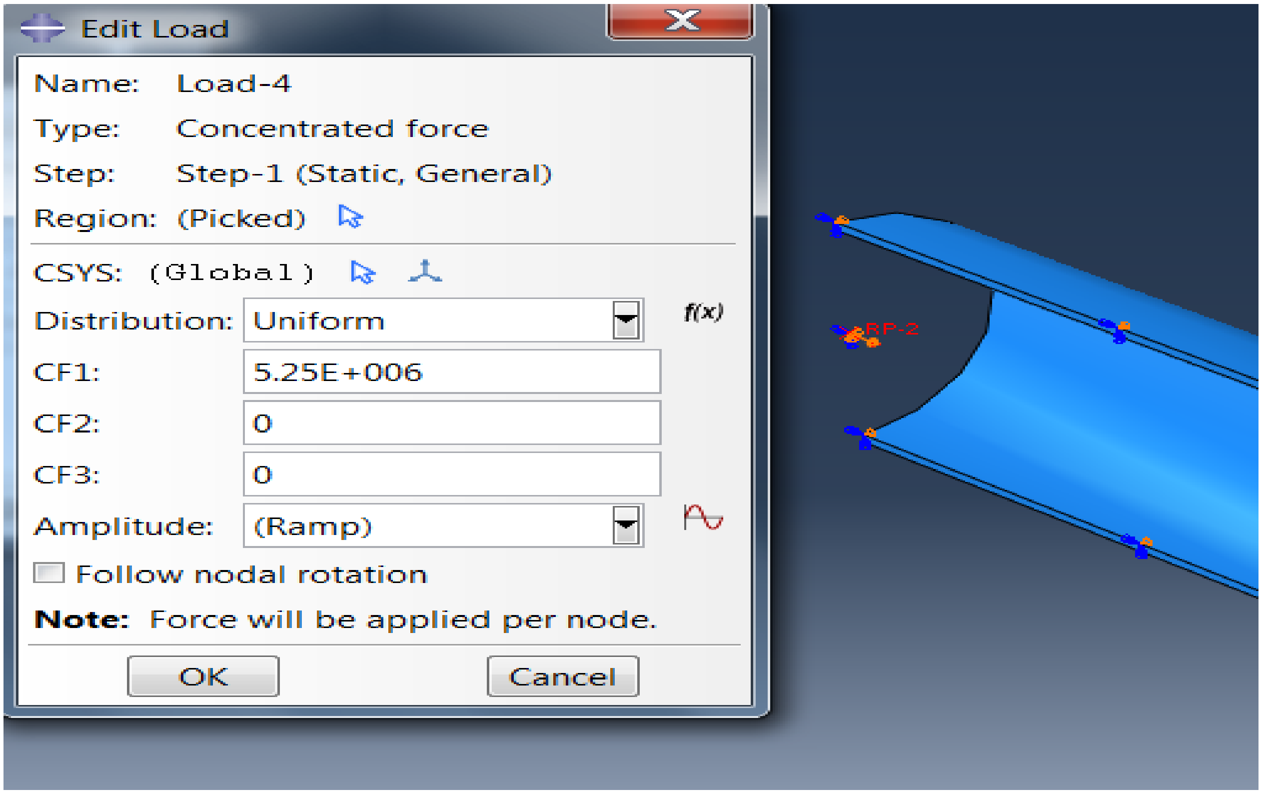

3.32 Load inputting

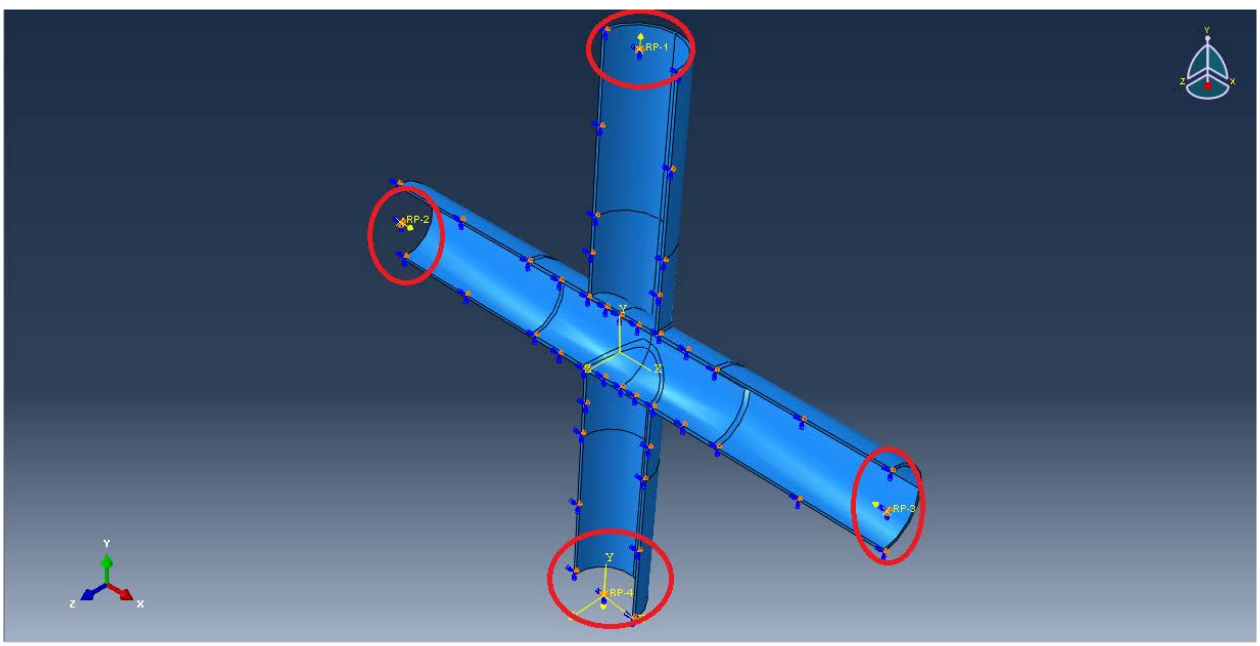

3.33 Applied load over view

Also about Load incrimination we just accept the ABAQUS, defaults, and as we see later on in elastic analyst load incrimination does not have any effect.

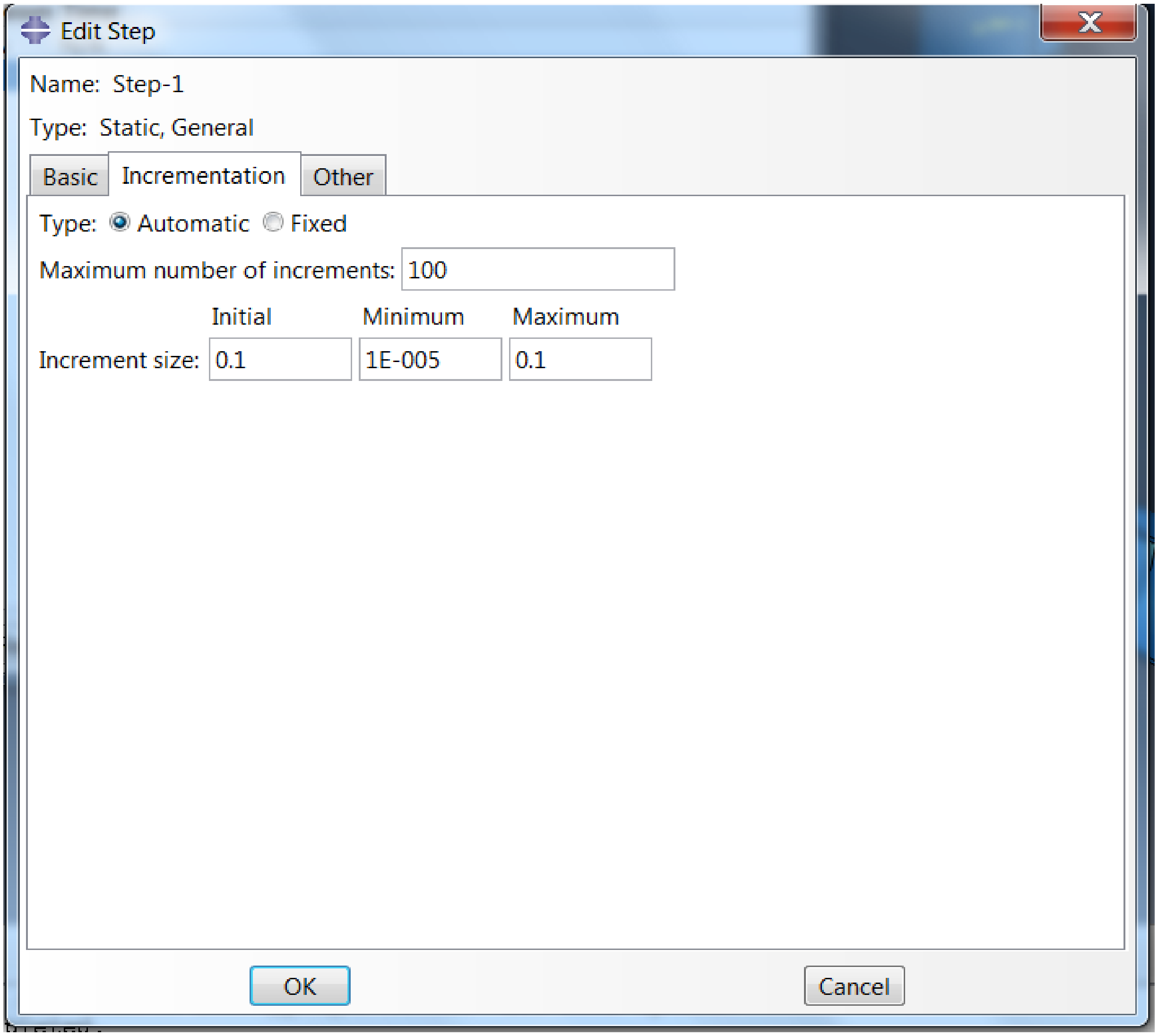

3.34 Load step inputting

3.8 Running the elastic model

Now we can run the elastic model for the first time,

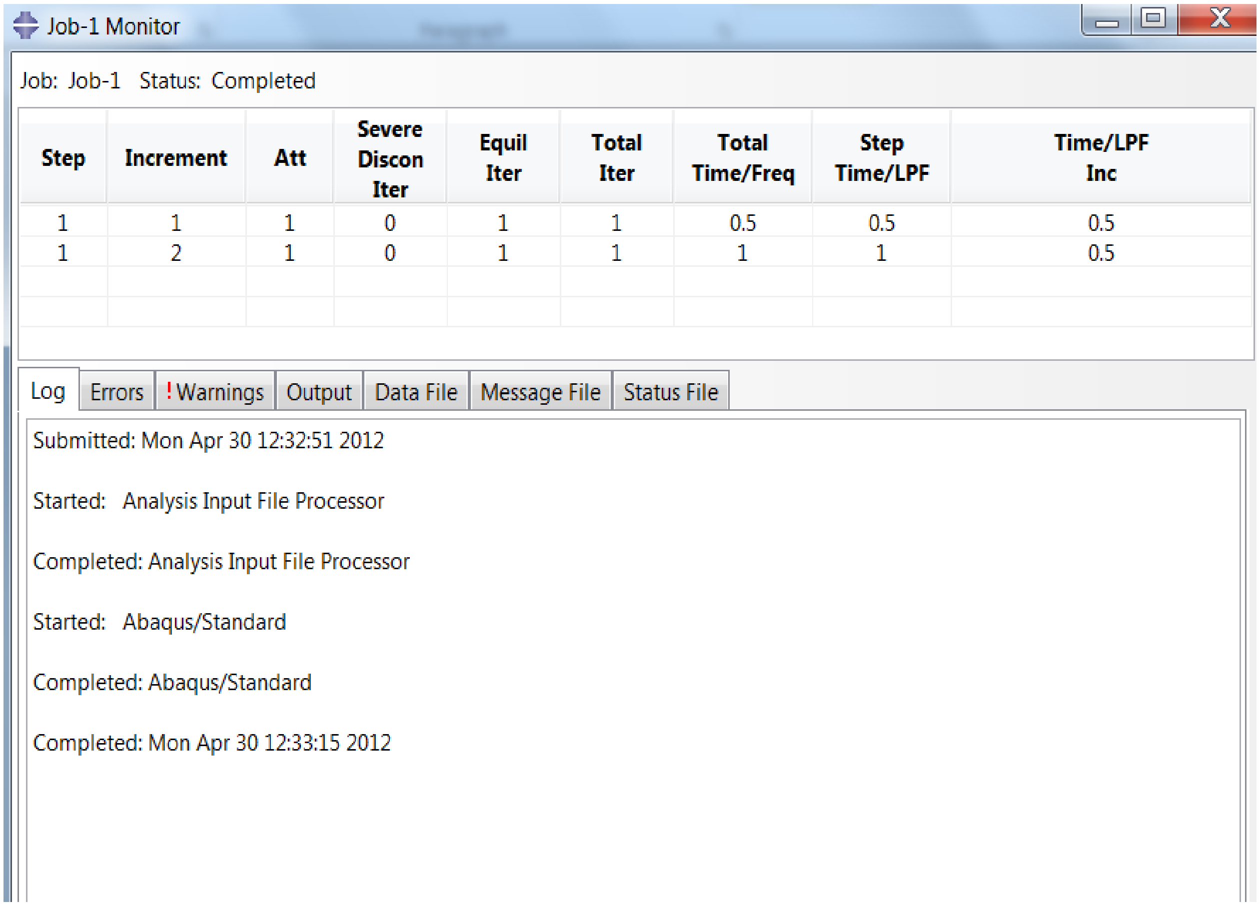

3.35 Running elastic model

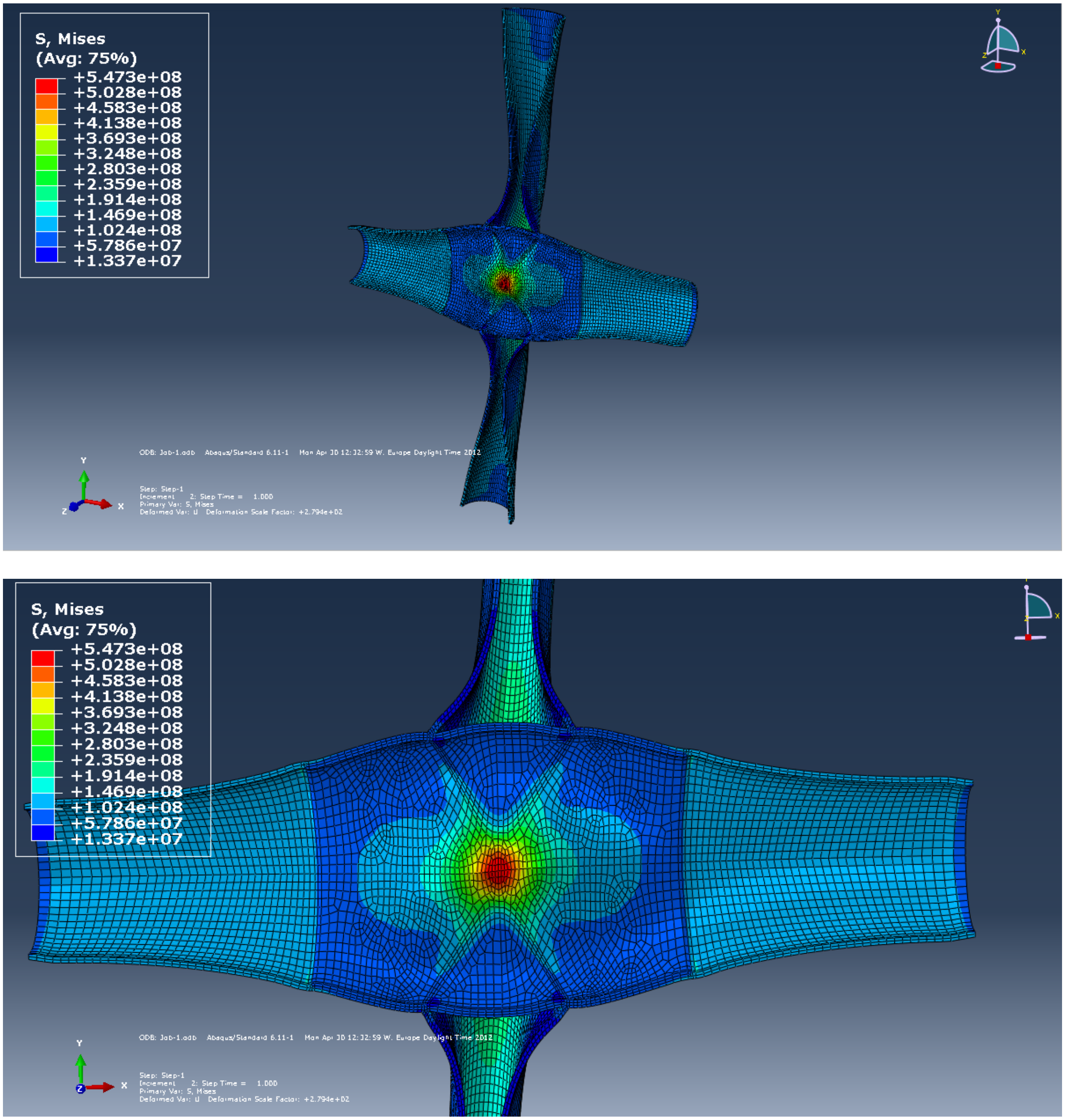

3.36 Maximum von Mises stress result

As expected the maximum of the stress has accorded in center of the joint.

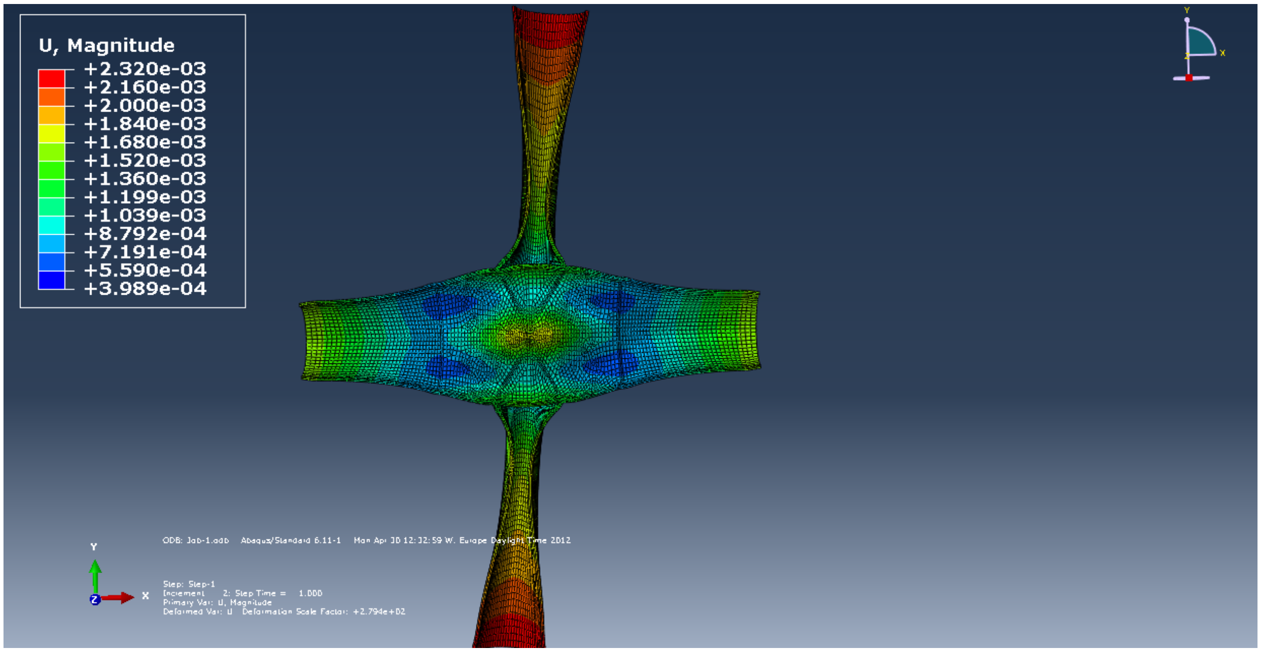

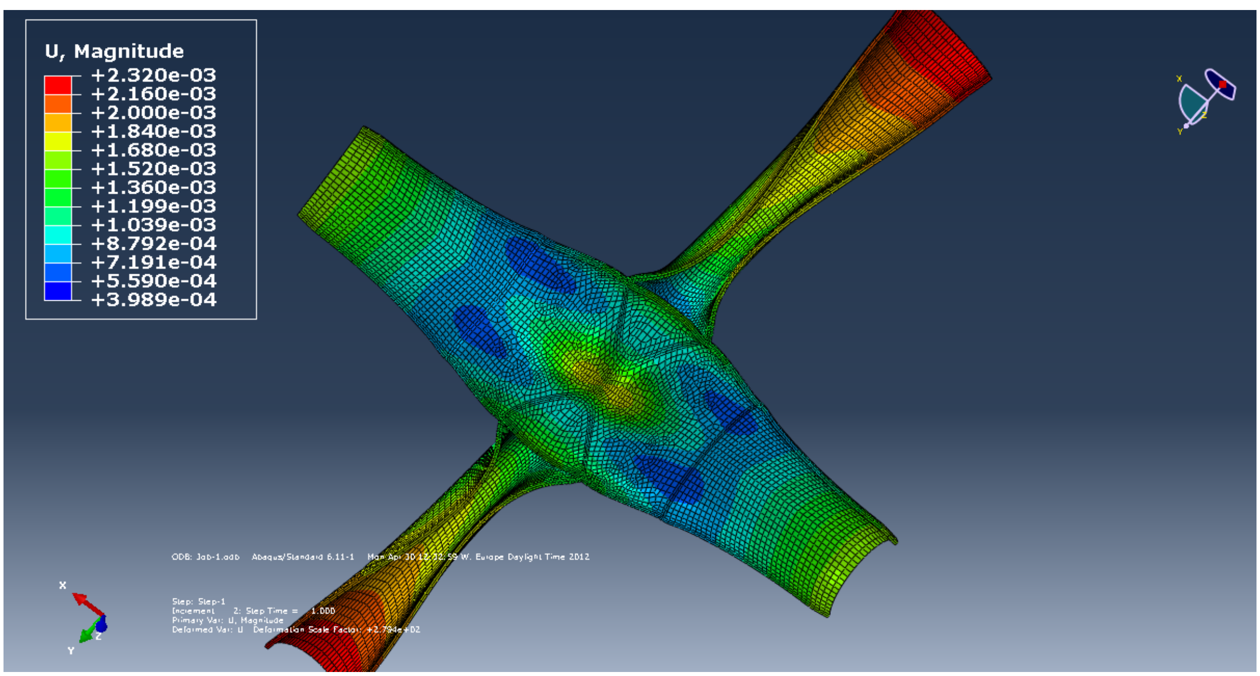

3.37 Exaggerated deflection of the joint

3.9 Von Mises Stress (20)

The von Mises yield criterion suggests that the yielding of materials begins when the second deviatory stress invariant J_2 reaches a critical value. For this reason, it is sometimes called the J_2- plasticity or J_2 flow theory. It is part of a plasticity theory that applies best to ductile materials, such as metals. Prior to yield, material response is assumed to be elastic.

In materials science and engineering the von Mises yield criterion can be also formulated in terms of the von Mises stress or equivalent tensile stress, σ_v, a scalar stress value that can be computed from the stress tensor. In this case, a material is said to start yielding when its von Mises stress reaches a critical value known as the yield strength, S_y. The von Mises stress is used to predict yielding of materials under any loading condition from results of simple uniaxial tensile tests. The von Mises stress satisfies the property that two stress states with equal distortion energy have equal von Mises stress.

Because the von Mises yield criterion is independent of the first stress invariant, J_1, it is applicable for the analysis of plastic deformation for ductile materials such as metals, as the onset of yield for these materials does not depend on the hydrostatic component of the stress tensor.

Although formulated by Maxwell in 1865, it is generally attributed to Richard Elder von Mises (1913). Titus Maksymilian Huber (1904), in a paper in Polish, anticipated to some extent this criterion. This criterion is also referred to as the Maxwell–Huber–Hacky–von Mises theory.

- **Mathematical formulation**

Mathematically the von Misses yield criterion is expressed as:

$$J_2 = k^2$$

Where k is the yield stress of the material in pure shear. As shown later in this article, at the onset of yielding, the magnitude of the shear yield stress in pure shear is √3 times lower than the tensile yield stress in the case of simple tension. Thus, we have:

$$k = \frac{S_y}{\sqrt{3}}$$

Where S_y is the yield strength of the material. If we set the von Misses stress equal to the yield strength and combine the above equations, the von Misses yield criterion and expressed as:

$$\sigma_v = S_y = \sqrt{3J_2}$$

Or

$$\sigma_v^2 = 3J_2 = 3k^2$$

Substituting J_2 with terms of the stress tensor components

$$\sigma_v^2 = \tfrac{1}{2}[(\sigma_{11} - \sigma_{22})^2 + (\sigma_{22} - \sigma_{33})^2 + (\sigma_{11} - \sigma_{33})^2 + 6(\sigma_{23}^2 + \sigma_{31}^2 + \sigma_{12}^2)]$$

This equation defines the yield surface as a circular cylinder whose yield curve, or intersection with the deviatory plane, is a circle with radius $\sqrt{2}k$, or $\sqrt{\tfrac{2}{3}}S_y$. This implies that the yield condition is independent of hydrostatic stresses.

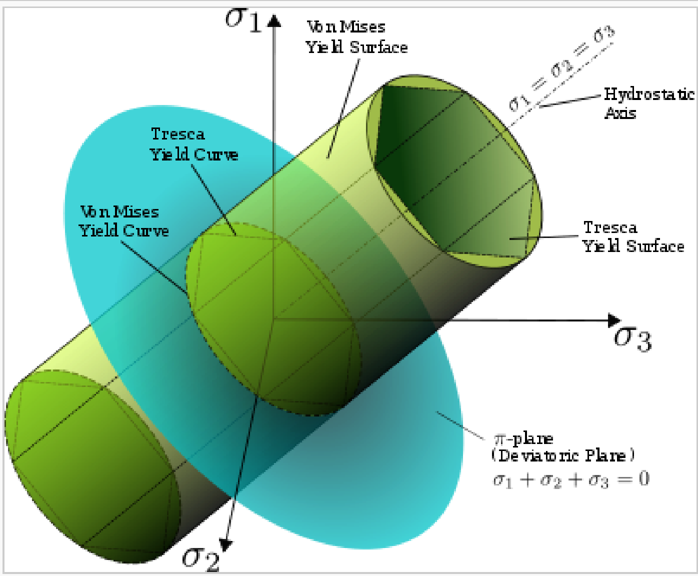

The von Mises yield surfaces in principal stress coordinates circumscribes a cylinder with radius $\sqrt{\tfrac{2}{3}}\sigma_y$ around the hydrostatic axis. Also shown is Tresca's hexagonal yield surface.

3.38 von Mises yield stress

❖ Reduced von Mises equation for different stress conditions

The above equation can be reduced and reorganized for practical use in different loading scenarios.

In the case of uniaxial stress or simple tension, $\sigma_1 \neq 0, \sigma_3 = \sigma_2 = 0$, the von Misses criterion simply reduces to

$\sigma_1 = S_y$,

Which means the material starts to yield when $\sigma_1$reaches the yield strength of the materialS_y, and is agreement with the definition of tensile (or compressive) yield strength.

It is also convenient to define an Equivalent tensile stress or von Misses stress, σ_v, which is used to predict yielding of materials under multiracial loading conditions using results from simple uniaxial tensile tests. Thus, we define

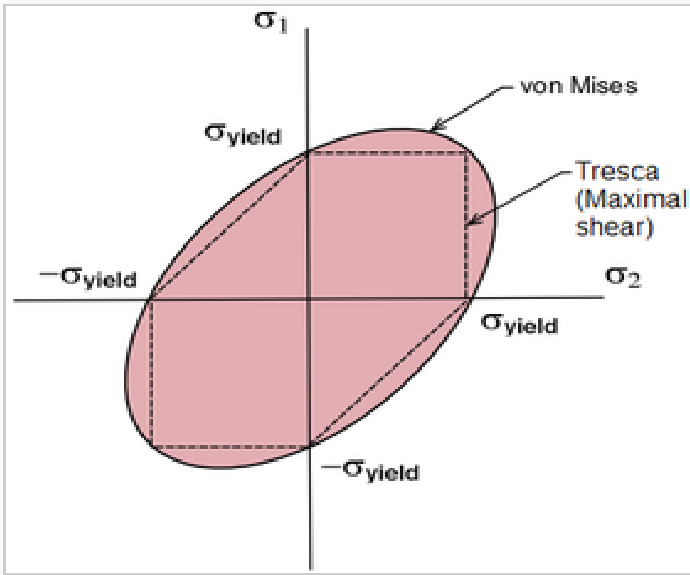

Projection of the von Mises yield criterion into the σ_1, σ_2 plane

3.39 Projection of the von Mises yield criterion

$$\begin{aligned}
\sigma_v &= \sqrt{3J_2} \\
&= \sqrt{\frac{(\sigma_{11}-\sigma_{22})^2+(\sigma_{22}-\sigma_{33})^2+(\sigma_{11}-\sigma_{33})^2+6(\sigma_{12}^2+\sigma_{23}^2+\sigma_{31}^2)}{2}} \\
&= \sqrt{\frac{(\sigma_1-\sigma_2)^2+(\sigma_2-\sigma_3)^2+(\sigma_1-\sigma_3)^2}{2}} \\
&= \sqrt{\tfrac{3}{2}\, s_{ij}s_{ij}}
\end{aligned}$$

Where are the components of the stress deviator tensor $\boldsymbol{\sigma}^{dev}$:

$$\boldsymbol{\sigma}^{dev} = \boldsymbol{\sigma} - \frac{1}{3}(\mathrm{tr}\ \boldsymbol{\sigma})\,\mathbf{I}$$

In this case, yielding occurs when the equivalent stress, σ_v, reaches the yield strength of the material in simple tension, σ_y. As an example, the stress state of a steel beam in compression differs from the stress state of a steel axle under torsion, even if both specimens are of the same material. In view of the stress tensor, which fully describes the stress state, this difference manifests in six degrees of freedom, because the stress tensor has six independent components. Therefore, it is difficult to tell which of the two specimens is closer to the yield point or has even reached it. However, by means of the von Mises yield criterion, which depends solely on the value of the scalar von Mises stress, i.e., one degree of freedom, this comparison is straightforward: A larger von Mises value implies that the material is closer to the yield point.

In the case of pure shear stress, $\sigma_{12} = \sigma_{21} \neq 0$, while all other $\sigma_{ij} = 0$, von Mises criterion becomes:

$$\sigma_{12} = k = \frac{S_y}{\sqrt{3}}.$$

This means that, at the onset of yielding, the magnitude of the shear stress in pure shear is $\sqrt{3}$ times lower than the tensile stress in the case of simple tension. The von Misses yield criterion for pure shear stress, expressed in principal stresses, is:

$$(\sigma_1 - \sigma_2)^2 + (\sigma_2 - \sigma_3)^2 + (\sigma_1 - \sigma_3)^2 = 6\sigma_{12}^2$$

In the case of **plane stress**, $\sigma_3 = 0$, the von Misses criterion becomes:

$$\sigma_1^2 - \sigma_1\sigma_2 + \sigma_2^2 = 3k^2 = S_y^2$$

This equation represents an ellipse in the plane $\sigma_1 - \sigma_2$, as shown in the Figure above.

The following table summarizes von Misses yield criterion for the different stress conditions.

Load scenario	Restrictions	Simplified von Mises equation
General	No restrictions	$\sigma_v = \sqrt{\frac{1}{2}[(\sigma_{11} - \sigma_{22})^2 + (\sigma_{22} - \sigma_{33})^2 + (\sigma_{33} - \sigma_{11})^2 + 6(\sigma_{12}^2 + \sigma_{23}^2 + \sigma_{31}^2)]}$
Principal stresses	$\sigma_{12} = \sigma_{13} = \sigma_{23} = 0$	$\sigma_v = \sqrt{\frac{1}{2}[(\sigma_1 - \sigma_2)^2 + (\sigma_1 - \sigma_3)^2 + (\sigma_2 - \sigma_3)^2]}$
Plane stress	$\sigma_3 = 0$ $\sigma_{31} = \sigma_{23} = 0$	$\sigma_v = \sqrt{\sigma_1^2 - \sigma_1\sigma_2 + \sigma_2^2 + 3\sigma_{12}^2}$
Pure shear	$\sigma_1 = \sigma_2 = \sigma_3 = 0$ $\sigma_{31} = \sigma_{23} = 0$	$\sigma_v = \sqrt{3}\sigma_{12}$
Uniaxial	$\sigma_2 = \sigma_3 = 0$ $\sigma_{12} = \sigma_{31} = \sigma_{23} = 0$	$\sigma_v = \sigma_1$

3.40 Von Mises yield criterion for the different stress conditions

❖ Physical interpretation of the von Mises yield criterion

Hencky (1924) offered a physical interpretation of von Misses criterion suggesting that yielding begins when the elastic energy of distortion reaches a critical value. For this, the von Misses criterion is also known as the maximum distortion strain energy criterion. This comes from the relation between J_2 and the elastic strain energy of distortion W_D:

$$W_D = \frac{J_2}{2G} \text{ with the elastic shear modulus } G = \frac{E}{2(1+\nu)}.$$

In 1937 Arpad L. Nadia suggested that yielding begins when the octahedral shear stress reaches a critical value, i.e. the octahedral shear stress of the material at yield in simple tension. In this case, the von Misses yield criterion is also known as the maximum octahedral shear stress criterion in view of the direct proportionality that exist between and the octahedral shear stress, J_2 , which by definition is:

$$\tau_{oct} = \sqrt{\tfrac{2}{3}J_2}$$

thus we have

$$\tau_{oct} = \tfrac{\sqrt{2}}{3}S_y$$

3.10 Study of mesh and Load incremination changing in elastic model

In this part we evaluate the effect of changing of mesh and initial load incremination in an elastic model. Because of that we compare 4 different models which 2 of them are same in meshing but different in initial load incrementation and the two others are same in Initial load incrementation but different in meshing and we will see the effect of them on an elastic joint model.Now we define four different models:

Model Name	Number of elements	Initial Load Inc
A	21377	0.1
B	21377	0.5
C	10700	0.1
D	10700	0.5

3.41 Initial load Inc studies

Model A & B has 3 elements along the chord and can but we have put 2 element in wide of chord length of model C& D.

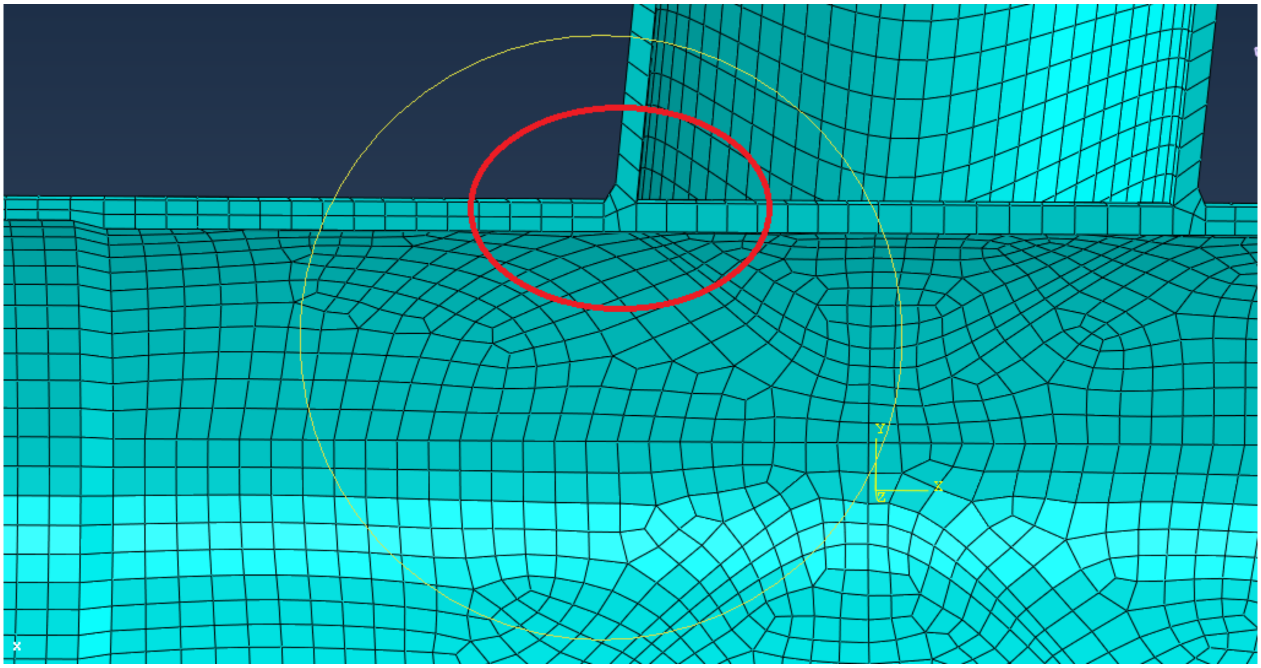

Meshing of model C & D (10700 elements)

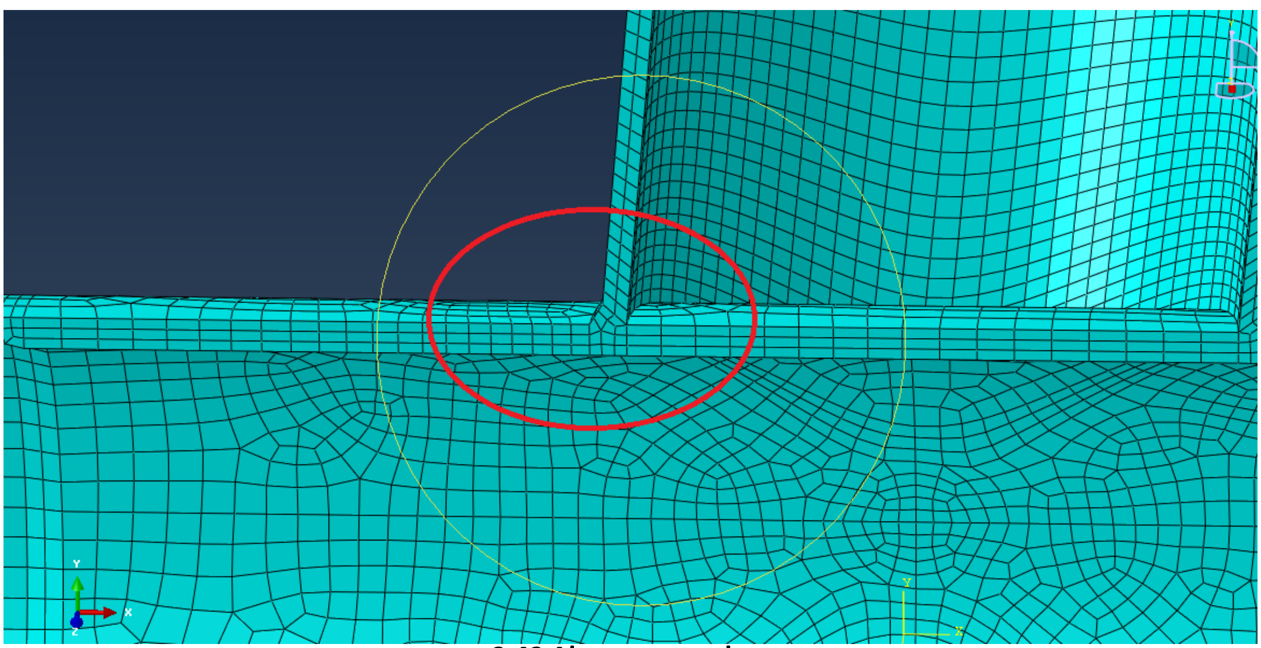

3.42 Abaqus snap shot

Meshing of model A & B (21377 elemnts)

Also Model B & D have initial load Inc of 0.5 which is abaqus default.

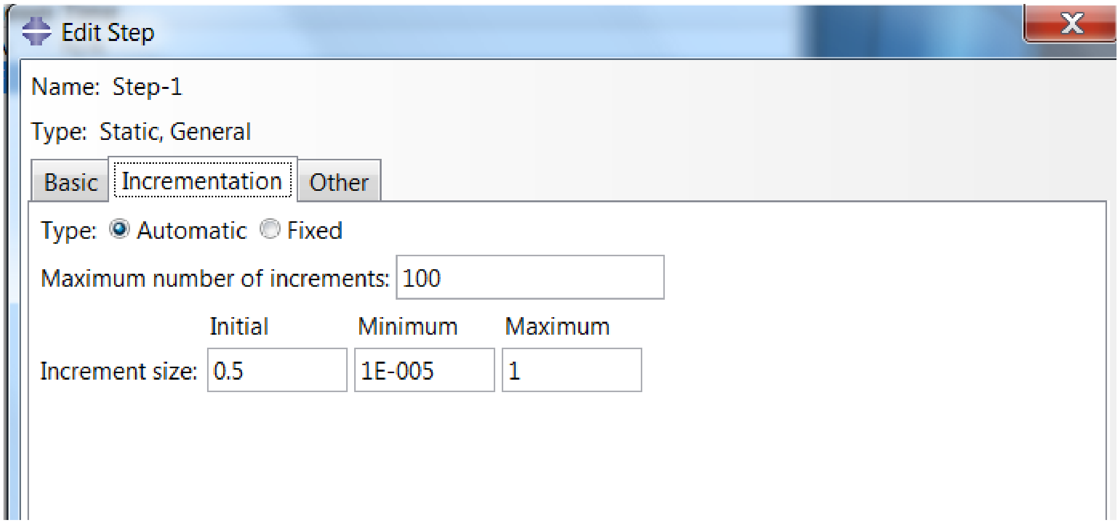

And Model A & C have initial Load inc of 0.1

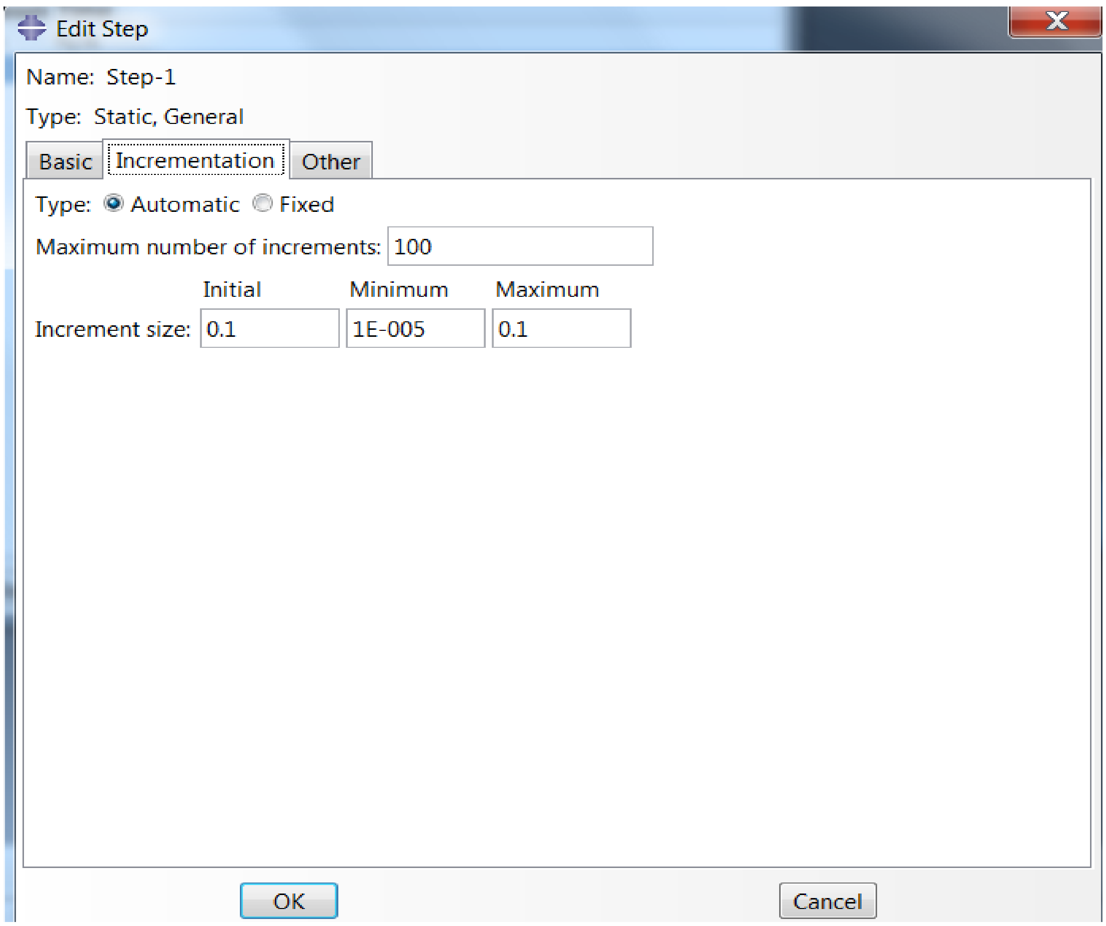

After running the elastic analysis the results are presented below:

Model Name	Max misses stress	Maximum deflection U
A	5.47e+8	2.32e-3
B	5.47e+8	2.32e-3
C	4.78e+8	2.34e-3
D	4.78e+8	2.34e-3

3.43 Initial load study results

As results shows changing in mesh (make it coarser) cause around 17% deference in maximum stress and not that much deference in deflection and changing initial load inc have no effects in results WHEN we are doing elastic analysis.

4 Plastic analysis By Abaqus

4.1 Introduction

In previous chapter we have modeled and analyzed the joint with elastic materials that concluded to an elastic analysis. We have described all stages to make a model, defining boundary conditions, constraints points and loading by details. It took around 20 seconds. After that we have performed some changes related to meshing and initial Load Inc and we observed the effect of each on an elastic analysis.

Now in this chapter we are going to perform a plastic analysis for same joint with same geometry characteristics. To reach this target first of all we need to define some sections made by plastic materials, then assign theses section to whole joint and as a result we will have plastic material joint. Then we can perform plastic analysis. For assigning plastic characteristics to the sections we have taken advantage of Ramberg-Osgood relations which we have provided a general explanation about it in previous chapters.

After performing plastic analysis we are aiming to do some studies about effect of element types (Linear & Quadratic) also elements deferent sizes on the maximum misses' stress and maximum deflection.

By this way we try to investigate an optimum way of meshing a model in plastic analysis.

4.2 Defining plastic materials

According to DNV reports for the mentioned joint to kinds of steel have been used that their specifications are shown below in the table:

Yield	Thickness (mm)	Grad I
	17-40	340 Mpa
	41-63	325 Mpa

4.1 Plastic material datas

The Ramberg–Osgood equation was created to describe the nonlinear relationship between stress and strain—that is, the stress–strain curve—in materials near their yield points. In its original form, the equation for strain (deformation) is:

$$\epsilon = \frac{\sigma}{E} + K\left(\frac{\sigma}{E}\right)^n$$

Where

ϵ is strain,

σ is stress,

E is Young's modulus, and

K and n are constants that depend on the material being considered.

The first term on the right side, σ / E, is equal to the elastic part of the strain, while the second term, $K(\sigma/E)^n$, accounts for the plastic part, the parameters K and n describing the hardening behavior of the material. Introducing the yield strength of the material, σ_0, and defining a new parameter, α, related to K as $\alpha = K(\sigma_0/E)^{n-1}$, it is convenient to rewrite the term on the extreme right side as follows:

$$K\left(\frac{\sigma}{E}\right)^n = \alpha\frac{\sigma_0}{E}\left(\frac{\sigma}{\sigma_0}\right)^n$$

Replacing in the first expression, the Ramberg–Osgood equation can be written as:

$$\epsilon = \frac{\sigma}{E} + \alpha\frac{\sigma_0}{E}\left(\frac{\sigma}{\sigma_0}\right)^n$$

According to mentioned equations, we are going to calculate plastic strains regarding to deferent stresses to reach some data as input for material property part in Abaqus.

Ramberg-Osgood: Stress vs. Strain

Yield Stress, Pa	σ_y	3.25E+08
	σ_t	4.60E+08
Strain at Yield	ε_y	0.005
Strain at ultimate tensile	ε_t	0.2
Modulus of Elasticity	E	2.1E+11
	A1	0.002
	A2	0.002
	B	0.017
	C (A1/A2)	0.707
	n	11.653
	K	1.94E+30
Stress Increments, Pa	$\Delta\sigma$	1.00E+07

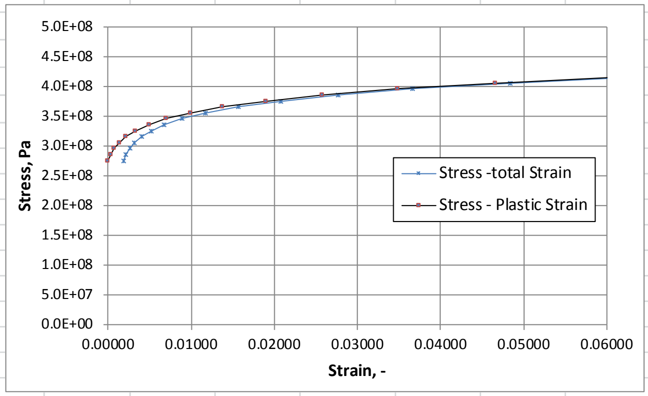

Total Strai	Stress	Plastic Strain	
ε_{tot}	σ	ε_{pl}	ε_{elstic}
0.00184	2.7625E+08	0.000000	0.0018
0.00215	2.8625E+08	0.000314	0.0018
0.00258	2.9625E+08	0.000749	0.0018
0.00319	3.0625E+08	0.001351	0.0018
0.00402	3.1625E+08	0.002183	0.0018
0.00516	3.2625E+08	0.003329	0.0018
0.00673	3.3625E+08	0.004899	0.0018
0.00887	3.4625E+08	0.007036	0.0018
0.01176	3.5625E+08	0.009925	0.0018
0.01564	3.6625E+08	0.013803	0.0018
0.02081	3.7625E+08	0.018975	0.0018
0.02766	3.8625E+08	0.025822	0.0018
0.03666	3.9625E+08	0.034827	0.0018
0.04843	4.0625E+08	0.046594	0.0018
0.06371	4.1625E+08	0.061873	0.0018
0.08343	4.2625E+08	0.081592	0.0018
0.10873	4.3625E+08	0.106894	0.0018
0.14101	4.4625E+08	0.139178	0.0018
0.18199	4.5625E+08	0.180151	0.0018
0.23372	4.6625E+08	0.231882	0.0018
0.29871	4.7625E+08	0.296875	0.0018
0.37998	4.8625E+08	0.378143	0.0018
0.48113	4.9625E+08	0.479297	0.0018
0.60649	5.0625E+08	0.604653	0.0018
0.76118	5.1625E+08	0.759349	0.0018
0.95131	5.2625E+08	0.949477	0.0018
1.18408	5.3625E+08	1.182242	0.0018
1.46797	5.4625E+08	1.466135	0.0018
1.81297	5.5625E+08	1.811134	0.0018
2.23076	5.6625E+08	2.228927	0.0018
2.73500	5.7625E+08	2.733168	0.0018
3.34160	5.8625E+08	3.339765	0.0018
4.06904	5.9625E+08	4.067202	0.0018
4.93873	6.0625E+08	4.936899	0.0018
5.97546	6.1625E+08	5.973623	0.0018
7.20777	6.2625E+08	7.205935	0.0018
8.66854	6.3625E+08	8.666701	
10.39549	6.4625E+08	10.39366	
12.43186	6.5625E+08	12.43003	
14.82706	6.6625E+08	14.82523	

4.2 Spread sheet for 325 MPa Yield

Ramberg-Osgood: Stress vs. Strain		
Yield Stress, Pa	σ_y	3.40E+08
	σ_t	4.60E+08
Strain at Yield	ε_y	0.005
Strain at ultimate tensile	ε_t	0.2
Modulus of Elasticity	E	2.1E+11
	A1	0.002
	A2	0.002
	B	0.017
	C (A1/A2)	0.739
	n	13.461
	K	1.25E+35
Stress Increments, Pa	$\Delta\sigma$	1.00E+07

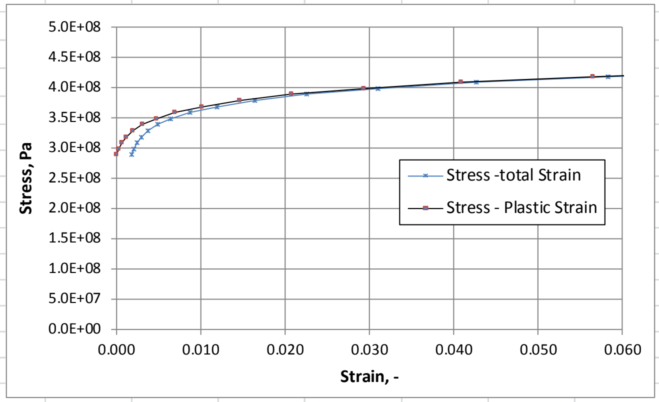

Total Strai	Stress	Plastic Strain
ε_{tot}	σ	ε_{pl}
0.002	2.8900E+08	0.000000
0.002	2.9900E+08	0.000268
0.002	3.0900E+08	0.000649
0.003	3.1900E+08	0.001197
0.004	3.2900E+08	0.001983
0.005	3.3900E+08	0.003108
0.006	3.4900E+08	0.004712
0.009	3.5900E+08	0.006984
0.012	3.6900E+08	0.010177
0.016	3.7900E+08	0.014634
0.023	3.8900E+08	0.020805
0.031	3.9900E+08	0.029287
0.043	4.0900E+08	0.04086
0.058	4.1900E+08	0.056535
0.079	4.2900E+08	0.077619
0.108	4.3900E+08	0.105791
0.145	4.4900E+08	0.143189
0.194	4.5900E+08	0.192529
0.259	4.6900E+08	0.257237
0.343	4.7900E+08	0.341615
0.453	4.8900E+08	0.45104
0.594	4.9900E+08	0.592199
0.775	5.0900E+08	0.773372
1.007	5.1900E+08	1.004769
1.301	5.2900E+08	1.298928
1.673	5.3900E+08	1.671183
2.142	5.4900E+08	2.14022
2.730	5.5900E+08	2.728721
3.466	5.6900E+08	3.464128
4.381	5.7900E+08	4.379527
5.516	5.8900E+08	5.514675
6.919	5.9900E+08	6.917196
8.646	6.0900E+08	8.643967
10.764	6.1900E+08	10.76271
13.356	6.2900E+08	13.35382
16.514	6.3900E+08	16.51251
20.353	6.4900E+08	20.35119
25.004	6.5900E+08	25.00225
30.623	6.6900E+08	30.62125
37.392	6.7900E+08	37.39047

4.3 Spread sheet for 340 MPa yield stress

Because just strains which are less than 10% are enough as input in abaqus, we have highlighted used data color of green.

We have defined two deferent sections for two kinds of steel and have assigned them related parts of the joint regarding their thicknesses.

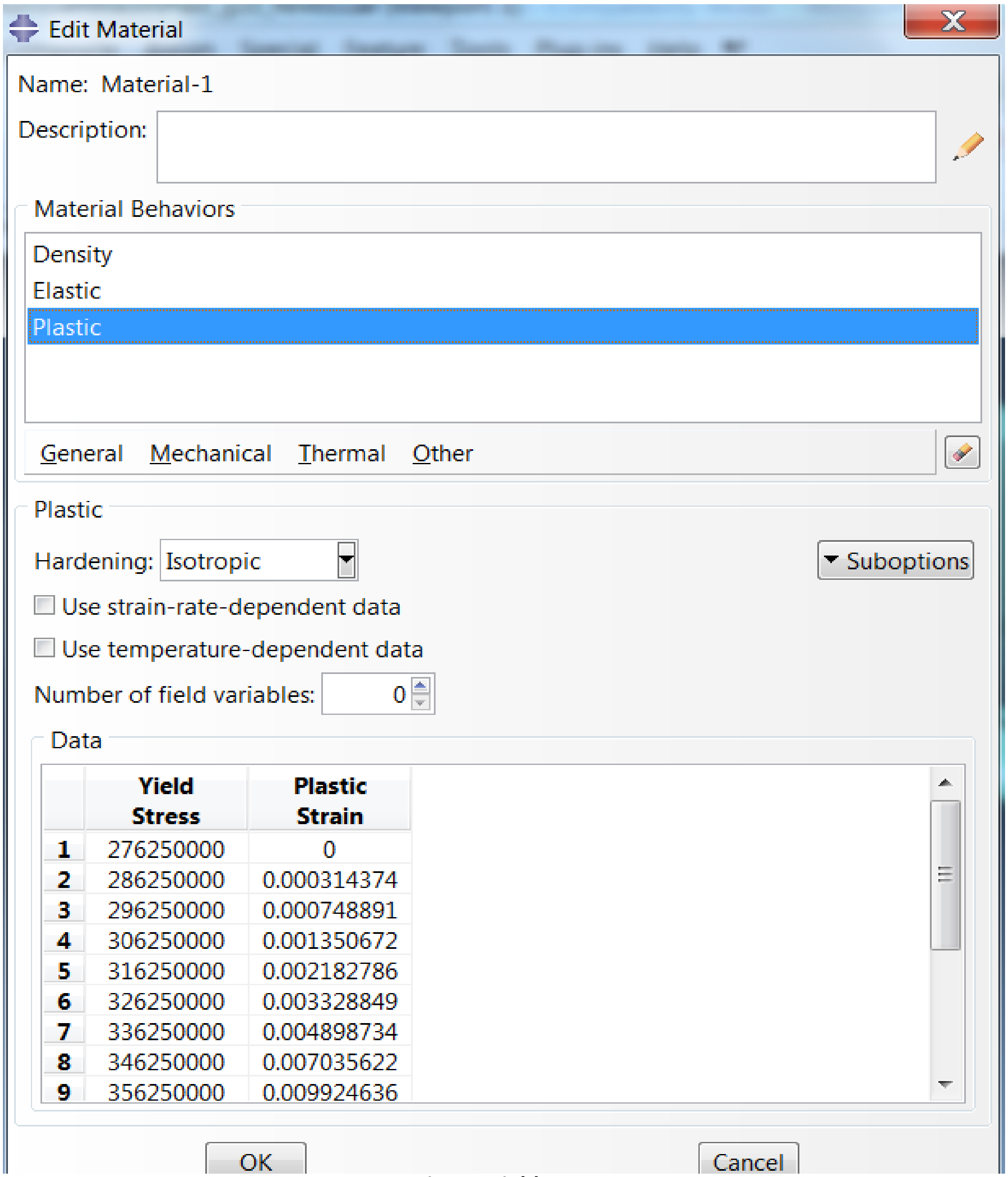

4.4 Section 1, Yield stress: 325 MPa

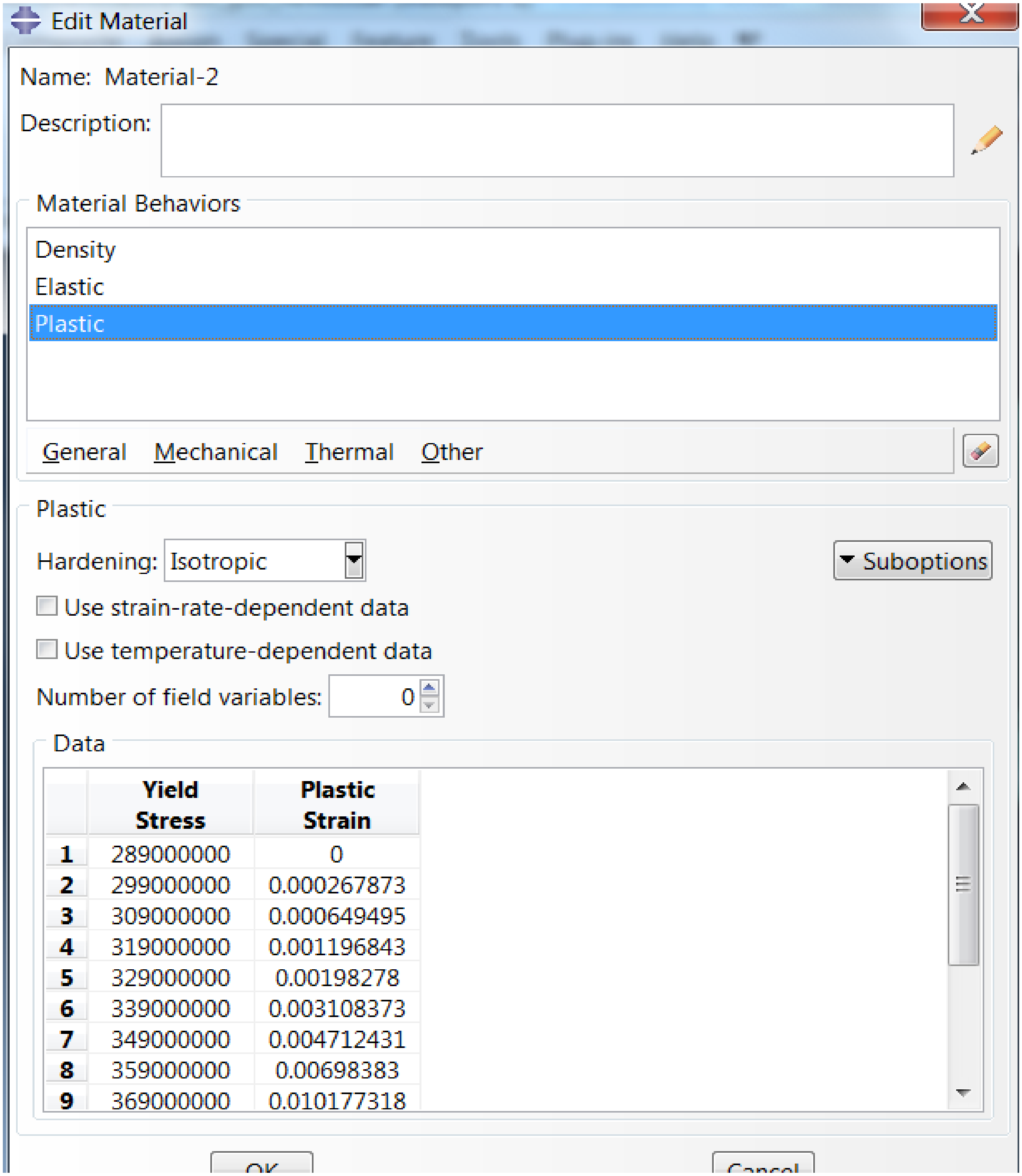

4.5 Section 2, Yield Stress: 340 MPa

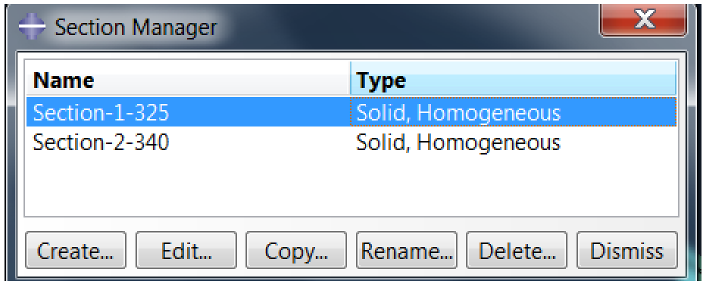

Boundary conditions and loading and meshing are quite same with the elastic model, although in future we will make some changes in this model and we will evaluate their effects.(C3D8R :An 8- node linear brick , reduced integration elements. **21377** elements have been produced in this stage)

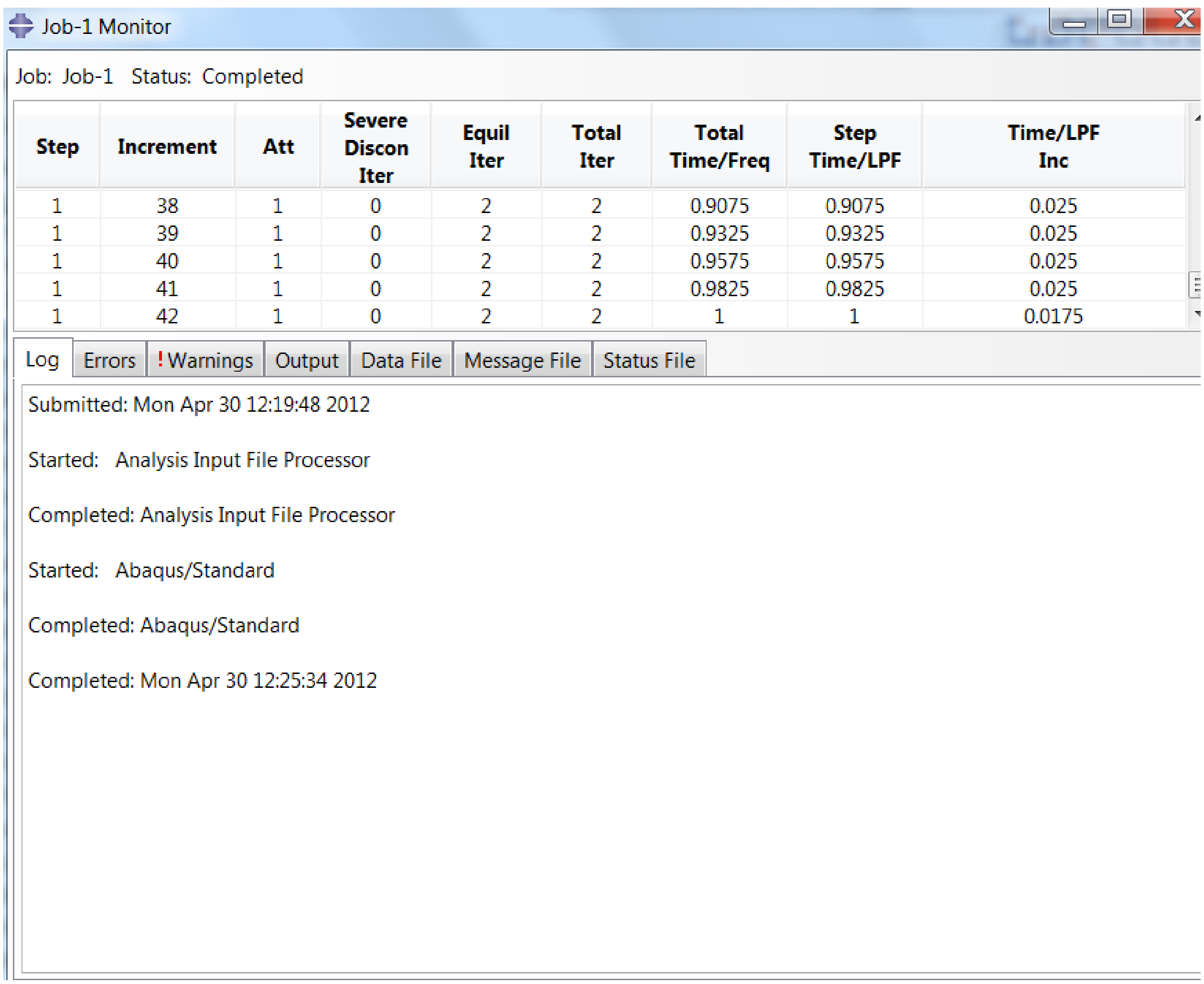

Step	Increment	Att	Severe Discon Iter	Equil Iter	Total Iter	Total Time/Freq	Step Time/LPF	Time/LPF Inc
1	38	1	0	2	2	0.9075	0.9075	0.025
1	39	1	0	2	2	0.9325	0.9325	0.025
1	40	1	0	2	2	0.9575	0.9575	0.025
1	41	1	0	2	2	0.9825	0.9825	0.025
1	42	1	0	2	2	1	1	0.0175

After around 7 minutes analysis completed.

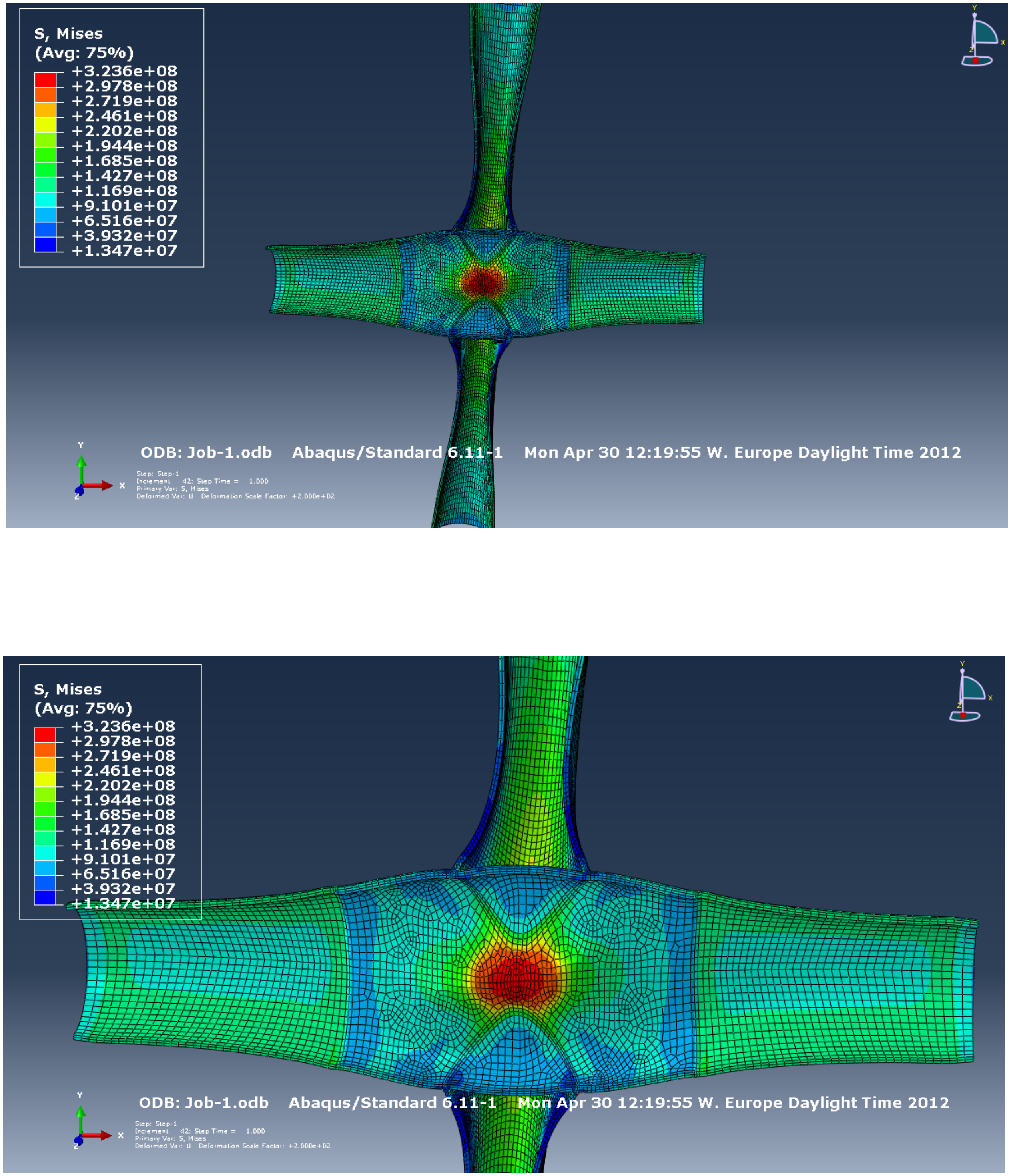

4.6 Plastic analysis result (von Mises stress)

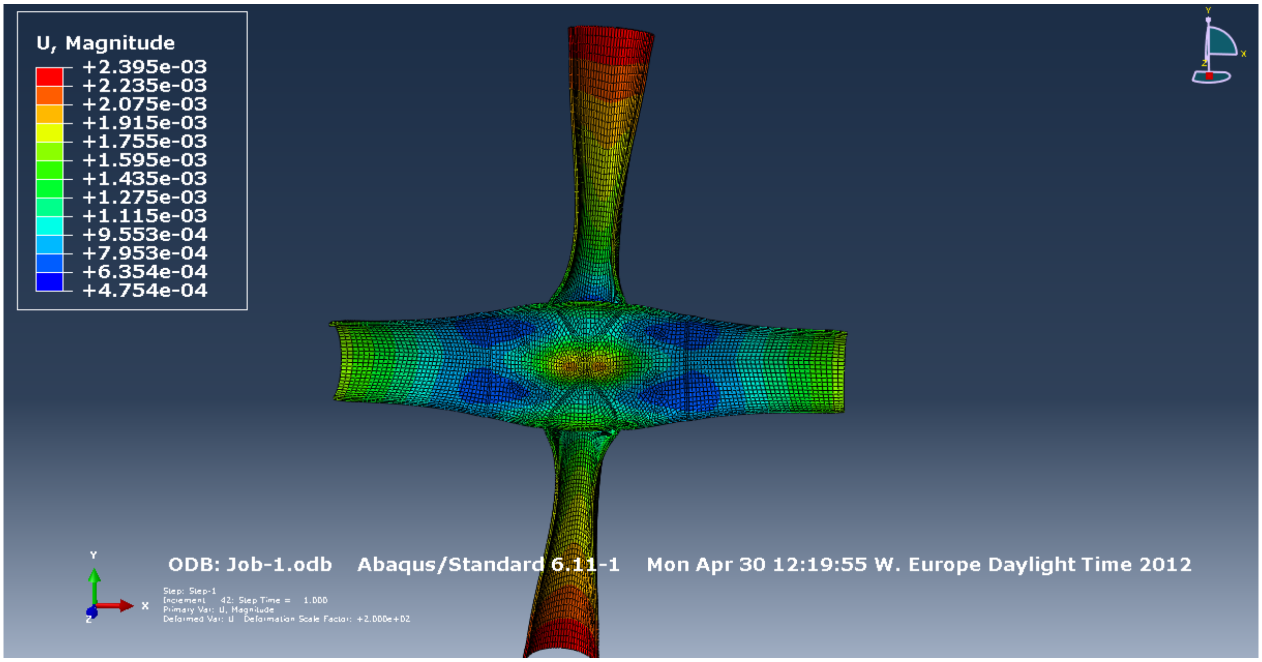

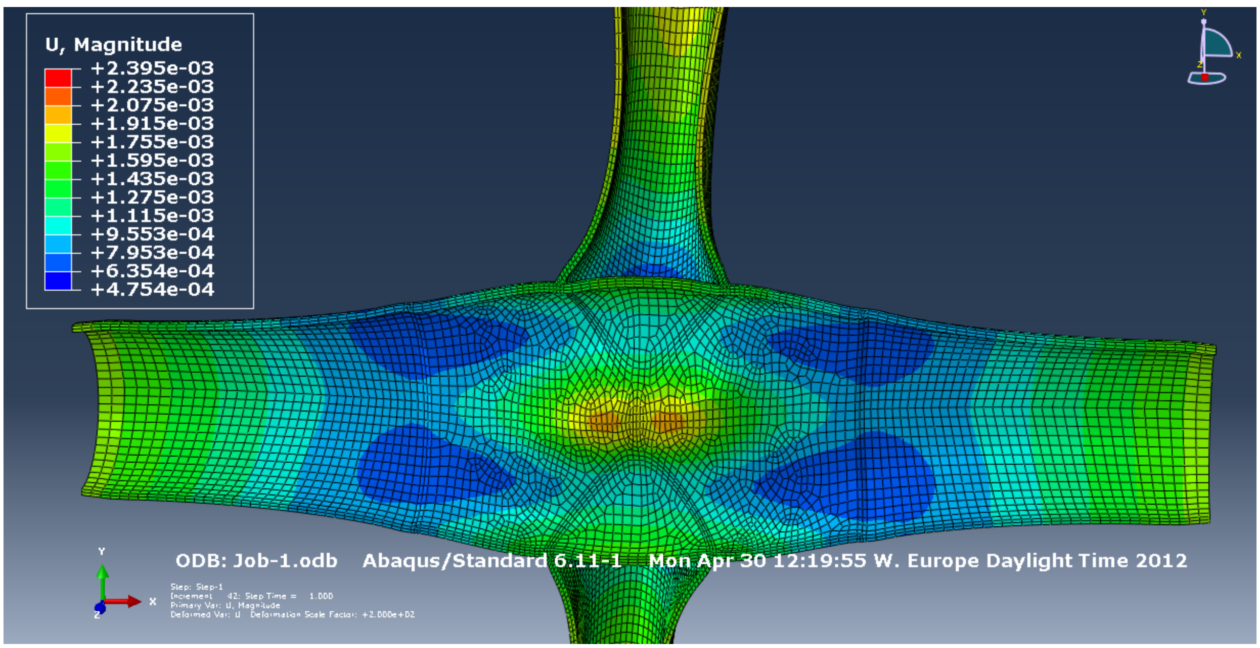

4.7 Plastic exaggerated deflections

As expected the maximum misses stress in elastic analysis is more than maximum misses' stress in plastic analysis in same model with same condition.

3.236e+8 Pa (Plastic) < 5.473 e+8 Pa (Elastic)

PEEQ is the equivalent plastic strain remaining when you remove the loads. If the material hasn't yielded then these will be zero everywhere. If it has yielded then you'll have this residual plastic strain and corresponding stresses at or below yield.

4.3 PEEQ and PE differences

In ABAQUS, PEEQ refers to the equivalent plastic strain, and PEMAG refers to the plastic strain magnitude. Both are scalar measures of the accumulated plastic strain. For proportional loading, the measures should be equal. However, for loading with reversals, PEEQ will continue to increase if the plastic strain rate is non-zero (regardless of sign). So, in general, PEMAG is the preferred measure.

PEEQ and PEMAG are generally used since they correspond to the plastic strain value on the uniaxial stress-strain curve. PE is used only if you are interested in component values / orientation.

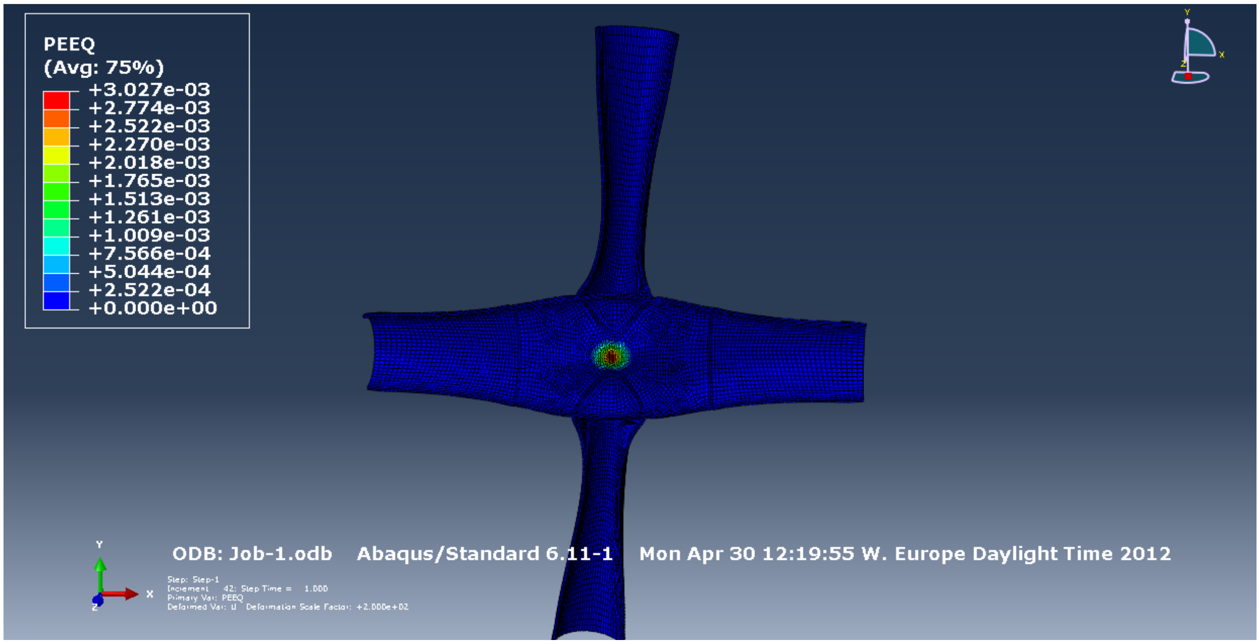

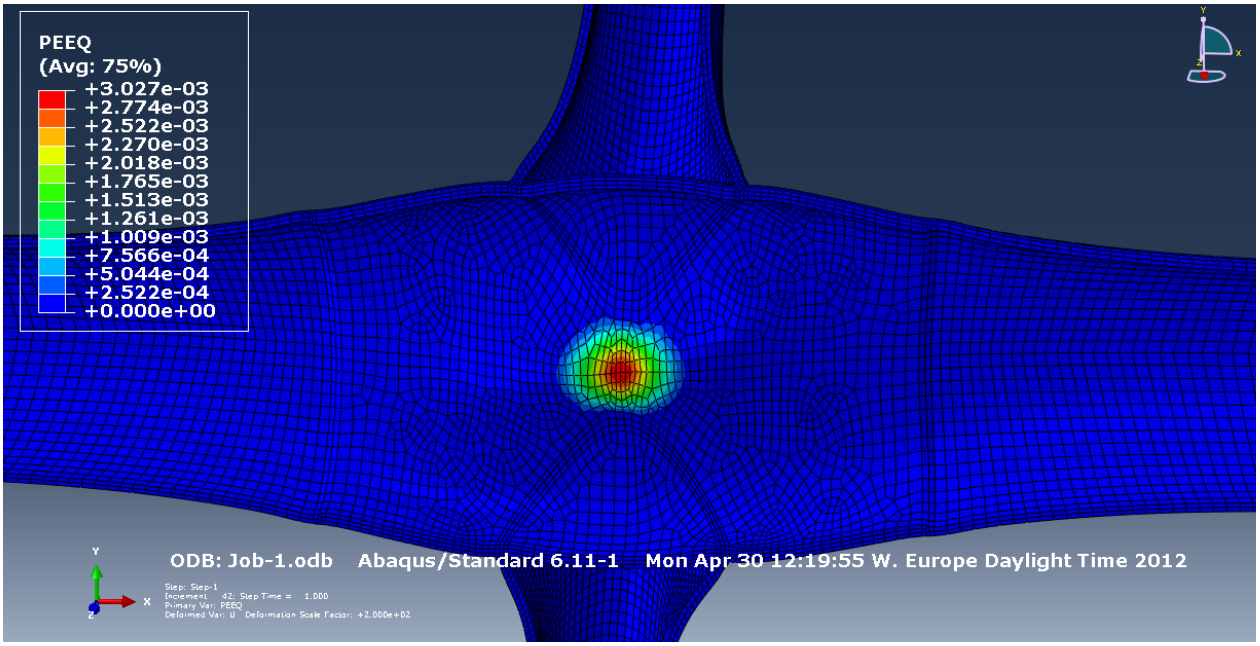

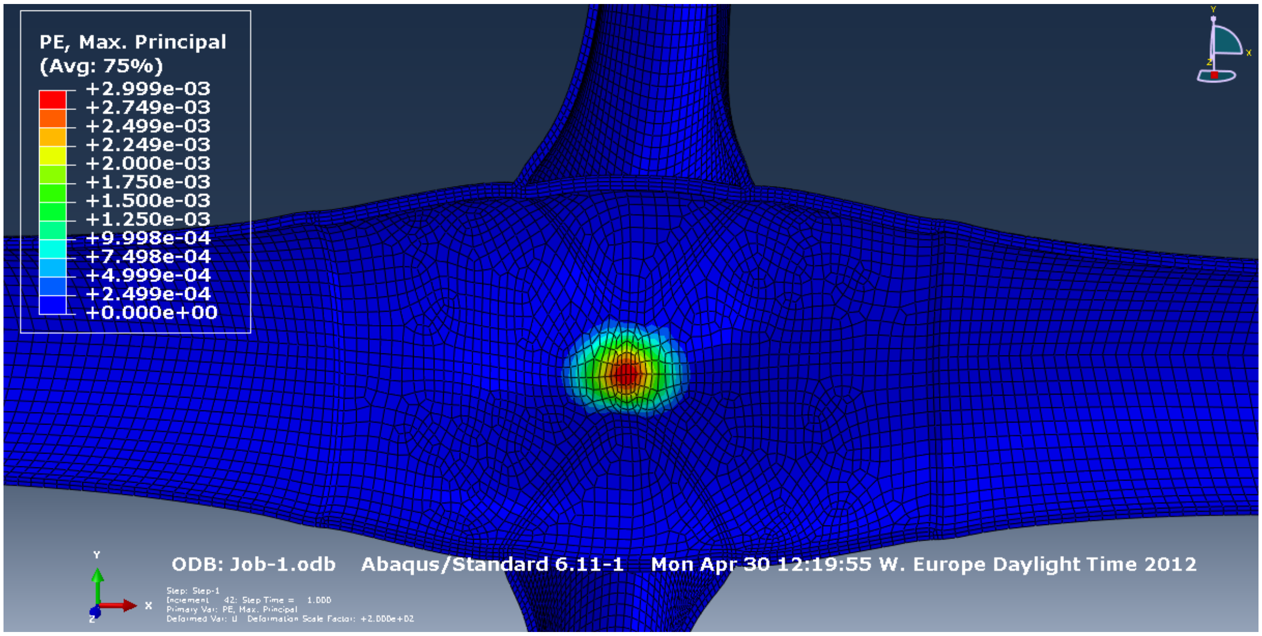

<u>4.8 PEEQ results</u>

4.4 Study of different element types (Linear & Quadratic) and meshing effects on Plastic analysis by ABAQUS

In this part we are going to evaluate effects of using different kinds of elements types in Plastic analysis. Especially we take a look to two different types of elements, linear elements with 8 nodes and Quadratic elements with 20 nodes.

Number of elements also is the other issue that is always matter of concern in all finite element analysis. Because there is direct relation between amount of elements and the time needed for analysis to be completed.

Considering all this factors and choosing an optimum way of meshing is something quite experimental and a good finite element analyst can make the best decision on each specific case. In this part, we compare 12 different model of same joint with same conditions, But different in amount of elements and also different in type of elements.

Model Name	Descriptions	Number of nodes in element	Total number of elements
A	Much Much Coarser-linear-8 nodes	8	1620
C	Much Coarser-Linear Element-8nodes	8	5232
E	Coarser Mesh-Linear Element-8nodes	8	10300
G	Coarse Mesh-Linear Element-8nodes	8	21377
I	Fine mesh-Linear Element-8 nodes	8	26696
K	Finer mesh-Linear Elements-8nodes	8	32337
L	Much Finer mesh-Linear Elements-8nodes	8	99297

<u>4.9 Linear 8 nodes elements models</u>

Model name	Descriptions	Number of nodes in element	Total number of elements
B	Much Much Coaser-Quadratic-20 nodes	20	1620
D	Much Coarser-Quadratic Element-20nodes	20	5233
F	Coarser Mesh-Quadratic Element-20nodes	20	10300
H	Coarse Mesh-Quadratic Elements-20 nodes	20	21377
J	Fine mesh-Quadratic Elements-20 nodes	20	26696

4.10 Quadratic 20 nodes elements models

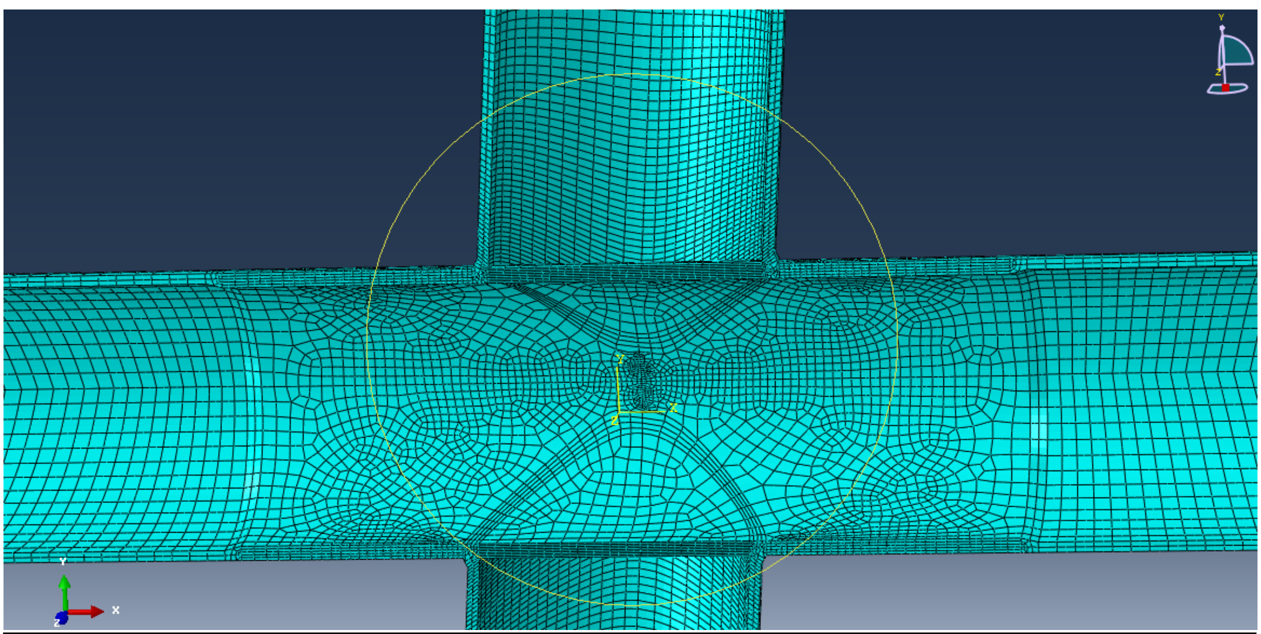

4.11 Model j with 26697 Quadratic elements

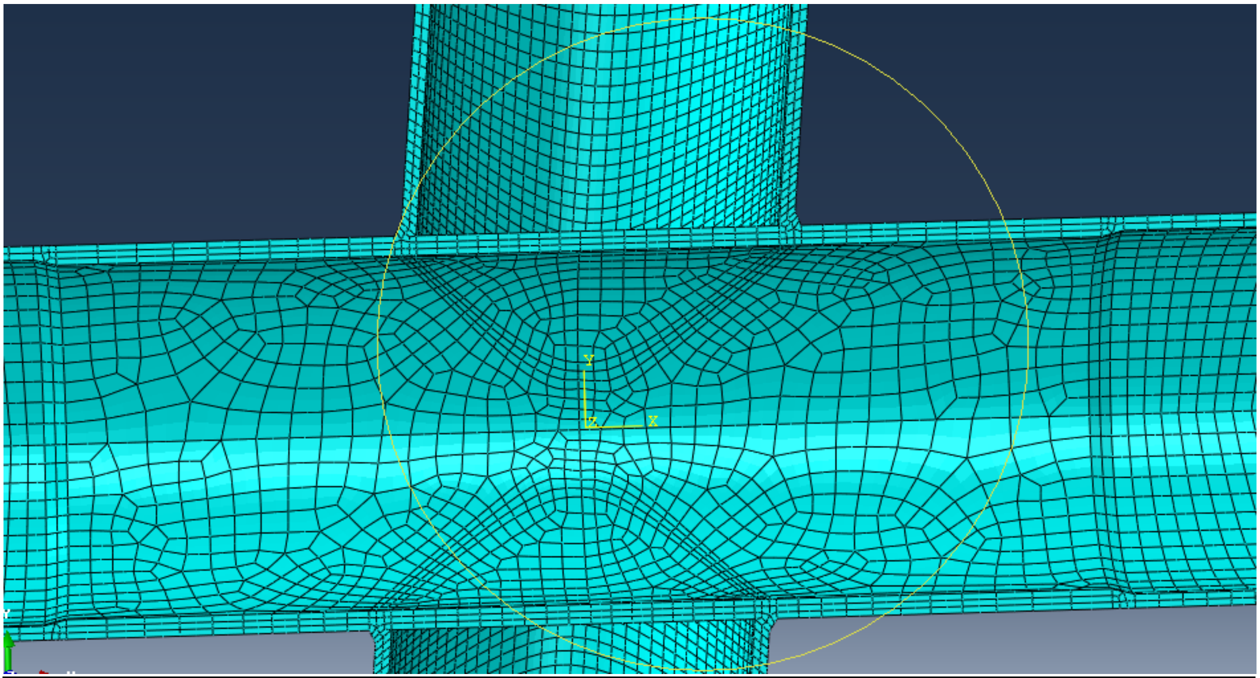

4.12 Model E with 10300 linear elements

As it is shown in examples pictures, changing in amount and size of elements has been done mainly on can area, because this is the area which is more critical for us and maximum of stresses have been observed in this area.

As we explained before changing the element type in abaqus is changeable in the element type box:

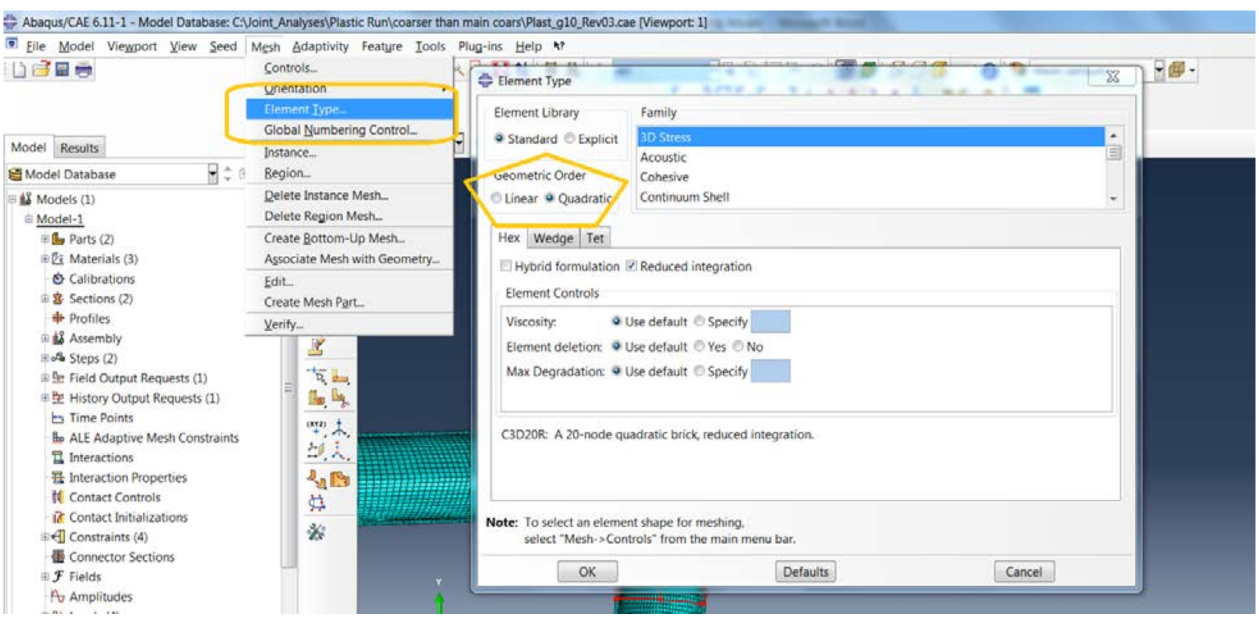

Number of elements and the other specifications of the model are available in Job-.dat files that will be created automatically in work directory file which we define for the software in advance. As an example some part of Job-.dat file related to elements for model K:

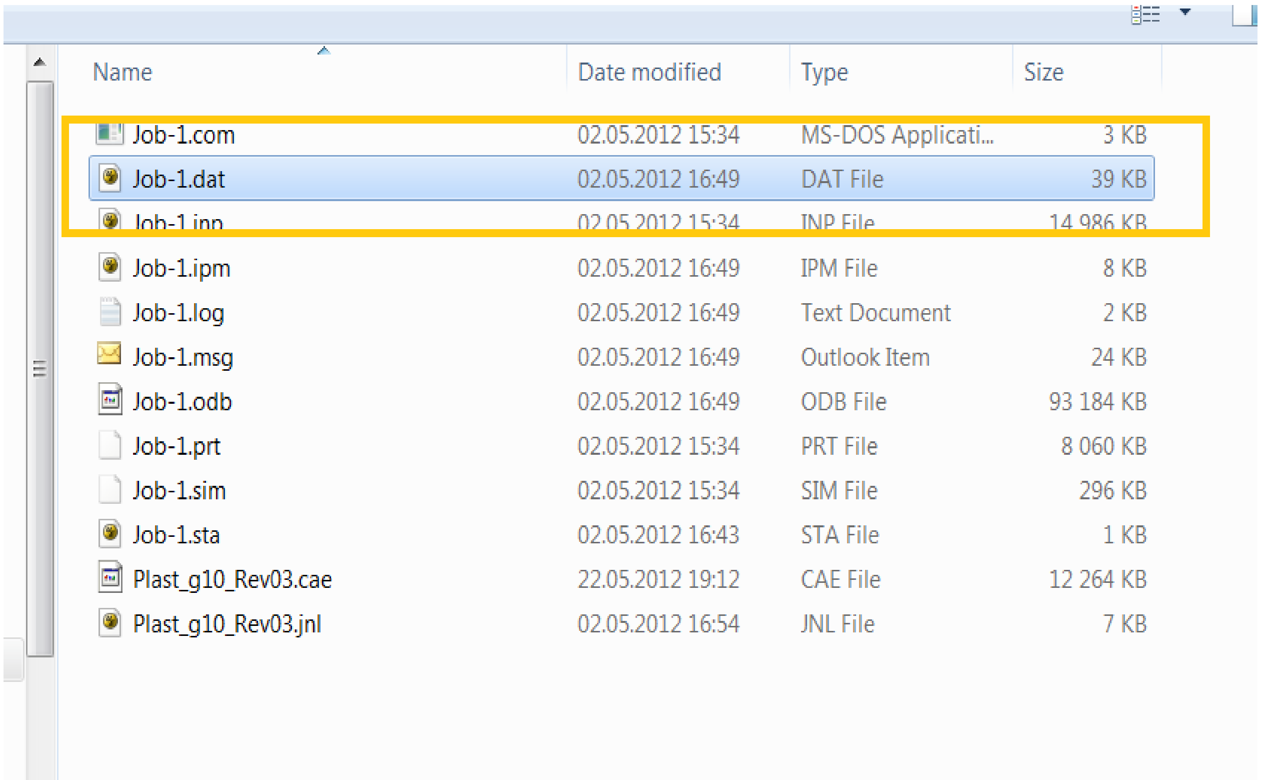

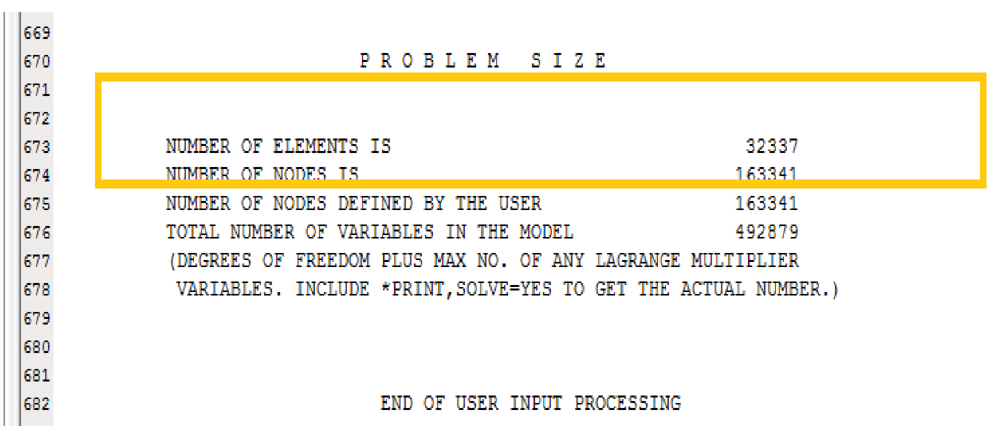

```
                         P R O B L E M   S I Z E


      NUMBER OF ELEMENTS IS                             32337
      NUMBER OF NODES IS                               163341
      NUMBER OF NODES DEFINED BY THE USER              163341
      TOTAL NUMBER OF VARIABLES IN THE MODEL           492879
      (DEGREES OF FREEDOM PLUS MAX NO. OF ANY LAGRANGE MULTIPLIER
       VARIABLES. INCLUDE *PRINT,SOLVE=YES TO GET THE ACTUAL NUMBER.)



                          END OF USER INPUT PROCESSING
```

All the 12 mentioned models have been analyzed and obtained results are presented in table below:

Model name	Description of model	Number of Nodes per Element	Total number of Elements	σ Mises (max)	PEEQ	Time elapse (min)
A	Much Much Coarser-linear-8 nodes	8	1620	3.05E+08	1.44E-03	0.4
B	Much Much Coaser-Quadratic-20 nodes	20	1620	3.62E+08	4.63E-03	2
C	Much Coarser-Linear Element-8nodes	8	5232	3.08E+08	1.63E-03	1.8
D	Much Coarser-Quadratic Element-20nodes	20	5233	3.62E+08	4.62E-03	12
E	Coarser Mesh-Linear Element-8nodes	8	10300	3.23E+08	2.88E-03	2.61
F	Coarser Mesh-Quadratic Element-20nodes	20	10300	3.45E+08	4.07E-03	18.4
G	**Coars Mesh-Linear Element-8nodes**	**8**	21377	3.24E+08	3.03E-03	5.47
H	**Coars Mesh-Quadratic Elements-20 nodes**	**20**	21377	3.44E+08	3.79E-03	53
I	Fine mesh-Linear Element-8 nodes	8	26696	3.24E+08	3.11E-03	6.81
J	Fine mesh-Quadratic Elements-20 nodes	20	26696	3.43E+08	3.77E-03	128
K	Finer mesh-Linear Elements-8nodes	8	32337	3.25E+08	3.23E-03	11
L	Much Finer mesh-Linear Elements- 8nodes	8	99297	3.26E+08	3.28E-03	57.5

4.13 Results for study of 12 models with different amount of mesh and element type

In this table all the models with linear elements are highlighted with color of green and models with Quadratic element types are highlighted with color of yellow.

As you can see the number of elements and the types of them in addition of maximum Mises stress and PEEQ and also time elapses for each one have been provided in the table.

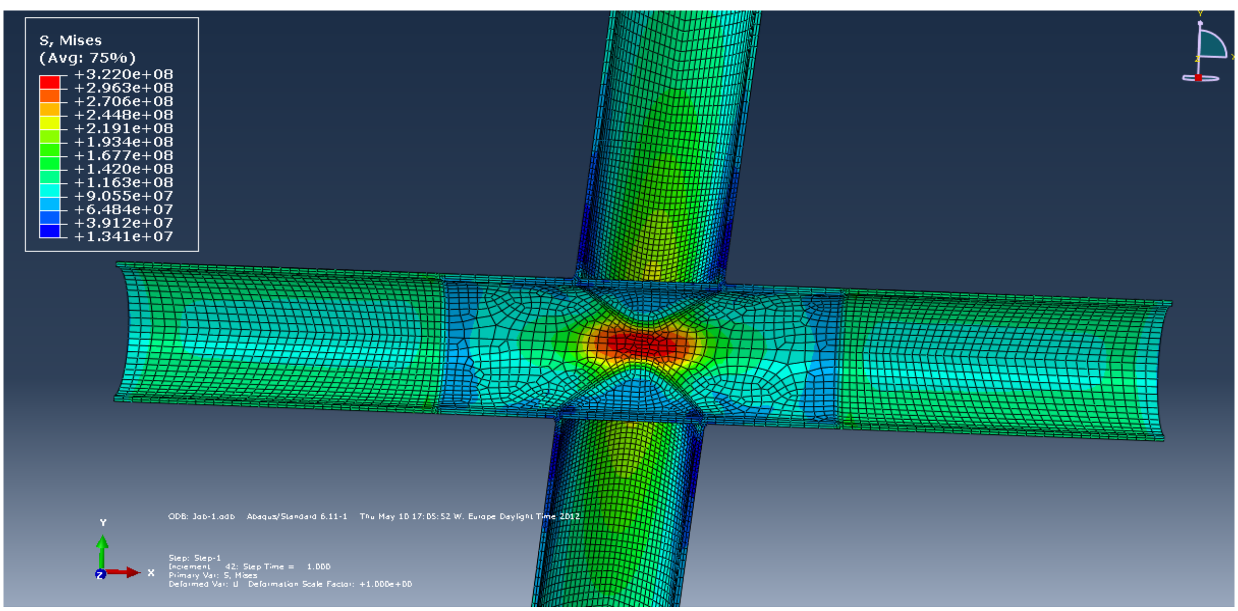

4.14 Von Mises' stress obtained after plastic analysis related for model E (as an example)

Furthermore two important diagrams are presented. In one of them you can see the comparison of all 12 models in aspect of max misses stress and the other contains PEEQ of all 12 models. Interpretation of each one will be presented also.

#Elements	σ Mises Linear	σ Mises Quadratic
1620	3.05E+08	3.62E+08
5232	3.08E+08	3.62E+08
10300	3.23E+08	3.45E+08
21377	3.24E+08	3.44E+08
26696	3.24E+08	3.43E+08
32337	3.25E+08	3.35E+08
99297	3.26E+08	3.29E+08

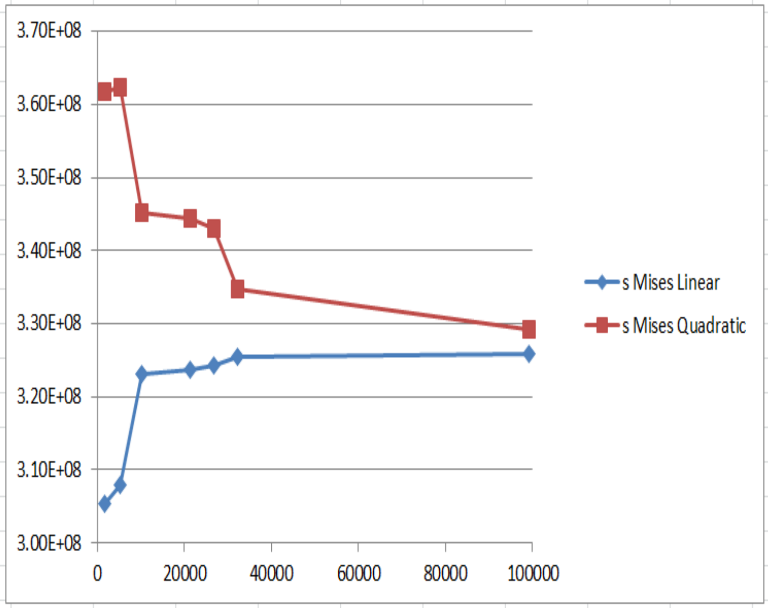

4.15 Comparison of Mises stress in linear and quadratic elements

This Diagram contains results of plastic analysis which have been meshed by two different elements types. 1st one is linear element type and 2nd one is Quadratic element type. X axis shows number elements and Y axis shows the obtained maximum misses stress. As is written the red line relates to linear ones and blue line shows the results for quadratic elements. As we see in beginning when we have relatively few amounts of elements (1620) the difference between linear and quadratic elements are significant (about 15%) but as it is obvious by increasing the amount of elements little by little the results of two different kinds got near together

Number Of elements	Differences between the results in percentage
1620	15%
5232	14%
10300	6%
21377	5.8%
26696	5.4%
32337	3%
99297	1%

4.16 Differences between the results of linear and quadratic elements in percentage

#Elements	PEEQ(Linear)	PEEQ (Quadratic)
1620	1.44E-03	4.63E-03
5232	1.63E-03	4.62E-03
10300	2.88E-03	4.07E-03
21377	3.03E-03	3.79E-03
26696	3.11E-03	3.77E-03
32337	3.23E-03	3.41E-03
99297	3.28E-03	3.15E-03

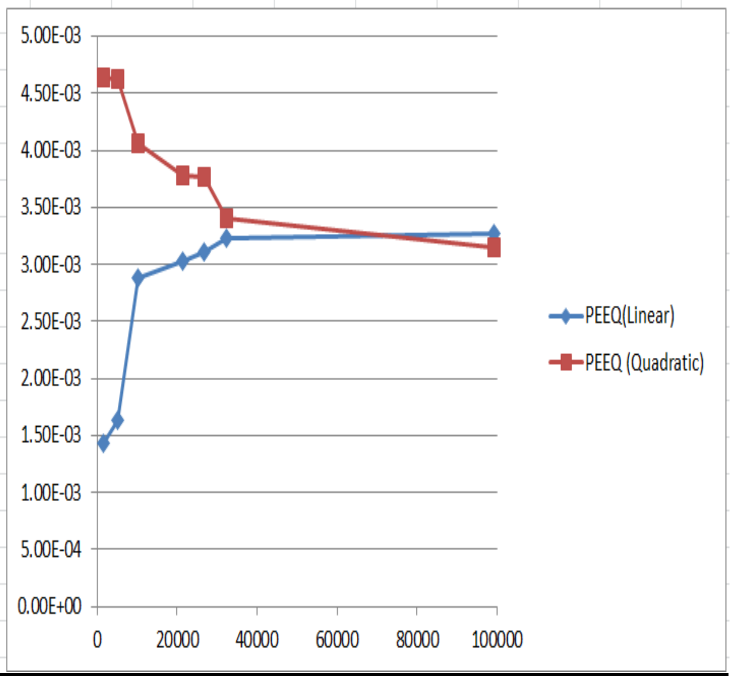

4.17 Comparison of PEEQ in linear and quadratic elements

This table and diagram is also about comparing the results PEEQ in different amount of element and two different types of elements, and again like what we saw about maximum misses stress by increasing the amount elements we will observe relatively same amount of PEEQ.

In conclusion we can say that it is obvious that in most cases quadratic elements with high amount of elements produce the most accurate results, but we should know that using quadratic elements and high amount elements hardly increase the time of analyses, and a well experienced finite element analyst can choose optimum way and amount of meshing.

5 Conclusions and Recommendations for further works

5.1 Conclusions

In conclusion I want really mention that doing this thesis have given me good knowledge and worthy skills about finite element modeling and analysis and made me to learn using a very powerful software, ABAQUS, which is lifelong treasure for my all professional life.

Also I have really touched this reality that for realistic FE analysis just knowing how to use software is not enough and we need to have deep knowledge about finite element concepts in advance. In this thesis I have done linear and non-linear FE analysis on the same case with same specifications and as we know and saw, considering the non linear behaviors of materials will guide us to most realistic results but in another hand there is a reality that concept of engineering is based on two principles, 1st mathematical accuracy, 2nd time managing and a well experienced engineer can decide a way which can fulfill both of these principles.

In technical aspect, we have performed comparisons between elastic and plastic analysis and also lots of comparison studies about using different types of elements and meshing techniques. Specifically we investigated differences between linear and quadratic elements. Based on finite element concepts we know that in most complicate shaped cases using much more dense meshes with quadratic 20 nodes elements will conclude to most accurate results.

And it is what we exactly saw in the results. In very coarse meshes the deference in results between linear and quadratic elements are quite significant, But by increasing the amount of elements and by make it more and more fine mesh the results of linear element types inclines to results obtained from quadratic elements type, for example in last compression which we used 99297 elements, difference in max von Mises stress between two types of elements was just 1% however this deference in beginning that we used just 1620 elements was about 15%.

Time elapse for each analysis is a factor which we should consider also always, and using quadratic elements and fine meshes increase time elapse in kind of exponentially, spending much more time means spending much more money and now this is a place that a knowledgeable and well experienced analyst can choose the most optimum way to save as much as possible time in one hand and reach to results with acceptable level of accuracy.

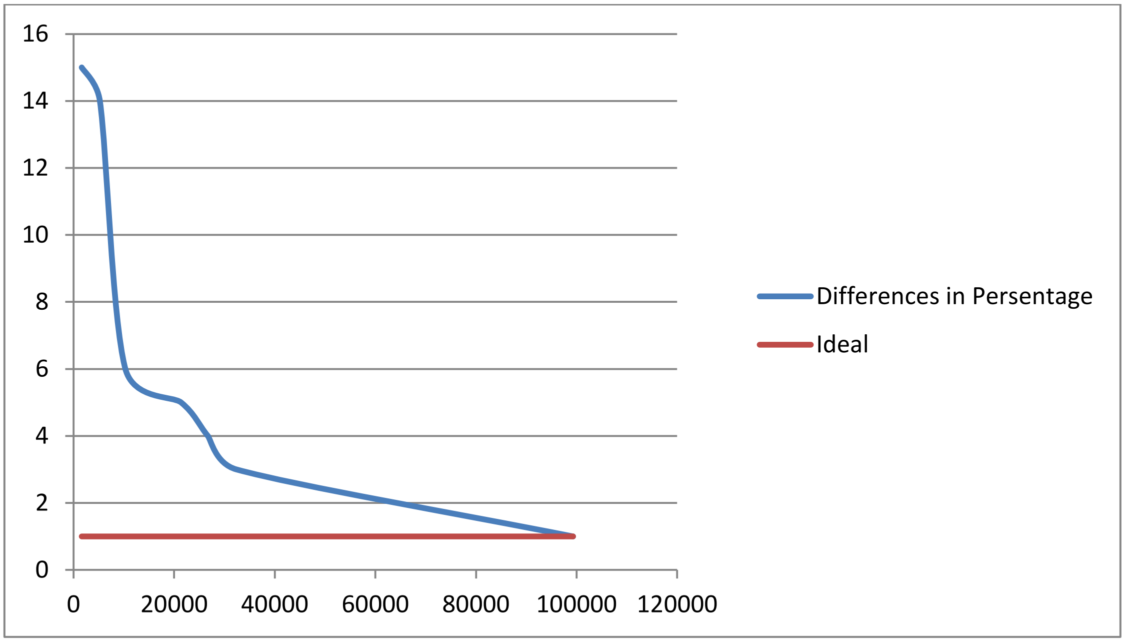

5.1 inclinations of the differences in results in percentage to 1%

As it is quite clear in this diagram, by increasing the number of elements fraction of quadratic results on the linear results inclines to 1 and differencing will decrease.

5.2 Recommendations for further works

Main point of this thesis was about comparison of elastic and plastic analysis and investigation of effects of using different kinds of meshing techniques and element types in X tubular joints by ABAQUS. We have reached to some interesting outputs from our studies. It can be continued with some other powerful FE analyzer softwares like ANSYS for example or etc to see the differences also we can extend the amount of samples, for example in this thesis we compared 12 different models it can be done with much more samples to have even more elastic observations. Also mainly in this thesis we compared linear 8nodes elements with quadratic 20nodes elements it can be done for some other types of elements like more even more complicated ones. Also as mentioned before generally there are some different mesh generating techniques in FE software like structured, sweep or bottom up, in this case we have used relatively all of them in different parts of the model, it would be interesting if we could define some fixed factors and parameters related to geometry of a model to help us in recognizing about where and when we should use each method.

In aspect tubular joints, this thesis was concentrated on X joints, as presented previously there are joint classifications in all standards and codes, due to extended usage of tubular joints in marine structures other types of joints like K or Y types are also good field of investigations in aspect of capacity and application.

References

(1) "Comparison of tubular joint strength provisions in codes and standards", HSE Health and safety executive, Bomel Limited, Ledger House, Forest Green Road Fifield Maidenhead, Berkshire SL6 2NR, United Kingdom, Accessed on 05.02.2012, http://www.hse.gov.uk/research/otopdf/2001/oto01082.pdf

(2) American Petroleum Institute. "Recommended practice for planning, Designing and constructing fixed offshore platforms - working stress design",
API RP2A-WSD, 20th edition, July 1993

(3) American Petroleum Institute. "Recommended practice for planning, designing and constructing fixed offshore platforms - load and resistance factor design", API RP2A-LRFD, 1st edition, July 1993

(4) Health and Safety Executive. "Offshore installations, guidance on design, construction and certification", 1990 plus amendments [withdrawn 1998]

(5) Department of Energy. "Background to the new static strength guidance for tubular joints in steel offshore structures", Offshore Technology Report, OTH 89 308, HMSO, 1990

(6) International Standards Organization. "Petroleum and Natural Gas Industries – Offshore Structures - Part 2: Fixed Steel Structures", First Edition, 1995

(7) International Standards Organisation. "Petroleum and Natural Gas Industries – Offshore Structures - Part 2: Fixed Steel Structures", Second Edition Draft B, November 1996; Draft C, July 1997; Committee Draft (CD), May 1999

(8) Dier, A F and Lalani, M. "New code formulations for tubular joint strength", International Symposium on Tubular Structures, 1997

(9) NORSOK Standard. "Design of Steel Structures", N-004, Rev 1, December 1998

(10) Yura, J A, Zettlemoyer, N and Edwards, I F. "Ultimate capacity equations for tubular joints", OTC Paper 3690, Offshore Technology Conference, Houston, May 1980

(11) Wikipedia, “Theory of elasticity” http://en.wikipedia.org/wiki/Solid_mechanics, Accessed on 25.03 2012
(12) “Theory of elasticity”, Accessed on 25.03.2012, http://seisweb.usask.ca/classes/GEOL335/2004/Lectures/PDF/Elasticity.pdf

(13) “Theory of Plasticity”, Accessed on 05.05.2012 http://www.scribd.com/doc/29556452/Elements-of-the-Theory-of-Plasticity

(14) Dieter, G.E., “Mechanical Metallurgy”, 1988, SI metric edition, McGraw-Hill, ISBN 0-07-100406-8

(15) Hibbeler,R.C., “Mechanics of materials”, 2005 SI second edition, Person Prentice Hall, ISBN 0-13-186-638-9

(16) Wikipedia, “Ranbarg-Osgood Relations”, Accessed on 15.05.2012, http://en.wikipedia.org/wiki/Ramberg%E2%80%93Osgood_relationship

(17) Abaqus 6.12 manual, available in abacus documentary file also in the website bellow (keep being updated with new versions), http://abaqus.ethz.ch:2080/v6.11/

(18) “Finite elements”, ftp://ftp.demec.ufpr.br/disciplinas/TM738/l2-elements.pdf, Accessed on 20.05.2012

(19) “Linear vs Quadratic element types”, http://old.nabble.com/Linear-Vs-NonLinear-elements-td30577463.html, Accessed on 20.05.2012

(20) Wikipedia, “Von Mises stress”, http://en.wikipedia.org/wiki/Von_Mises_yield_criterion, Accessed on 1.06.2012

(21) “FE Mesh Generation for Circular Tubular Joints with or Without Cracks”, Junjie Cao, Guojing Yang and Jeffrey A. Packer, University of Toronto, The Seventh International Offshore and Polar Engineering Conference, May 25 - 30, 1997 , Honolulu, Hawaii, USA